A framework for the impact assessment of low discharges on the performance of inland waterway transport

TU Delft

Royal HaskoningDHV
Enhancing Society Together

S. Kievits

A framework for the impact assessment of low discharges on the performance of inland waterway transport

by

Servaas Kievits

Student number	4207947	
Thesis committee	Prof. dr. ir. M. Van Koningsveld	TU Delft (Chair)
	Ir. M. Bos	Royal HaskoningDHV
	Prof. dr. ir. P. Van Gelder	TU Delft
	Ir. J. Lansen	TU Delft
	Dr. Ir. P. Taneja	TU Delft

TU Delft

Royal HaskoningDHV
Enhancing Society Together

Preface

This research marks the final stage of the master Civil Engineering at the faculty of Civil Engineering and Geosciences of the Delft University of Technology. It has therefore been the final effort in obtaining the title of Master of Science in the field of Hydraulic Engineering.

This thesis has been performed in collaboration with Royal HaskoningDHV, a renowned engineering and project management consultancy. The maritime sector of Royal HaskoningDHV makes a large effort incorporating digitization in their way of working. In line with that ambition, this research contributes to the expanding set of digital tools that become available to engineers. I would like to thank Royal HaskoningDHV for offering me the opportunity to perform my thesis in their Rotterdam office. I would like to thank the people there for showing their curiosity about my work and for their support when needed.

I would like to take this opportunity to express special gratitude to the people that have guided me through this thesis. To start, I would like to thank Mark van Koningsveld, the chair of my committee, for his endless enthusiasm on the topic of simulating maritime logistics. Moreover, I would like to express my gratitude to Matthijs Bos and Joost Lansen of Royal HaskoningDHV for supervising the relaxed way they did, and for challenging me to stay sharp throughout the process. In addition, I would like to thank my other committee members, Pieter van Gelder and Poonam Taneja, for showing confidence in my approach and for providing me with useful feedback. Lastly, I would like to thank Joris Den Uijl whom I have spent several hours with, explaining me inexplicable Python errors. It has been a joy.

Servaas Kievits
Rotterdam, November 2019

Contents

List of Abbreviations

IWT	Inland waterway transport
LSM	Landelijk Sobek Model
SLR	Sea level rise
IPCC	Intergovernmental Panel on Climate Change
RCP	Representative Concentration Pathways
G_L	Climate scenario with moderate global warming and low change in circulation pattern
G_H	Climate scenario with moderate global warming and high change in circulation pattern
W_L	Climate scenario with high global warming and low change in circulation pattern
W_H	Climate scenario with high global warming and high change in circulation pattern
LAD	Least Available Depth
CCR	Central Commission for the Navigation of the Rhine
ALW	Agreed Low Water level
EMO	Europees Massagoed Overslag
EECV	Ertsoverslag Europoort C.V.
JIT	Just-in-time
OpenCLSim	Open-source Complex Logistics Simulation
DES	Discrete Event Simulation
ABS	Agent Based Simulation
IVS-90	Informatie en Volgsysteem Scheepvaart (1990)
RMSE	Root Mean Squared Error
CV(RMSE)	Coefficient of Variation of the Root Mean Squared Error
PCC	Pearson Correlation Coefficient
EYD	Estimated yearly damage
PVEYD	Present value of estimated yearly damage
BCR	Benefit-Cost Ratio

List of Figures

List of Tables

Abstract

Ports are crucial nodes in global supply chains, thereby making economic development depend on port performance. One of the indicators of port performance is intermodal hinterland connectivity. Inland waterway transport (IWT) is one of the three main modalities for inland transport of dry, liquid and containerized cargo. As IWT performs well on cost-competitiveness, environmental friendliness, and congestion-related issues, authorities strive to shift freight transport from road to water, thereby aiming to increase its share of the modal split. Inland waterway connections, however, are vulnerable to the growing impact of climate change as in 2018, when the Netherlands was struck by 6 months of low discharge on the Rhine branches. A combination of higher temperatures and more extreme seasonal differences in precipitation is expected to increasingly impact the discharge of the Rhine in the future. In summer, this will result in low water events happening more frequent and more intense in parts of Europe. Low water levels pose a larger threat to inland navigation than high water events because of their usually longer duration. The effects of climate change on IWT in combination with an expected increase of port downtime could result in a reduced annual transport capacity, thereby weakening the reputation of IWT and increasing the costs of cargo shipment.

In the light of climate change, low discharges are expected to happen more often. The drought in North-Western Europe in 2018 therefore marks the beginning of an exploration of long-term measures that reduce the impact of future low discharges on the IWT performance. The objective of this research is to provide more insight into the consequences of climate change-induced low discharges on the performance of IWT and to assist in making justified adaptation decisions. A simulation model that includes the effects of climate change on the network parameters to study the performance of the IWT system does not exist. During this research, an IWT performance model has been developed that is capable of studying the capacity and vulnerability of the inland waterway system to low water depths, and simultaneously can be used to propose the most effective measures to strengthen the position of IWT. Due to the vital role of the Rhine as transport corridor in North-Western Europe and the recent issues with low discharges in 2018 for the German steel manufacturers, this research considers a case study on the iron ore and coal transport between Rotterdam and Duisburg.

A model was developed to simulate the performance of an IWT network to varying discharges. The objective of this IWT performance model is to accurately express the performance of the IWT system in key performance indicators describing the transported cargo and the costs of transport. The chosen model concept is the Python package OpenCLSim which is available at the GitHub of the TU Delft Hydraulic Engineering department. This model concept is set up as a combination of Discrete Event Simulation (DES) and Agent-Based Simulation (ABS). The DES describes the discrete events that represent the logistical chain of IWT and the ABS includes the vessels and berth equipment required to carry out the various activities in the simulation.

To assess the quality of the logistic simulations, the model has successfully been subjected to a number of validity tests related to the functioning of the load factor, the number of trips, the transport demand and the transport costs. Consequently, the model was calibrated on two parameters that have a high uncertainty and a significant impact on the simulation; the manoeuvring time per trip and the vessel capacity. For this purpose, an IVS-90 data-set was obtained that describes the observed transported weight and number of trips for dry bulk transport originating from Rotterdam in 2018. After calibration, the model shows a correlation coefficient for the transported cargo of $r = 0.794$ and for the number of trips of $r = 0.921$. From these values, it can be concluded that the results of the IWT performance model are relatively accurate with reality.

A base scenario was set, corresponding to a discharge profile that undershoots the agreed limit for low discharge of 1020 m^3/s for the maximum allowable number of days, i.e. 5% of the year. Daily projections of the water depth on the Rhine are obtained by extrapolation of the representative, dry year 1976 with two climate scenarios to the year 2050. Similar to 1976, the obtained number of days with low water depths then has a return period of $T = 10\ years$. The RUST- and the STOOM-scenario of the Deltaprogram have been used, representing respectively moderate and rapid climate change. The water depths encountered in the RUST-scenario and the STOOM-scenario have been compared to the base scenario. To put into perspective these impacts, a model run for the reference scenario of 2018 has been incorporated in the comparison. The studied scenarios that are used to assess the impact of low discharges are shown in Figure 2. Moreover, the

significant water depths of $3.0m$ and $2.25m$, that denote the depths beneath which the 6-barge push convoys and the smaller convoys, respectively, become inactive, are depicted.

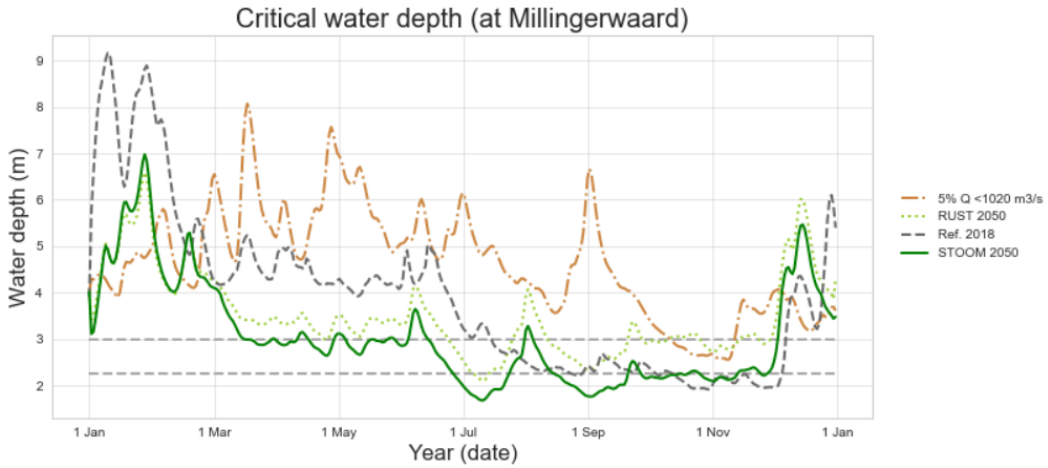

Figure 2: Critical water depth at Millingerwaard for all scenarios

When assessing the impact of low discharges, a comparison of model outcomes given the set of input values is presented in Table 1. The RUST-scenario shows a relatively small reduction of transported weight whereas the STOOM-scenario shows a decrease of 21% compared to the base scenario. Both scenarios show large growth of the projected costs of 70% and 192% of the costs in the base scenario, respectively. Consequently, it is concluded that the critical water depth profile of 2018, which has a return period of $T = 20\ years$, is more extreme than the projections of the RUST-scenario for the year 2050 with a return period of $T = 10\ years$. The critical water depth profile of the STOOM-scenario in 2050 with a return period of $T = 10\ years$, however, is projected to be more extreme than the reference scenario of 2018 by estimating values for the transported weight and the transport costs that exceed the model results of 2018 by approximately 50%. This follows from more days in the year with a critical water depth below $2.25m$, which is the limit beneath which the smaller push-barge convoys stop operation and the transport capacity of the network becomes insufficient. Figures 3 and 4 show the trend of the transported cargo and the transport costs for the various scenarios throughout the simulation.

	Unit	**Base scenario**	**RUST [%]**	**STOOM [%]**	**Ref. 2018 [%]**
Transported weight	$[tons]$	26,048,467	−6.7	−21.0	−13.0
Total costs	[€]	62,180,575	+70.3	+191.5	+120.4

Table 1: Relative impact of climate scenarios and reference 2018

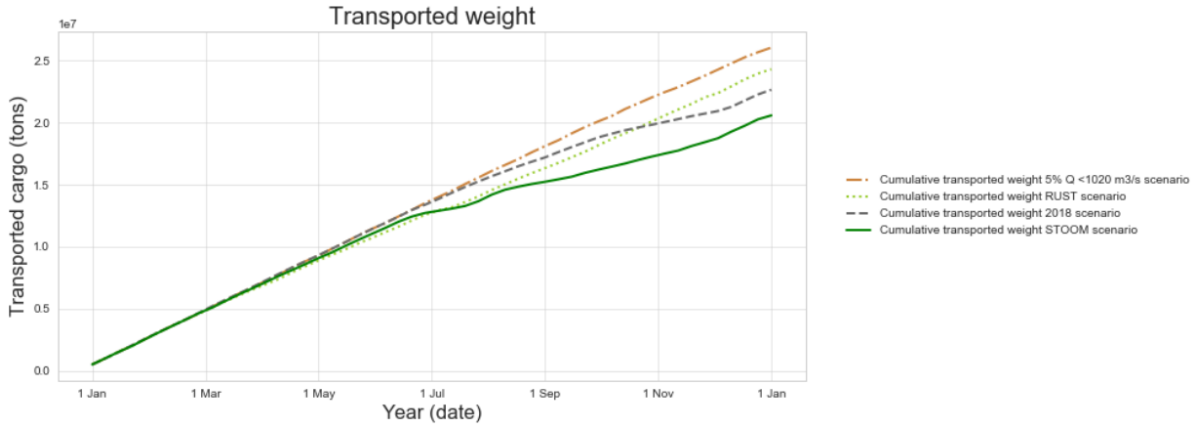

Figure 3: Cumulative transported weight in impact scenarios

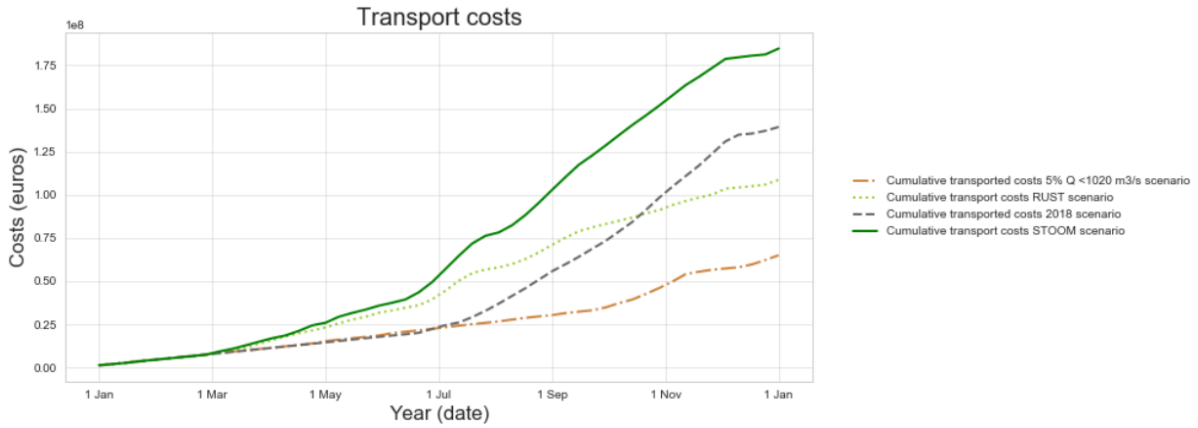

Figure 4: Cumulative transport costs in impact scenarios

When low water depths recover to become sufficient again for unrestricted loading, so does the network capacity required to compensate an arisen transport deficit. Consequently, the water depth profile induces changes in the model output that do not only follow from the critical water depth but also from the frequency of occurrence and consecutiveness of these low water depths. These changes are best seen in the cumulative trends of the transported weight and the transport costs in Figures 3 and 4. These trends show a varying steepness throughout the year, depending on the water depth and the successiveness of low water days.

A high-level application of the IWT model was included for practical purposes. Different adaptation measures have been tested to see the effect of each measure on the key performance indicators of the IWT performance. The improvement per adaptation measure was assessed by a comparison with the original impact scenario, for the RUST-scenario and the STOOM-scenario, respectively. From this comparison, the differences both in transported weight and transport costs have been computed. The reduction of expected costs was translated to its present value in order to evaluate whether the investment in each adaptation measure would be justified. The feasibility of a measure was determined both by the effect of a measure on the transported cargo and by the benefit-cost ratio (BCR) between the potential saving in transport costs and the implementation costs. This has shown the practical application of the IWT performance model in the assessment of the economic feasibility of adaptation measures.

It follows from this thesis that low discharges, in combination with navigational restrictions, could cause substantial losses for the IWT in 2050 in terms of transported cargo and transport costs. The restrictions to navigation posed by authorities were not included in earlier research. This has led to earlier research underestimating the potential damages of periods of low water depths. Due to its proven significance, navigational restrictions should therefore be included in future studies. Following from literature, the accurate modeling of IWT should include various local effects that follow from regulations, fleet composition or waterway characteristics. This research is the first study on the impact of low water depths on the IWT performance that does not take the load factor as the only variable but that includes other network parameters as the active fleet size and the number of trips to provide a comprehensive picture of the IWT performance in periods of low discharge. With this overview, the impact of periods of low discharge on the performance of the IWT can be studied and the effect of changes in the IWT system on different performance indicators can be assessed.

1 Introduction

1.1. Context

Ports play a key role in the globalized economy of the 21st century. Providing import and export possibilities to economies, they facilitate the global trade on which economies thrive. From the fact that around 80% of all cargo worldwide is transported through maritime logistics, it follows that current-day society and global economies immensely rely on the well-functioning of maritime supply chains. Ports are crucial nodes in these chains, making economic development dependent on port performance.

One of the indicators of port performance is intermodal hinterland connectivity (De Langen and Sharypova, 2013). Although being considered essential for the development of ports, reliable hinterland connections are vulnerable to the impacts of climate change (Nugroho, 2016). This vulnerability follows partly from the geographical locations of ports in coastal areas with relatively high susceptibility to sea level rise and storms. Moreover river flooding or drought due to variations in river discharge are expected to impact roads, rail and inland waterways (Stenek et al., 2011).

Inland waterway transport (IWT) is one of the three main modalities for inland transport of dry, liquid and containerized cargo. Already since the Roman empire the Rhine has facilitated trade of goods in North-Western Europe. In 2017, the freight transport in the Netherlands by inland navigation made up 44.7% of the freight transported by road, rail and IWT (Eurostat, 2019). As IWT performs well on cost-competitiveness, environmental friendliness, and congestion-related issues, authorities strive to shift freight transport from road to water, thereby aiming to increase this share of the modal split (Desquesnes et al., 2016, Hendrickx and Breemersch, 2012, Jonkeren et al., 2011, Kallas, 2011). Providing hinterland transport for the ports of Rotterdam and Amsterdam and supplying millions of people, the Rhine therefore is regarded as a vital transport corridor. A map of the Rhine can be seen in Figure 1.1. The colors mark different stretches of the Rhine.

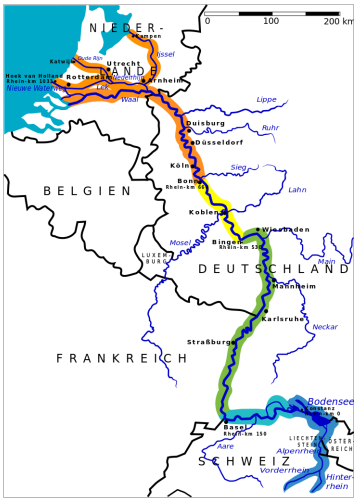

Figure 1.1: Map of the Rhine (Ullrich, 2012)

Following the vulnerability of hinterland connections, climate change is increasingly suggested as the main cause of disruption of inland waterway transport (Levermann, 2014, Van Meijeren et al., 2011). A combination of higher temperatures and more extreme seasonal differences in precipitation are expected to impact the discharge of the Rhine (Sperna Weiland et al., 2015). In summer, this results in low water events happening more often and more intense in parts of North-Western Europe (Van Meijeren et al., 2011). It is understood that low water levels pose a larger threat to inland navigation than high water events because of their usually longer duration (Fischer et al., 2015). In recent years, Dutch container vessels have not experienced situations of restricted load factors following from low water levels (Volker and Volker, 2015). Bulk barges, however, do experience limitations to the load factor as a result of insufficient water depths more often. The draught of the vessels when loaded is larger than for container vessels, making these barges more susceptible to low water levels. For this reason this research focuses on dry bulk transport.

Inland shipping is affected by decreasing water depths in three different ways (Dorsser, 2015):

1. A reduction of the transport capacity
2. A restricted number of barges that a push convoy may transport at once
3. Logistical restrictions to remain sailing as e.g. reduced speed and time windows for sailing

The effects of climate change on IWT, in combination with an expected increase of port downtime, could result in reduced annual transport capacity, thereby weakening the reputation of IWT and increasing the costs of cargo shipment. In the long term, this might lead to a modal shift to road and/or rail, counteracting the efforts made by authorities (Hendrickx and Breemersch, 2012, Kallas, 2011).

Figure 1.2: Drought on the Rhine in 2018 (Hitij, 2018)

In 2018, the Netherlands was struck by 6 months of low discharge causing insufficient water depths on the Rhine branches, see Figure 1.2. This has caused stress on the transport capacity of the IWT network. As a result of the low water depths, some vessels could remain sailing with less cargo while others had to stop operation. There was a general lack of suitable vessels, personnel and transshipment capacity in ports (Van Hussen et al., 2019). As cargo was divided over more vessels, loading and unloading stages in ports were interrupted more often and hence took longer. Moreover, since the maximum number of suitable vessels was deployed, congestion occurred on the river. These effects led to a further delay of transported cargo. Other modalities were only partly able to compensate for the reduced transport capacity. Transport by road was restricted in capacity by material and personnel whereas rail transport could not cope with short-time variations in demand as it too is restricted in capacity (Van Hussen et al., 2019). Figure 1.3 stresses the relevance of this drought by showing the titles of newspaper articles during this period.

Drought has hit Europe's Rhine River and its commerce hard: 'Everyone's hoping for rain'

(a)

Rhine drought leaves Europe's industry high and dry

(b)

Figure 1.3: Newspapers report on the Rhine drought of 2018 (Kirschbaum, 2018, Sheppard and Chazan, 2018)

Water authorities have reserves of fresh water that are distributed among social and economic needs during a drought. In order to prioritize the provision of fresh water among sectors, the Dutch government makes use of a so-called 'verdringingsreeks' (Rijkswaterstaat, 2019b). This verdringingsreeks is shown in Figure 1.4. It denotes a priority ranking of activities and industries. Safety and avoiding irreversible damage to nature is given the highest priority. Navigation, however, is seen to be of the lowest priority. This means that the IWT sector will have to find means to cope with future low discharges as available water could be directed to other causes. This advocates the application of preventive measures and the formation of a plan for low river discharge that is integral with other activities and industries.

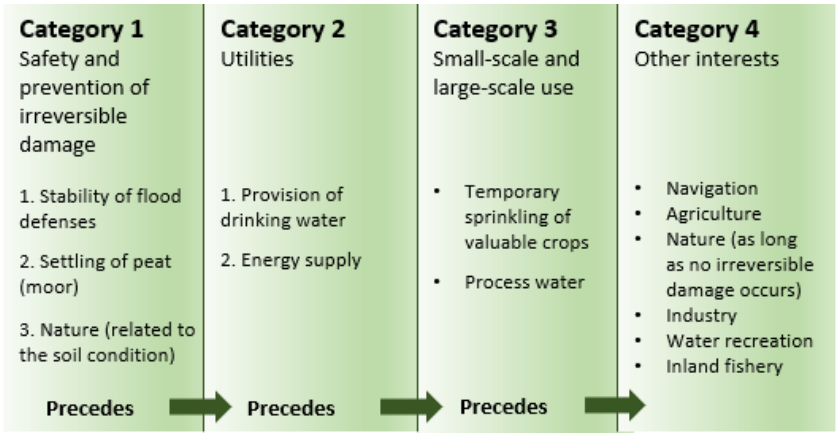

Figure 1.4: Navigation has the lowest priority for fresh water in times of drought (Rijkswaterstaat, 2019b)

The IWT sector currently has a set of possible measures to deploy in order to reduce the impact of a period with low discharge (Van Hussen et al., 2019). These measures are classified as reactive to insufficient water depths and not pro-active or preventive. The possible measures are the following:

- Using alternative routes
- Increase efficiency (e.g. by sailing with coupled barges)
- Different way of exploitation (e.g. day-and-night sailing instead of only during daytime)
- Use of different vessel types (better suited to low water depths)
- Compensating by other modalities as truck or train
- Temporary storage of cargo and use from stockpile
- Adjusting the production to lower demand

During the drought of 2018 a combination of these measures was applied. Since many economic sectors and geographical areas were affected by a decrease of the IWT performance, the effect of each of these measures to reduce damage is deemed difficult to quantify. Moreover, in the light of climate change, low discharges are expected to happen more often. The drought of 2018 therefore marks the beginning of an exploration of structural measures that reduce the impact of future low discharges on the IWT performance.

1.2. Problem statement

The importance of a navigable Rhine to the economy of North-Western Europe is well-known. With climate change affecting the seasonal discharge and therewith the available water depths, the reliability of inland waterway transport is put under serious stress.

Many studies have been performed on the consequences of disruptions in the IWT system (Beuthe et al., 2013, Colin et al., 2016, DiPietro et al., 2014, Hendrickx and Breemersch, 2012, Jonkeren et al., 2008, Koetse and Rietveld, 2009, Millerd, 2007, Nachtmann and Oztanriseven, 2014, Scholten et al., 2011, 2014, Zheng and Kim, 2017). In an economic sense, Jonkeren et al. (2008) finds an average annual welfare loss of €28 million on the river Rhine due to low water levels related to droughts. Moreover, Nachtmann and Oztanriseven (2014) found a potential impact 6 months after a major disruption on the IWT system of Arkansas, US of $450 million and DiPietro et al. (2014) found losses of $ 0.56 – 1.7 billion as a result of a year-long closure of a waterway after infrastructure failure. In literature, these disruptions focus on large-scale events. In addition, only the costs and hindrance of such an event are considered, instead of suggesting preventive measures.

Scholten et al. (2011, 2014) go a step further by including the indirect costs of IWT disruption by connecting climate conditions to a deviation of the optimal storage. In this way, they are able to describe the relation between low water levels and times of decreased production. Moreover, they make a first effort to propose measures. Scholten et al. (2014) studied three potential measures where they rank the potential of a seasonal modal shift above both smaller vessels and increased storage capacity. Although their research provides important insights into the advantages and disadvantages of three possible measures, the linear relations between load factor and transport capacity used do not give the desired level of detail about IWT performance nor do three measures cover the set of possibilities.

Rothstein and Scholten (2017) and Fischer et al. (2015) have performed case studies on disruption impact on the Danube and rivers in Germany but did not draw generic conclusions in terms of important factors or main characteristics. On the contrary, Christodoulou and Demirel (2018) conclude from their study on continental scale that pilot projects should be done in detail in order to find the contributing factors to the impact of climate change on ports and inland waterways (IWW). All authors mentioned take a lower maximum load factor as the only variable without looking at other network parameters such as fleet size and nr. of trips that could improve or worsen the performance of the IWT.

In conclusion, prior research has focused on the performance of the IWT system only being dependent on the maximum load factor that results from the normative water depth instead of the performance being a dynamic play of multiple network parameters. The exact role of each parameter in the play is only slightly covered in literature while this understanding of the system is crucial for policymakers to propose the correct adaptation measures. Moreover, only three measures have been compared in the same study which assists authorities marginally in the correct and pragmatic application of adaptation measures.

The following knowledge gaps have been identified:

- There is little knowledge on the influence of the dynamic behaviour of network parameters on the overall performance of IWT.
- Due to simplified relations between the water level and the transport capacity, the factors contributing to the performance of the IWT network have not yet been modeled in the detail that is required to draw generic conclusions on the behaviour of the network.
- A comprehensive tool to assess the effect of measures is lacking so that only few measures have been considered in present research.

When looking at the unwanted consequences and economic impact that reduced workability in IWT might have, authorities must recognize the relevance of system vulnerability and take up adaptation measures. In order to be able to make a deliberate decision on these measures, it is important to know what damage is expected, what the relevant contributors are and in what sectors adaptation measures will be most effective.

1.3. Research objective

Well-informed adaptation decisions can only be made with a complete picture of the potential damages and effective measures. This research therefore aims to provide more insight into the consequences of climate change-induced drought on the performance of IWT and to assist in making justified adaptation decisions. In the absence of a simulation model that uses the effects of climate change on the reduced performance of the IWT system to come up with effective measures, this research aims to compose a model that studies

the capacity and vulnerability of the inland waterway system to low water levels, and simultaneously can be used to propose the most effective measures to strengthen the position of IWT. Due to the vital role of the Rhine as transport corridor in North-Western Europe and the recent issues with low discharges in 2018 for the German steel manufacturers, this research considers a case study on the iron ore and coal transport between Rotterdam and Duisburg.

This research addresses the following research question:

"What is the impact of climate change-induced low discharges on the network performance of inland waterway transport in the year 2050 and what adaptation measure promises to be most effective in reducing this impact?"

To answer the research question, the study addresses the following sub-questions:

1. **What are the characteristics of the inland waterway transport network between Rotterdam and Duisburg in the year 2050?**
   A literature study on the different elements that contribute to the IWT system of the Rhine will help both set up the IWT network in the model and understand the effects of different network parameters. Moreover, this will provide the hydraulic conditions that should be put on the network in the model.

2. **How can the performance of an inland waterway network, as a result of low discharges, be simulated?**
   In order to study the behaviour of a network, insight in the reactions of individual network components to varying water depths is required. A simulation that meets the functional requirements will provide this insight.

   (a) *What parameters indicate the performance of an IWT network?*

   (b) *Can the performance indicators be reproduced for a reference period of low water depths?*

3. **What is the impact of periods with low discharge on the performance of the IWT network between Rotterdam and Duisburg?**
   A computation of the impact of insufficient water depths on the IWT performance will show the damages that can be expected to result from climate change-induced low discharges. Moreover, this will set a base scenario that can be used in applications.

4. **What adaptation measure to enhance the IWT network performance is most promising in terms of benefits and costs?**
   A first effort in studying effective measures will both show practical applications of this research and aid authorities in the decision-making on adaptation measures.

1.4. Research scope

For the distinct iron ore and coal transport link between Rotterdam and Duisburg, it is considered easy to filter characteristics that can then be used in the simulation model. Iron ore and coal can be stockpiled in order to decrease the impact of drought when compared to e.g. perishable goods. This research does adopt the characteristics of iron ore and coal transport and includes the effect of stockpiling. The part of the supply chain that is treated within this research is denoted 'from stockpile to stockpile' as is shown in Figure 1.5. This includes the (i) loading, (ii) sailing and (iii) unloading stages of the transport, but excludes the various port processes.

The current status of the network, modalities, and cargo volumes are used in this research. Estimating the future situation deals with uncertainty and is not relevant to the research objective. A seasonal modal shift is, however, discussed as a potential adaptation measure.

The river bed of the modeled river reach is assumed to be at a fixed level. As such, elevation of the river bed by sedimentation, an eroding bed, dredging or lowering of the bed due to land subsidence is outside the scope of this research. Moreover, the water levels on the different branches are assumed to be directly dependent on the varying discharge of the Rhine near Lobith. Rainfall run-off within the geographical boundaries of the system is therefore not considered to add significantly to the river discharge. The effect of sea level rise is excluded as the focus of this research is on the upstream river branches where the depth limited sections are. In the impact area of sea level rise, the channels are artificially deepened and are for that reason not

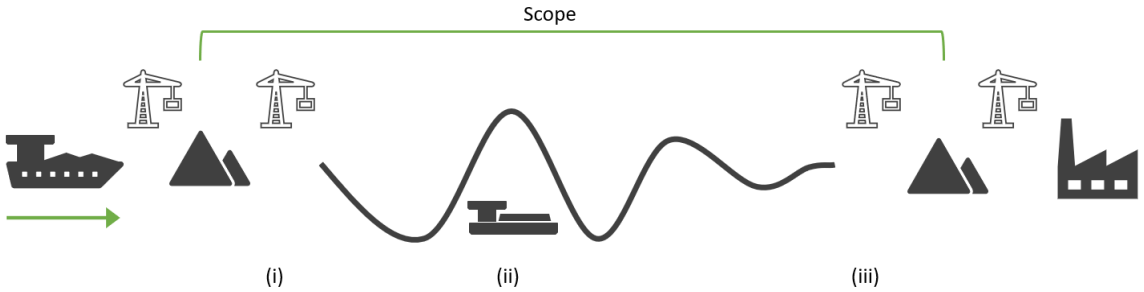

Figure 1.5: 'From stockpile to stockpile' demarcation

susceptible to depth restrictions. Moreover, this study will not consider floods as a result of coastal storm surges or tides, nor river floods.

The scope of the model is further defined in Chapter 3 based on a literature study performed in Chapter 2.

1.5. Research approach

The objective of this research is to study the behaviour and boundaries of the inland waterway system by composing a model that studies the performance and vulnerability in times of low river discharge. In order to provide insight into the impact of drought on the network performance the development of an integrated model is required. This model must be fed with the correct input to achieve reliable results. A literature study is therefore performed at the start of the research. This study serves both to gain a deeper understanding of all elements of the IWT system and as a source for quantitative data. Moreover, the literature study addresses the effects of climate change on the IWT system and evaluates drought projections.

This research contains a combination of two models that contribute to answering the main research question; the Landelijk Sobek Model[1] (LSM) which is a *Sobek*-model of the Dutch Rhine branches and the IWT performance model. A *Sobek*-model is a computational 1D-model, solving the continuity equation and the momentum equation of flow (Overduin, 2018). It is widely used due to its low complexity and high usability. However, in contrast to more sophisticated 2D-models, it does not include the effects of cross-sectional variations in the water level and therefore loses some accuracy. The level of detail including 1D-phenomena, however, is considered sufficient to serve the objective of this research. Moreover, compared to these other models (e.g. Waqua, D-flow FM and Delft3D) *Sobek* proves better on computational effort and thus calculation time required. In addition, the LSM is a validated model thereby saving on time and effort validating. For these reasons, a choice has been made to use this *Sobek*-model. The LSM is able to determine the water depth for all branches of the river Rhine depending on the discharge entering the Netherlands at Lobith. Following several climate projections, the expected changes in this discharge can be computed. These can therefore be used in the *Sobek*-model to compute new projected (navigable) water depths on all Rhine branches.

Secondly, the IWT performance model requires the output of the LSM to create a representative network in a case study. Serving the goal of computing the transport by vessels in a set period, the IWT performance model is set up as a simulation model describing a supply chain. The code language Python accommodates packages that can be used to create and study simulations on complex networks as, for example, supply chains. The 'NetworkX'-package [2] can be used to generate and manipulate networks. With the 'SimPy'-package [3], a simulation can be designed that describes the various steps in a transport process. A combination of these packages in Python therefore serves the purpose of a simulation model well. The fact that individual barges can be modeled easily, that the language is relatively easy to learn and the community setting of the Codelab at the Delft University of Technology, caused the selection of Python as computing language.

Upon validation and calibration of the IWT performance model, a base scenario can be set. Various measures will be tested to show the applicability of the model. The feasibility of these measures will follow from the measure-effectiveness and a cost evaluation, considered for two climate projections. The conclusion of this research addresses the applicability of the developed IWT performance model and provides the most promising adaptation measure to strengthen the position of IWT under low river discharge.

[1] Provided by the Helpdesk Water on 08-05-2019, https://www.helpdeskwater.nl/
[2] NetworkX, https://networkx.github.io/
[3] SimPy, https://simpy.readthedocs.io/en/latest/

1.6. Guide to the reader

1.6.1. Thesis outline

The remainder of this thesis is organized as follows. Chapter 2 considers the current and future state of the Rhine in the light of climate change. This chapter addresses the first sub-question *"What are the characteristics of the inland waterway transport network between Rotterdam and Duisburg in the year 2050?"*. It does so by studying climate change projections, their effect on the river discharge and the dry bulk transport between Rotterdam and Duisburg.

A model is developed in order to simulate and express the performance of the IWT system. Chapter 3 addresses the different elements that contribute to the model development. This chapter addresses the sub-question *How can the performance of an inland waterway network, as a result of low water depths, be simulated?* The selected modeling concept, the elements of the IWT performance model and its structure are discussed in this chapter. Consequently, the model is validated and calibrated in Chapter 4. The model is subjected to several validation tests after which it is calibrated on measured data from reality.

The application of the well-functioning model is shown in Chapter 5 by first setting a base scenario that shows the impact of drought in the year 2050, and then studying the effect of various adaptation measures to reduce this impact. As such, this chapter addresses the sub-question *"What is the impact of periods with low discharge on the performance of the IWT network?"*. The tested adaptation measures are identified in Section 2.4 and are studied in terms of measure effectiveness and costs. These are used to address the final sub-question *"What adaptation measure is considered most promising to enhance the IWT network performance while taking costs into account?"*.

Chapter 6 sets the context in which the model results should be interpreted and discusses the outcomes of this study. Moreover, this chapter draws conclusions in order to address the main research question and it proposes recommendations for further research.

The research framework and thesis outline are visualized in Figure 1.6. The blocks with grey backgrounds denote that modeling is to be done in those parts. The green blocks only require literature research. Moreover, the blue blocks highlight the input or output of the different chapters.

1.6.2. Glossary

Throughout this research, definitions have been used that could also be used in a different context. In order to read this thesis in the correct context of IWT transport, a list of definitions is provided. This list is intended to help the reader to correctly perceive and understand the background of this research.

Climate change
: A change in climate patterns apparent from the 20th century onwards.

Critical river section
: The river section with the Least Available Depth (LAD) that is crossed during transport. The load factor is determined based on the water depth on this location.

Disruption
: A disturbance that limits the transport processes.

Indirect economic impact
: Variation in costs for actors in the supply chain that do not transport themselves and are therefore dependent on sufficient supply of resources and the costs of transport.

Load factor
: The degree to which the vessel capacity can be used for transport. Computed by dividing the allowed capacity by the vessel capacity.

Network performance
: The ability of a supply network to meet the demand while keeping the costs low, given by key performance indicators.

Supply chain
: A sequence of processes from the manufacturer, shipper, seller to the user of a commodity.

Transport capacity
The actual ability to transport cargo. Is given by the product of the load factor, the vessel capacity and the vessel fleet. Can also be computed per vessel or for a whole network.

Transport cycle
The processes of the supply chain that concern transport. In this research includes loading, sailing filled, unloading, sailing empty and possibly waiting.

Hydrological summer
Definition from the field of hydrology, discerning the 6 months from June to November in which generally the least precipitation is expected.

Hydrological winter
Definition from the field of hydrology, discerning the 6 months from December to May in which generally the most precipitation is expected.

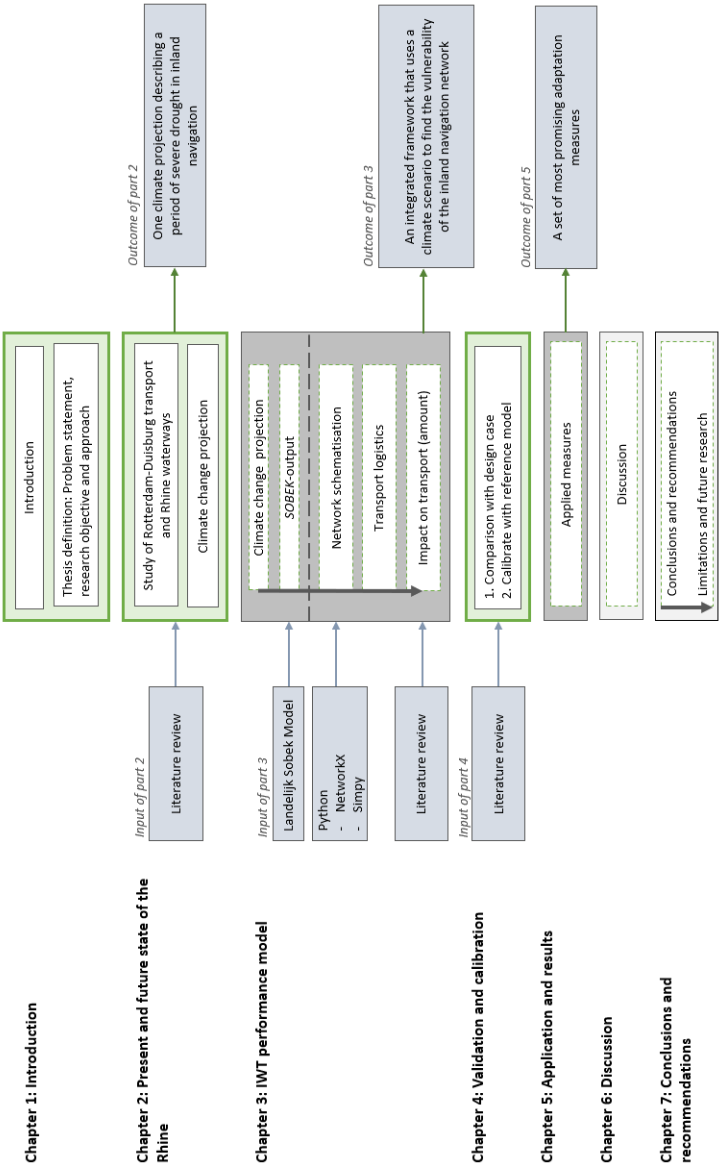

Figure 1.6: Research framework

2

Present and future state of the Rhine

This chapter presents the literature study and contributes to a deeper understanding of all elements of the IWT system. It provides background information and discusses relevant parameters and factors that influence the performance of an IWT network. This chapter addresses the following research question:

What are the characteristics of the inland waterway transport network between Rotterdam and Duisburg in the year 2050?

This chapter can be subdivided into three parts: climate change, waterways, and transport. Section 2.1 discusses the relevant effects of climate change and climate projections and proposes discharge scenarios. In Section 2.2, the infrastructural function of the Rhine branches is discussed. Consequently, in Section 2.3, the present transport situation is studied. This includes the transport demand, the fleet, and other characteristic numbers. Moreover, it describes how vessels determine their load factor. This chapter will conclude with Section 2.5 which presents the answer to the above question.

2.1. Climate change

2.1.1. Relevant climate effects

A wide range of climate effects that could impact processes within IWT is considered. This section will evaluate these effects and will identify the most relevant effects of climate change.

Both in ports and inland navigation, operations will possibly experience visibility issues as a consequence of more frequent intense precipitation (Nugroho, 2016). Yearly hours of fogginess (i.e. in the Netherlands), however, are expected to reduce drastically as a result of decreasing air pollution (Klein Tank et al., 2015). Predictions made for hailstorms deal with large uncertainties (Field et al., 2014) and are for that reason not taken into consideration. The frequency of precipitation events will likely decline and the number of more intense storms will increase (Field et al., 2014). Nevertheless, annual precipitation for the Rhine catchment area is expected to increase on average thereby impacting the seasonal discharge (Sperna Weiland et al., 2015). Moreover, as a result of melting glaciers due to increasing temperatures the snow-fed discharge throughout the year will increase in the short term, e.g. in the Rhine (Hiemstra, 2018). In addition, the Rhine, being a combined rain-fed and snow-fed river, in winter increasingly shifts towards rain-fed as rising temperatures cause snow to melt before reaching the ground (Sperna Weiland et al., 2015). Consequently, there is no ice to melt in summer so that a discharge deficit occurs and seasonality in discharge is enlarged. As this could result in effects on high and low water levels and thereby on the navigability and/or load factors, the variations of river discharge are studied in Section 2.1.2. Near the river mouth, sea level rise (SLR) is expected to heighten inland water levels, possibly reinforced by higher river discharge in winter months. This results in a reduced bridge clearance for vessels. This reduction might lead container vessels to have to sail with a restricted number of containers in order to not exceed a certain height (Hiemstra, 2018). This possible effect is not relevant for this research as dry bulk vessels are not restricted in height but only in draught. With high water levels, inland navigation can be stopped by law as vessels might produce waves that will damage infrastructure. Besides that, the currents that vessels create are stronger in deeper water and might therefore limit the navigability (Rothstein and Scholten, 2017). SLR is not studied in this research as it affects the downstream reaches of a river system whereas the bottlenecks that result from drought are expected upstream. In

contrast to higher water levels, droughts are understood to be events happening more often during summer and more intense in some parts of Europe (Van Meijeren et al., 2011). For inland waterways, it is understood that low water levels pose a larger threat to navigation than high water events because of their usually longer duration (Fischer et al., 2015). The impact of these events on the river discharge in summer will therefore be scrutinized in Section 2.1.2.

Christodoulou and Demirel (2018) stated that higher temperatures and extreme heat have relatively limited impacts on inland waterways compared to the described impacts of climate change. The most relevant effects of climate change have thus been identified. An overview of the considered climate effects is given in Table 2.1.

Cause	Effect	Impact	Relevant	In scope
Intense precipitation	Visibility issues	Limited operational hours	Yes	No
Hailstorms	Visibility issues	Limited operational hours	Yes	No
Temperature rise	Melting of glaciers	High winter discharge	Yes	Yes
Temperature rise	Melting of glaciers	Low summer discharge	Yes	Yes
Sea level rise	Reduced bridge clearance	Restricted container height	No	-
Sea level rise	Damaging waves from vessels	Restricted speed	Yes	No

Table 2.1: Relevance of climate effects for IWT

2.1.2. Climate projections

The Intergovernmental Panel on Climate Change (IPCC) has released a report in 2013 that projects climate change relative to a reference period of 1986 – 2005 based on four scenarios (Representative Concentration Pathways, RCP) (Stocker et al., 2013). These scenarios are named 'RCP2.6', 'RCP4.5', 'RCP6.0' and 'RCP8.5' and are associated with low to high emission cases in the coming decades respectively. These scenarios include different developments in world population, economy, and technology (Klein Tank et al., 2015). The Dutch case is best studied by the Dutch weather authority KNMI. A reference period of 1981 – 2010 is used as input for the KNMI climate models EC-Earth and RACMO$_2$, adding to the analysis of all calculation results from IPCC models. The outcomes of these calculations were grouped in terms of global mean temperature rise and change in air circulation and further categorized into climate scenarios. Four scenarios are proposed that reflect four cornerstones (see Figure 2.1a) between which human-induced climate change is likely to occur (Klein Tank et al., 2015). The scenarios are named G_L, G_H, W_L and W_H where global warming is represented by G (1.0 °C in 2050 and 1.5 °C in 2085) and W (2.0 °C in 2050 and 3.5 °C in 2085) and the change in circulation patterns by L (relatively dry winters and wet summers) and H (relatively humid winters and drier summers). These four KNMI'14 scenarios do not correspond directly to the four scenarios as proposed by the IPCC. Instead, the G_L and G_H match the lower end of the RCP4.5 and RCP6.0 scenarios and W_L and W_H match the upper end of RCP8.5, the high emission scenario, both in 2050 and 2085, see Figure 2.1b. After publication of these scenarios, it was realized that the decrease in precipitation during the hydrological summer may have been underestimated. An additional climate scenario, $W_{H,dry}$, was thus added which distinguishes by a stronger reduction of summer precipitation (Lenderink and Beersma, 2015). Moreover, the Deltaprogram run by the Dutch government proposes four different climate scenarios: 'DRUK', 'STOOM', 'RUST' and 'WARM' (Wolters et al., 2018). These scenarios are based on the most extreme KNMI'14 scenarios G_L and W_H but are extended with socio-economic projections. DRUK and STOOM are in that sense coupled with socio-economic growth whereas RUST and WARM describe situations of socio-economic stagnation. Furthermore, DRUK and RUST correspond with G_L and STOOM and WARM are linked to W_H. An overview is shown in Table 2.2.

Scenario	Socio-economic growth	KNMI scenario
DRUK	+	G_L
RUST	-	G_L
STOOM	+	W_H
WARM	-	W_H

Table 2.2: Deltaprogram climate scenarios

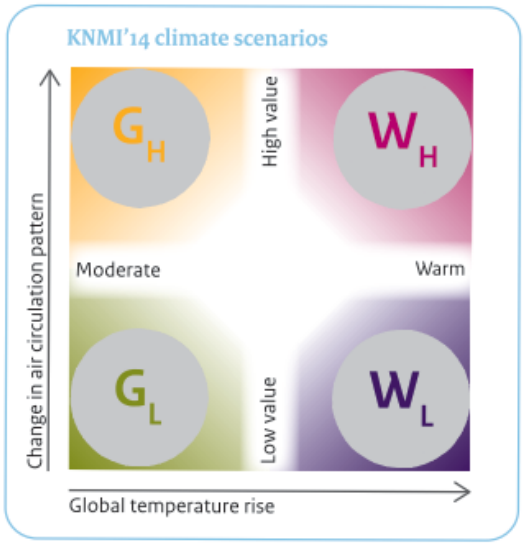

(a) KNMI'14 climate scenarios

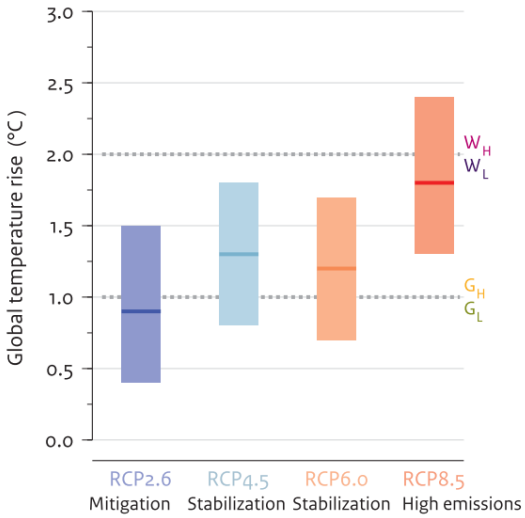

(b) IPCC and KNMI scenarios compared

Figure 2.1: KNMI'14 projections (Klein Tank et al., 2015)

Winter discharge

On a global scale, it was found that river discharges will generally increase at high latitudes during the wet season (Pachauri et al., 2007). This is in line with the results of Kienzle et al. (2012)[p. 85] who projected "significantly higher streamflow between October and June" for western Canada. This seasonality is also included by Fischer et al. (2015) who have studied the impact of climate change on the German parts of Rhine, Elbe and Danube river basins. An increase is shown in the mean discharge of the Rhine basin in the hydrological winter on both the short-term (up to 20% in 2050) and the long-term (up to 30% in 2085), corresponding to a discernible increasing trend in precipitation. Moreover, the high water levels, that are associated with these increased river discharges, show a significant growth in exceedance days (Fischer et al., 2015).

Consequently, when considering the Rhine on a national level, the KNMI'14 scenarios are studied. Research has been carried out by Sperna Weiland et al. (2015), studying the implications of the KNMI'14 climate scenarios for the mean discharge of the Rhine. These changing discharges were computed by first down-scaling climate scenarios to the sub-catchment areas of hydrological rainfall - runoff models. Their projections show that winter discharges will increase considerably for all 5 scenarios relative to the reference discharge of 2,585 m^3/s (Sperna Weiland et al., 2015).

Summer discharge

The annual mean discharges hardly show significant changes. Having seen the increase in winter discharges throughout Europe, it can be concluded that summer discharges will decrease. On a global scale, this is seen in Canada where a lower streamflow in the Cline River from July to September is projected (Kienzle et al., 2012). The same change is projected in Europe in the short-term for the Danube where a general tendency towards lower discharges can be discerned for the hydrological summer of up to 20% (Fischer et al., 2015). As summer precipitation shows a declining trend, this tendency is projected to continue towards the end of the century (up to 35% in 2085). The mean discharge of the German Rhine basin does not show a significant change in the short-term during the summer but the decreasing summer precipitation and increasing temperature could on the long-term decrease baseflows and mean discharge up to 25% in 2085 (Fischer et al., 2015).

Considering the Dutch case, all climate scenarios of the KNMI project growth of the precipitation deficit in the summer (Klein Tank et al., 2015). Consequently, less water will flow through the Rhine and hence the mean discharges in the hydrological summer will be lower. For the Dutch Rhine, projections of mean summer discharges predominantly show decreases in both the short-term and the long-term (Sperna Weiland et al., 2015). Only the G_L-scenario both in the near future (2050) and in the distant future (2085) shows projections of slight increases.

Case projections
The Deltaprogram logically uses their four projections when performing research. As such, all research carried out in the spirit of this program therefore incorporates the G_L or W_H climate projection. Two scenarios are used in this research; The RUST-scenario, representing socio-economic stagnation and a moderate climate change, and the STOOM-scenario, representing socio-economic growth and a rapid climate change. These scenarios are scrutinized to see the dependence of the results of this study on the input river discharge that follows from these climate scenarios. Although the KNMI proposes a dry $W_{H,dry}$-scenario that describes the most extreme cases of drought, there has been chosen to continue with STOOM, the W_H-scenario, for the sake of comparability to prior research. Moreover, this scenario is more complete as a socio-economic projection for 2050 is included. It is expected that this will help interpret the results of the study in the correct context and as such gives more weight to the expected implications.

To make a projection of the Rhine discharge in a dry year, historic data is extrapolated to 2050 under both scenarios. Within the Deltaprogram the daily discharge for every year in the past century was extrapolated to a daily discharge in 2050 for every scenario. As this research aims to study the impact of drought, a representative, dry year should be filtered from the data-set. The historic year 1976 was recorded to be a dry year with a return period of $T = 10\ years$ (Mens et al., 2018). The choice has therefore been made to make use of extrapolated daily discharges of the year 1976, thereby maintaining the return period. This way, a time-series consisting of daily discharges at Lobith is created that represents the discharge in the year 2050 with a return period of $T = 10\ years$.

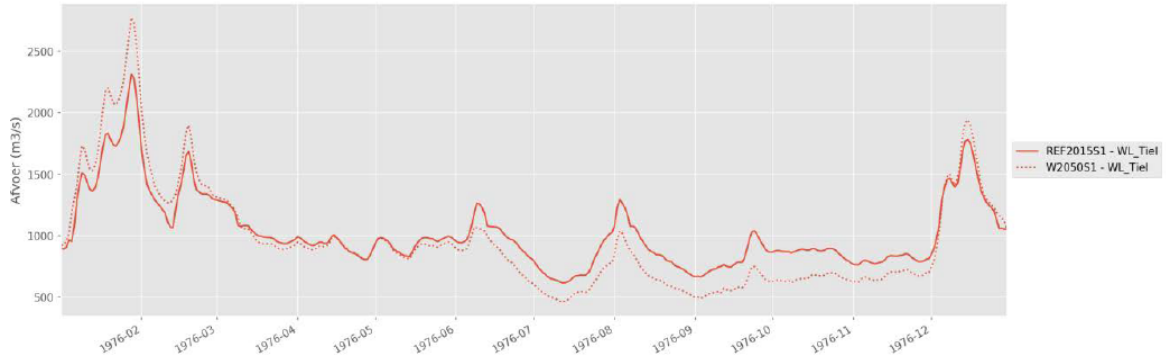

Figure 2.2: Transformation of year 1976 with T = 10 by STOOM scenario to 2050 (Mens et al., 2018)

2.2. Waterway analysis

2.2.1. The Rhine

Besides a large river in Western Europe stretching 1320 km, measured in Rhine kilometers (rkm), the Rhine is one of the most important transport corridors in this area. It is categorized as a snowmelt-fed mountain river since it springs in the Swiss Alps, but it flows out in the North Sea as a combined rain- and snowmelt-fed river. As such, it travels through six European countries, providing IWT between the port of Rotterdam and the European hinterland. The Rhine in the Netherlands can be subdivided into six branches: Upper-Rhine (Bovenrijn), Waal, Pannerdensch Kanaal, IJssel, Lower-Rhine (Nederrijn) and Lek. Directly after crossing the Dutch-German border at Lobith, the Upper-Rhine splits at the Pannerdensche Kop in the Waal and the Pannerdensch Kanaal which in its turn bifurcates again at the IJsselkop into the Lower-Rhine and the IJssel. Upon crossing the Amsterdam-Rijnkanaal the Lower-Rhine becomes the Lek. In a regular year, the average discharge of the Rhine at Lobith is 2600 m^3/s of which approximately two-thirds are directed to the Waal. The Upper-Rhine has a discharge distribution of 2/3 (Waal), 1/3 (Pannerdensch Kanaal) that again is subdivided in 1/9 (IJssel), 2/9 (Lower-Rhine/Lek) of the total discharge (Havinga, 2016). In times of drought, however, most of the water is directed towards the Waal in order to continue navigation operations.

Usually, IWT makes use of the Waal and Upper-Rhine on its route to Duisburg. Nevertheless, transport via the Lek, Lower-Rhine and Pannerdensch Kanaal is possible as it is seen as back-up of the Waal in the case of a calamity that blocks Waal-transport (Volker and Volker, 2015).

The Lek and Lower-Rhine
The Lek and Lower-Rhine is a discharge-regulated river by three weirs. These weirs are located at Driel (rkm

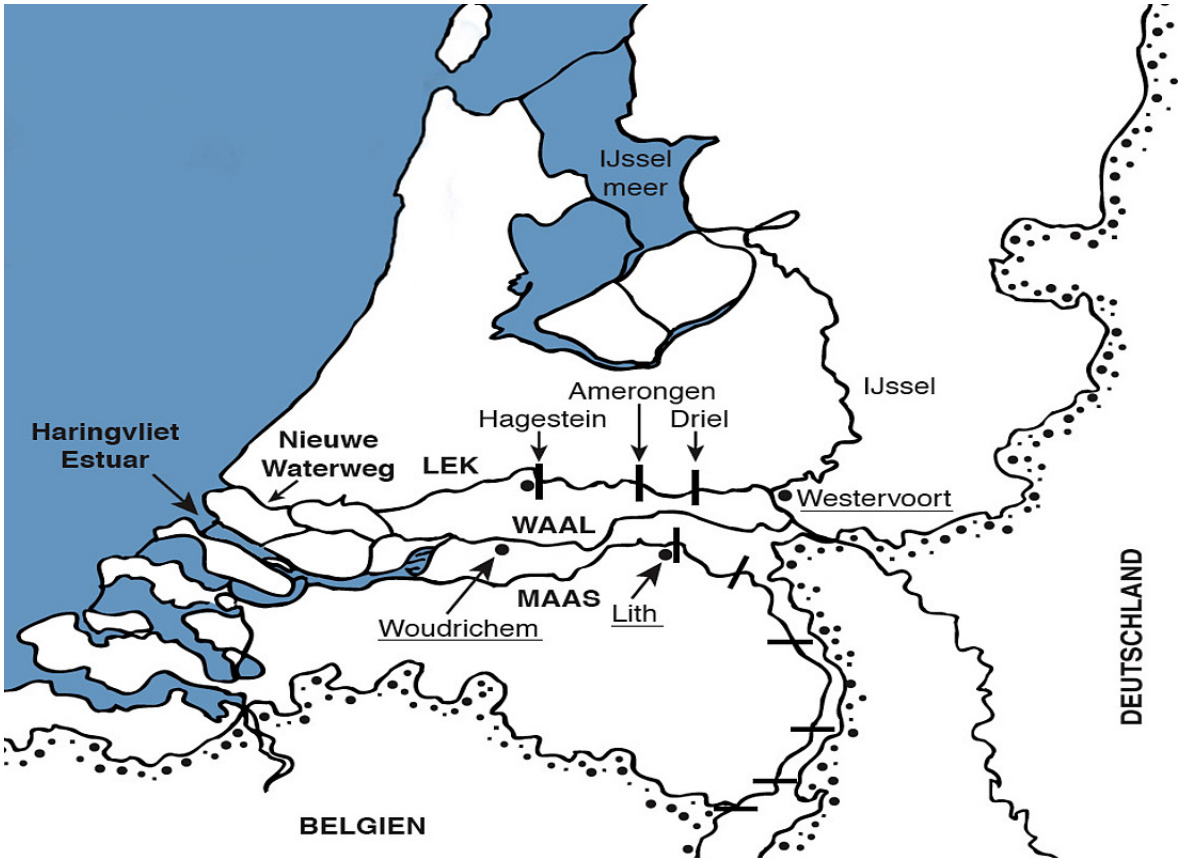

Figure 2.3: The Rhine branches and the Meuse in the Netherlands (ICBR)

891.5), Amerongen (rkm 922.3) and Hagenstein (rkm 946.9), as indicated in Figure 2.3. At low flow conditions, the weirs allow for a minimum discharge of 25 m^3/s thereby directing most water towards the IJssel and the Waal. This causes the Lower-Rhine to be the first stretch where water levels become too low for continuation of IWT in periods of low discharge. Besides the delay that results from passing the weirs, this is the reason that captains opt for a different route. Under regular flow conditions, the Least Available Depth (LAD) on the Lek and Lower-Rhine is found upstream of the port of Arnhem, between the Driel weir and IJsselkop. The sandbar that causes this LAD limits the loading depth of vessels by 70 cm (Volker and Volker, 2015).

The Waal
The Waal is the most important transport corridor in the Netherlands in terms of economic interest. Yearly more than 100,000 vessels travel the Waal to transport 130 $mln\ tonnes$ of cargo. To accommodate navigation on the Rhine in periods of low water levels, policymakers have agreed on certain requirements concerning the navigable depth and width under low flow conditions. The Waal (and Upper-Rhine) has a depth requirement of 2.80 m and a width requirement of 150 m corresponding to a discharge at Lobith of 1020 m^3/s and consequently a discharge of 820 m^3/s in the Waal. Before, the critical point on this part of the Rhine was located in Germany but due to erosion around the hard layer in the bend at Nijmegen, this point has shifted to the Netherlands (Schulz, 2018). Rijkswaterstaat, the Dutch water authority, has stated that the location normative for loading is susceptible to change; Beuningen, St. Andries and Erlecom also show extremely low water levels in periods of drought (Volker and Volker, 2015).

2.2.2. Future plans and measures
International agreements following from the Central Commission for the Navigation of the Rhine (CCR) state a guaranteed water depth in case a so-called Agreed Low Water Level (ALW) is reached. This ALW is a level that is not undercut more than 5% of the year on average (Dorsser, 2015). As a result of climate change more extreme discharges might enter the Dutch Rhine system in the future. This will bring a different ALW for different climate projections. For projections of a dry climate as is described in Section 2.1, the ALW is

expected to decrease significantly which will potentially impact the load factor. Presently, Rijkswaterstaat maintains the depth of the Rhine branches solely with dredging (Havinga, 2016). In the past, hard substrate layers have been constructed in the bends of Nijmegen and St. Andries in order to enhance inland navigation by widening of the river. As measurements during the drought of 2018 have shown that the actual water depth fell short, efforts are currently made to solve the issues (CBRB, 2019, Schulz, 2018). With the critical point for loading under low discharges expected to vary between several locations, adaptation measures concerning multiple river sections could become necessary in the near future.

The back-up route via the Lek and Lower-Rhine is deemed inadequate as the capacity of the weirs is considered insufficient by both captains and shippers (Volker and Volker, 2015). Due to the intensive use of the Waal, a calamity is seen as a realistic threat leaving no alternatives as the cargo volumes exceed the capacity of both rail and road transport.

2.3. Transport analysis

2.3.1. Port of Rotterdam

The throughput of the Port of Rotterdam in 2017 equaled 467 mln tonnes, divided into dry bulk (80 mln tonnes), liquid bulk (214 mln tonnes), container transport (142 mln tonnes) and breakbulk (30 mln tonnes) (Port of Rotterdam, 2018). In 2017, the Port of Rotterdam has handled 158 mln tonnes of cargo from IWT. With 112 mln tonnes leaving the port by inland vessel and 46 mln tonnes being exported, Rotterdam has the highest share of outgoing transport by IWT of all European seaports (CCR, 2018).

Focusing on dry bulk, 17 terminals contribute to Rotterdam's position as the largest dry bulk port in Europe. More specific, iron ores are handled at 2 terminals, being Europees Massagoed Overslag (EMO) and Ertsoverslag Europoort C.V. (EECV), and coals at 7 terminals, again including EMO and EECV. Whereas EMO provides transport for customers throughout Europe, EECV only provides iron ores and coal for the German steel industry, as the terminal is owned by steel concerns ThyssenKrupp Stahl and Hüttenwerke Krupp Mannesmann (Port of Rotterdam, a,b). The locations of the Port of Rotterdam and the port of Duisburg are shown in Figure 2.4.

Figure 2.4: Route between Rotterdam and Duisburg, retrieved from Google Maps

Being Europe's largest port for container and both liquid and dry bulk, the Port of Rotterdam makes efforts to maintain and strengthen the position of 'Global Hub', as is expressed in Port Vision 2030 (Port of Rotterdam, 2011). Following this ambition "Rotterdam will form an integrated network with its hinterland and it will be a frontrunner in creating and maintaining sustainable and efficient chains" (Port of Rotterdam, 2011, p. 30). As such, Port of Rotterdam believes that a substantial improvement in the quality of rail and IWT is crucial for realizing a modal shift from road towards less emitting modalities. Following the ambition to expand the share of rail and IWT, the numbers regarding IWT are likely to increase in the future.

2.3.2. Transport Rotterdam - Duisburg

It is stated in the 2018 annual report of the CCR that IWT dominates in transporting dry bulk with a share of 86% (CCR, 2018). In 2017, 31.2 mln tonnes of iron ore and scrap were transported to Rotterdam of which 29.3 mln tonnes imported and just 1.9 mln tonnes being exported. More or less the same can be said about coal transport where 25.8 mln tonnes of coal were transported in 2017 with 25.2 mln tonnes imported and

only 0.5 mln tonnes being exported (Port of Rotterdam, 2018). Together these segments make up the larger share of handled dry bulk in the port area. The numbers are presented in Table 2.3 at the end of this section.

Being one of two main iron ore terminals in the port area, EECV discharges on average 24 mln tonnes of iron ore for her German clients yearly. Moreover, it handles coal at a capacity of 8 mln tonnes per year (Ertsoverslagbedrijf Europoort CV, 2018). The steel industry in the port of Duisburg, Duisport, together handled 36.5 mln tonnes of cargo transported by IWT in 2017 (CCR, 2018). Comparing these amounts, it can be said that the EECV terminal provides most of the iron ore and coal resources for the Duisburg steel industry. The sum of the iron ore transport (24 mln tonnes) and coal transport (8 mln tonnes) is thus taken as the yearly transport that leaves EECV for Duisburg.

2.3.3. Fleet Rotterdam - Duisburg

As Dorsser (2015)[p. 263] writes, "impact studies often apply a certain fleet mix to take the effects on the various barge types properly into account but this approach requires detailed insight in the very long term development of the fleet mix up to the year 2100, which cannot be obtained at such a very long time horizon". Although the horizon in this research concerns the year 2050, the same conclusion regarding the fleet mix is applied. A representative fleet is therefore sought and used in further steps. It follows that the IWT of iron ore and coal to the hinterland happens predominantly with 6-barge push convoys (Port of Rotterdam, 2016). These convoys can transport up to 16,000 tons of dry bulk at a time (Port of Rotterdam, b). On average this means that each barge can transport approximately 2,700 tons per trip. To translate this maximum capacity to barge dimensions, obtained letters with measurements (in Dutch: meetbrieven) are used. These letters represent real barges used for operations and do therefore represent reality accurately. The measuring letters of three barges that all have maximum capacities around 2,700 tons bring draughts when loaded of 3.50 m, 3.95 m and 4.02 m. Following C. Van Dorsser's method to select a vessel size, the middle one of these barges is selected as the representative barge (Dorsser, 2015). This barge has an empty draught equal to 0.65 m. From the obtained letter with measurements of the representative barge, a more or less linear relationship between the load factor and the draught can be found.

During the drought of 2018, a different fleet mix was used for dry bulk transport [1]. Due to safety policy, the 6-barge push convoys were taken out of operation when the transport capacity dropped below 55%, corresponding to a minimum water depth of approximately 3.00 m. As the width of waterways decreases much more than the water depth, the wide and/or long 6-barge push convoys can no longer sail through river bends safely. These push convoys were then restricted to sail with 4, 2 or 1 barge(s), respectively. At a transport capacity of 35%, corresponding to a minimum water depth of 2.25 m, these too had to stop operations. All dry bulk transport was then shifted to Rhine vessels and coupled barges that continued sailing. These vessel classes, however, appear to have been available in too small numbers to maintain the transport capacity and therewith the network performance. When the water levels recovered, the active fleet of Rhine vessels and coupled barges rapidly decreased and 6-barge push convoys became active again. The vessel types are depicted in Figure 2.5. The characteristics of Rhine vessels follow from the guidelines for design of waterways (Koedijk et al., 2017). The capacity, draught and fleet size of each vessel type can be seen in Table 2.3 at the end of this section.

[1] Open website of Rijkswaterstaat accessed on 25-09-2019; https://bivas.chartasoftware.com/Scenarios

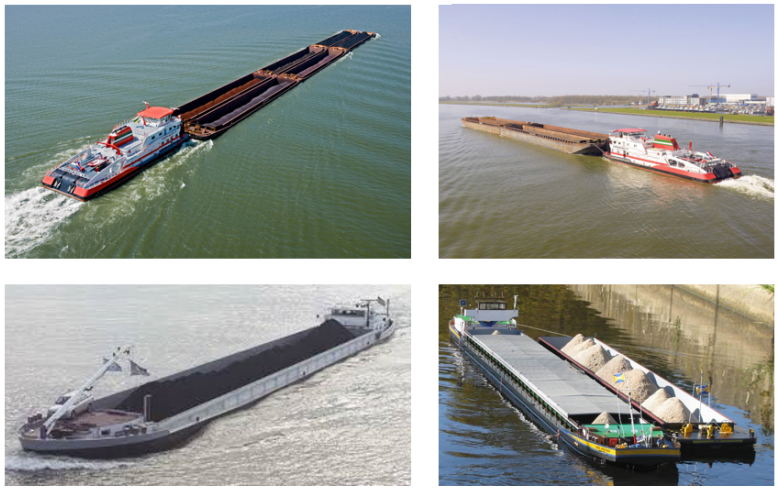

Figure 2.5: The 4 vessel types used for dry bulk transport on the Rhine: 6-barge push convoy (top left), smaller push convoy (top right), Rhine vessel (bottom left) and coupled barge combination (bottom right) (Jonkman, Kock, 2017, Quist and Verheij, 2010)

Data concerning the fleet size had to be provided by EECV or ThyssenKrupp Veerhaven, the fleet operator, but due to sensitivity of the data, no cooperation was found. Due to the importance of a number to the fleet size, an estimation is therefore made, based on Figure 2.7 that shows the observed trips per week from Europoort to Duisburg in 2018. The push convoys (both the 6-barge and the 4-/2-/1-barge) appear nearly constant as not more than 40 trips are undertaken weekly. With a trip cycle of almost 1.75 days, the fleet size of pusher boats is estimated on 10. The limits of operation described earlier were seen to be surpassed by the critical water depths in 2018, see Figure 2.6. While more barges become available after the 6-barge push convoys stop operation, the number of trips undertaken by push-barge convoys does not change significantly. It can thus be concluded that the fleet size of the pusher boats poses the limit to push-barge transport. In addition, the Rhine vessels show a maximum of approximately 60 trips per week. From the same calculation, a fleet size of 15 Rhine vessels follows. The trips of coupled barges peak when other barge transport stops. It is unclear whether vessels sail with one or two barges coupled. The capacity per vessel sailing with coupled barges will be checked in Section 4.2. For now, 20 coupled barge combinations are assumed, following from Figure 2.7 and a cycle time of 1.75 days. This is adopted as the fleet size. The design characteristics of the fleet are given in Table 2.3. It can be concluded, when comparing Figures 2.6 and 2.7, that a low critical water depth increases the number of trips by a factor 3, mainly due to the Rhine vessels and coupled barges that become active.

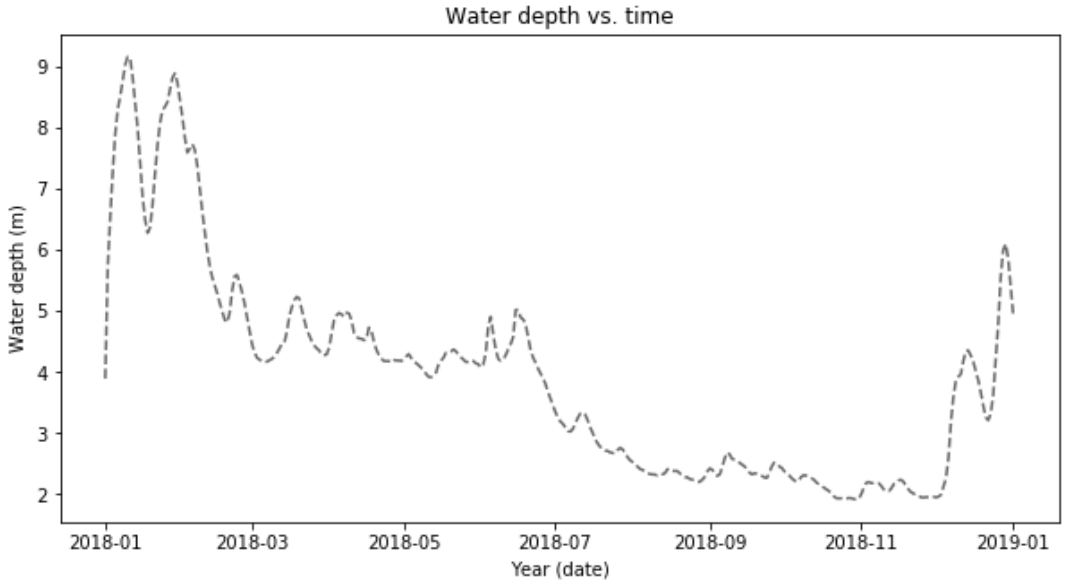

Figure 2.6: The critical water depth at Millingerwaard in 2018, computed with data from Rijkswaterstaat Waterinfo

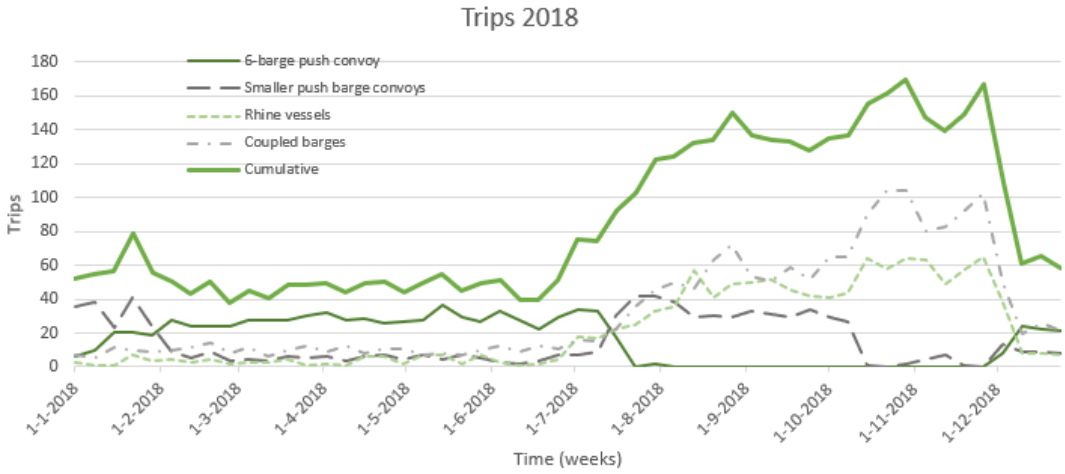

Figure 2.7: The observed weekly nr. of trips of different vessel classes in 2018 (Rijkswaterstaat, 2019a)

2.3.4. Navigability

In times of low river discharge, the water depths on several sections of the transport route become insufficient for unrestricted navigation. One of these sections is normative and restricts the maximum draught and load factor of inland barges. In the past, this crucial section of the Rhine for transport to Cologne was located in Germany but it appears that the water depth in the Waal has decreased so much that the critical section is now found in the Netherlands (Dorsser, 2015, Schulz, 2018). For the Waal, the guaranteed depth under low discharge conditions is equal to 2.80 m. Moreover, a minimum navigable river width has been agreed upon. For the Waal, this is equal to 150 m (Schulz, 2018). Measurements during the drought of 2018, however, showed that the guaranteed depth fell 40 to 60 cm short in some locations along the Waal (Schulz, 2018). To get to a loading factor, shippers use the following equations 2.1 and 2.2:

$$Actual\ water\ depth\ (m) = Gauge\ value\ Lobith\ (m) + Guaranteed\ water\ depth\ (m) - ALW\ (m) \quad (2.1)$$

$$Loading\ depth\ (m) = Actual\ water\ depth\ (m) - Safety\ margin\ (m) \quad (2.2)$$

The loading depth is dependent on the required safety margin beside the available water depth. The safety margin consists of the under keel clearance and a margin for the effect of 'squat'. The under keel clearance

varies depending on the type of cargo shipped (smaller margins for bulk than for transport of chemicals), the type of river bottom (larger margins applied for rock bottoms than for sand) and the trim angle of the barge (Dorsser, 2015). The applied under keel clearance to avoid running aground falls between 0.20 and 0.40 m in general (Dorsser, 2015). For the insensitivity of the goods but for the presence of a rock protection layer (at the bend of Nijmegen, see Section 2.2) there has been chosen to apply an under keel clearance of 0.25 m. Sailing vessels in shallow water create an area of reduced pressure around the vessel. This reduced pressure 'pulls' the ship down so that the hull comes even closer to the bed. This effect is called 'squat'. For vessels sailing in constricted waterways, as is the case for IWT, squat is in the order of 0.50 m (Van der Walle, 2006). Squat is added to the under keel clearance to define the required safety margin.

	Unit	**Value**
Dry bulk transport	[tons/year]	32 mln
Barge capacity	[tons]	2,700
Rhine vessel capacity	[tons]	2,000
Barge draught empty	[m]	0.65
Barge draught full	[m]	3.95
Rhine vessel draught empty	[m]	1.20
Rhine vessel draught full	[m]	3.0
Safety margin	[m]	0.75
Fleet size	[pusher boats]	10
Fleet size	[Rhine vessels]	15
Fleet size	[coupled barges]	20

Table 2.3: Characteristics of Rotterdam-Duisburg transport

2.4. Adaptation measures

This section concerns the possible adaptation measures that can help make the IWT system more resilient to climate change-induced droughts. The studied adaptation measures follow from literature. Of these options, the most promising measures in terms of effectiveness on the network performance will be identified. This first analysis does consider ease of implementation in the rigid considered IWT market. It does not yet consider a cost estimation although this is closely related to implementation. Costs will be weighed against the effectiveness of the most promising measures, which will be tested in Chapter 5.

2.4.1. Potential measures

Following severe drought events in 2003 and 2006 in North-Western Europe, many adaptation measures have been proposed for the Rhine (Scholten et al., 2011). These adaptation measures can be categorized as follows:

- **Logistic measures**; concern the traffic situation, sailing windows and the use of multiple modalities
- **Equipment measures**; relate to the vessels used for IWT
- **Infrastructural measures**; concern engineering adaptations to the waterway
- **Site measures**; include measures at the origin and destination site

Several potential adaptation measures are listed below. These have been suggested in literature and are scrutinized in this research. Three measures are titled most promising to be used further in this research.

Logistic measure: Seasonal modal shift

Due to the seasonality in river discharge, and consequently droughts occurring in autumn, an adaptation measure ideally can be deployed seasonally. Such a measure is a seasonal modal shift as proposed by Scholten et al. (2014). If the transport share of inland navigation is lowered in the dry season by shifting transport to other modalities such as road and rail, the network will potentially be less impacted by drought. On the long-term, a seasonal reduction of inland navigation of 20% is projected to bring the days of reduced storage down to 1% for a steel manufacturer along the Rhine (Scholten et al., 2014). Though promising, this reduction of transport via inland navigation requires a growth in transport by truck or train. Set aside the fact that dry bulk transport by truck is not common, transport by road might bring congestion issues, high

emissions and therewith costs related to delay and greenhouse gases. Moreover, this shift counters the policy of shifting road transport to other modalities. Rail transport is still seen to struggle and requires cooperative actors to overcome technical and political obstacles (Kallas, 2011). Nonetheless, European funded projects are advocating rail transport industrialization and the entrance of new technologies into the rail economy (Castagnetti, 2012). Despite these efforts, in recent years the rail freight has not attracted new market share and it is doubtful whether a seasonal modal shift will be enough to attract investments and political efforts.

Equipment measure: Additional pusher boats
Increasing the number of convoys that can be deployed increases the capacity of the network. An increase of the pusher boat fleet on the Lower Rhine of 33% is seen as realistic (Scholten et al., 2011). The issues with low water depths, however, occur due to the draught of the barges. Additional pusher boats will therefore increase the capacity of the network both before and after drought, but will have no effect during a period of low discharges.

The construction of new pusher boats brings considerable costs. Many vessels in IWT are privately owned. As such, a new vessel requires a relatively high investment. Without suitable push barges, the pusher boats become idle in the dry season and hence do not generate revenue. First, smaller barges are required for additional pusher boats to have an effect during the dry season. The threshold for investing in additional pusher boats therewith is expected to become too high.

Equipment measure: Smaller (and lighter) barges
This adaptation measure considers the deployment of smaller and thus lighter barges. These barges have a lower capacity and are only used in dry periods. Due to their lower capacity, the barges have a draught when loaded that is lower than the original barges. They are therefore less restricted by the water level and will be able to sail with a higher load factor in times of low discharge. A further reduction in barge size however is limited to the technical and economic feasibility (Scholten et al., 2014). The relative effect that this measure will have is to remain sailing when conventional push-barge convoys cannot operate anymore. Introducing this measure, the pusher boats still limit the number of convoys present in the network but they can now remain sailing instead of becoming inactive during extremely low water levels. Transport can thus continue, be it at a lower scale. The barges will have to be built which brings costs. In addition, the construction of pusher boats could add to the feasibility of this measure. This also brings costs. These costs will be scrutinized in a later stage of this research.

Infrastructural measure: River training
Currently, the water depth on the Rhine is maintained by dredging. The locations with the lowest water levels could be deepened by river engineering measures. In the summer of 2019, the decision was made to start solving the problems occurring in the bend of Nijmegen (CBRB, 2019). It is expected that the lowest point will then shift to one of the other locations found in Section 2.2.1. Other river engineering measures could thus become necessary in the future. These could involve the introduction of e.g. hydraulic works to guarantee sufficient water depth or a sediment nourishment to reduce the bed subsidence. Some options are shown in Figures 2.8a and 2.8b. River engineering measures are expected to be costly and rigorous but do affect water depths positively on the long-term. Moreover, the effect of solving one bottleneck on the network performance relative to solving several is unknown. For that reason, an optimum could be found between estimated costs and impact. Following, river engineering measures will be studied in Section 5.

Site measure: Increase storage in destination
The transport to Duisburg aims for a just-in-time (JIT) delivery (Burgers, 2005, Ertsoverslagbedrijf Europoort CV, 2018). This contributes to the vulnerability of the supply chain. As JIT means no buffer stocks and minimal units on transport, a disruption in the supply chain for several days could make production facilities more vulnerable to a shutdown (Henriet et al., 2012). Increased storage in the destination results in higher resilience of the IWT network. This measure, however, introduces several difficulties. Increasing of the storage does not account for seasonality. In wet periods, the size of the storage does therefore exceed the required capacity. Whether this underutilized storage affects the potential of the adaptation measure depends on the costs of the storage capacity (Scholten et al., 2014). Finding space to store resources, possibly by constructing additional storage buildings, comes at a cost that is site- and company-specific. Iron ore and coal are stockpiled in the open air, thereby only requiring open space. The costs for increased stockpile capacity are therefore expected to be limited. This adds to the feasibility of this adaptation measure.

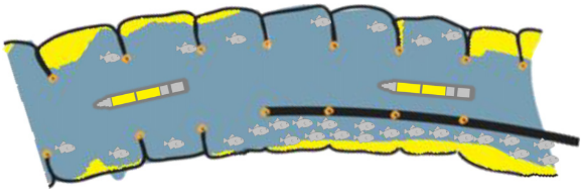

(a) Longitudinal dams as river training works (Collas et al., 2018)

(b) Sediment nourishment to reduce bed subsidence (Van der Mark, 2019)

Figure 2.8: Examples of potential river training works

Site measure: Relocation of industries
Relocation of companies could help in making them less susceptible to low water levels. They can move to locations with better connections to other transport modes or they can move along the river to a location before the bottleneck so that transport will be less affected. It follows from a survey that more than half of the interviewed companies does not consider relocation as a feasible option, mostly due to the investment and their immobility (Scholten et al., 2011). The German steel manufacturers are considered to be immobile due to their large factories and owned terminals. The measure of relocation is therefore assumed to have low potential.

2.4.2. Promising measures

The adaptation measures that have been identified to be the most promising in terms of ease of implementation and estimated economic feasibility are the following:

1. Smaller (and lighter) barges
2. River training
3. Increase storage in destination

They involve equipment, infrastructural and site measures. These adaptation measures will be represented schematically in the model. Smaller and lighter barges can be modeled by adjusting the barge characteristics, river engineering measures are represented by adjusting the water depths, and increased storage is posed to the model manually. Moreover, their effectiveness in relation to the implementation costs is considered in Chapter 5.

2.5. Conclusion

This chapter has studied various elements of the IWT network between Rotterdam and Duisburg. By doing so, this chapter has addressed the following research question:

What are the characteristics of the inland waterway transport network between Rotterdam and Duisburg in the year 2050?

The literature study on projections of climate change showed that the annual precipitation for the Rhine catchment area is expected to increase on average thereby impacting the seasonal discharge. In addition, the Rhine, being a combined rain-fed and snow-fed river, in winter increasingly shifts towards rain-fed as rising temperatures cause snow to melt before reaching the ground. Consequently, there is no ice to melt in summer so that a discharge deficit occurs and seasonality in discharge is enlarged. The choice has been made to make use of daily discharges from the year 1976 to extrapolate both with the RUST- and the STOOM-scenario of the Deltaprogram, which represent socio-economic stagnation and moderate climate change and socio-economic growth and rapid climate change, respectively. In this way, a time-series consisting of daily discharges at Lobith is created that represents the discharge in the year 2050 with a return period of $T = 10\ years$ and can be used in further modeling efforts.

To accommodate navigation on the Rhine in periods of low water levels, policymakers have agreed on requirements concerning the navigable depth and width under low flow conditions. The Waal (and Upper-Rhine) has a depth requirement of 2.80 m and a width requirement of 150 m which correspond to a discharge at Lobith of 1020 m^3/s and consequently to a discharge of 820 m^3/s in the Waal. For projections of a dry climate however, the Agreed Low Water Level (ALW) is expected to decrease significantly whilst the depth requirement should be maintained. In addition, with the critical point for loading under low discharges expected to vary between several locations, adaptation measures concerning multiple river sections could become necessary in the near future.

Usually, the IWT makes use of the Waal and Upper-Rhine on its route to Duisburg. Nevertheless, transport via the Lek, Lower-Rhine and Pannerdensch Kanaal is possible as it is seen as back-up of the Waal in the case of a calamity that blocks Waal-transport. This back-up route however is deemed inadequate as the capacity of the weirs is considered insufficient. Under regular flow conditions, the Least Available Depth (LAD) on the Lek and Lower-Rhine is found upstream of the port of Arnhem whereas the LAD on the Waal is found near Nijmegen. Rijkwaterstaat states however that Beuningen, St. Andries an Erlecom also show extremely low water levels in periods of drought.

This analysis of the transport corridor between Rotterdam and Duisburg has led to identifying several characteristics. A representative barge has been selected and a safety margin of 0.75 m was assumed. A calculation was made to estimate the fleet size. This resulted in a fleet of 10 push barges, 15 Rhine vessels and 20 vessels with coupled barges. These numbers will be used in the simulation model.

Possible adaptation measures that can help making the IWT system more resilient to climate change-induced droughts are tested. Several measures have been identified to be the most promising in terms of effect and ease of implementation. These measures are schematically represented in the model and will demonstrate the use of the simulation model.

3

IWT performance model

In Chapter 2 the characteristics of the IWT system have been identified. Moreover, a data-set was extracted that describes a low discharge projection for the year 2050. In this chapter, an effort is made to model the network performance. Two models are used in this research to schematize the functioning of an IWT network: the LSM describing the hydraulic conditions and the IWT performance model simulating the logistics. The LSM was received as a validated model and is thus used instead of built. For the sake of conciseness, the theory behind the LSM model, boundary conditions and the input values can be found in Appendix A. This chapter addresses the first section of the answer to the following research question:

How can the performance of an inland waterway network, as a result of low discharges, be simulated?

As such, this chapter answers the following sub-question:

What parameters indicate the performance of an IWT network?

The model outline is considered in Section 3.1. The different sets of required input data for the IWT performance model are described in Section 3.2. The output of the model is addressed in Section 3.3. Consequently, Section 3.4 holds the conclusion regarding the IWT performance model and provides an answer to the above question.

3.1. Model outline

The model that was developed in this research is the IWT performance model. This model requires the output of the LSM to create a network. Serving the goal of computing the distributed share of cargo by vessels in a set period, this model must be able to simulate the cargo transport on each connection within the network. Hence, this representation is set up as a simulation model that describes a chain of transport.

3.1.1. Model objective

The objective of the study is to provide conclusions on the behaviour and boundaries of the inland waterway system by composing a model that studies the performance and vulnerability in times of drought. The performance of the network can be captured by key performance indicators describing the transported cargo and the costs of transport. The objective of the developed IWT performance model thus is to express the performance of an IWT system in indicators. In order to do so, the model has several requirements.

- The information of every vessel contributes to a deep understanding of the vessel behaviour. Every vessel must therefore represent an individual entity in the model. Moreover, a high degree of detail is asked in the application of the model, e.g. to study the effects of adaptation measures. The model, therefore, must consider each single vessel as an individual entity that reconsiders the work method at every step in the simulation and that collects information on its activities to provide detailed insight.
- The network performance should be expressed in key performance indicators. The model therefore must accommodate a coupling between projections of variation of the discharge regime and the transport capacity to translate water levels to network performance. A complete network with water depths

and section widths are required to make the model generically applicable for the ship-routing, responsible for the sailing time and width-restrictions of vessels, and for the testing of multiple measures on several critical river sections.

3.1.2. Modeling concept

As stated, the model must be able to simulate the cargo transport on each connection within the network in order to compute the cargo distributed by barges. More specifically, the model should meet the defined requirements. The chosen model concept is the Open Source Complex Logistics Simulation (OpenCLSim) which is available at the GitHub of the TU Delft Hydraulic Engineering department (Van Koningsveld et al., 2019). This model concept is set up as a combination of Discrete Event Simulation (DES) and Agent Based Simulation (ABS) and is developed in a Simpy simulation environment in Python. OpenCLSim has a wide applicability as it has been used to model plume development, the planning of constructing a layered dike and to assess the energy consumption of dredging projects (den Uijl, 2018, Van Der Bilt, 2019). The motivation for this concept follows its extensive applicability.

In DES modeling, the discrete events are activities in an order of execution within a simulation with a start- and a stop-condition and therefore a fixed duration. DES evaluates the state of the model as it evolves in time induced by these predefined events (Law and Kelton, 2000). This type of simulation modeling has proven to be a useful method in cases where events can easily be discerned, as e.g. ship routing and scheduling (Van Der Bilt, 2019). Upon correct validation of a simulation, DES can be used to gain better understanding of the behaviour of a system (Law and Kelton, 2000). The events in a IWT cycle, i.e. loading, sailing loaded, unloading and sailing empty, can be seen as a series of discrete events. All equipment required to carry out these events such as vessels and (un)loading cranes can be seen as an autonomous entity, i.e. an agent. In ABS modeling, the behaviour of each agent depends on the interactions with other agents. In other words, the events in each transport cycle of every vessel will be impacted by the events of other vessels. Together this represents the interactive behaviour of vessels within an IWT system. The combination of DES and ABS in OpenCLSim and its purpose in this research are presented in Figure 3.1.

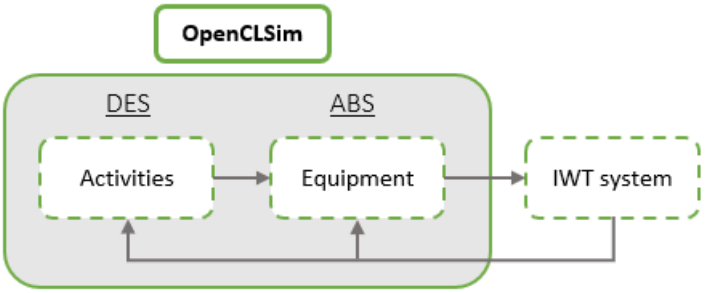

Figure 3.1: DES and ABS are combined in OpenCLSim

OpenCLSim makes use of a predefined *work method* that is given to the model to set out the conditions of the discrete events that take place. The work method consists of *equipment* to carry out the events, *sites* between which the events take place, and *activities* that describe the actual processes. For each of these components a standardized set of input variables is required. With this set of input, the model is able to describe the logistics of the IWT system. The model uses the predefined steps of the work method to create discrete events. These discrete events follow the configuration that was specified in the work method. As such, the model simulates every process in the transport chain between the origin and the destination in the correct order. An overview of the work method is provided in Figure 3.2.

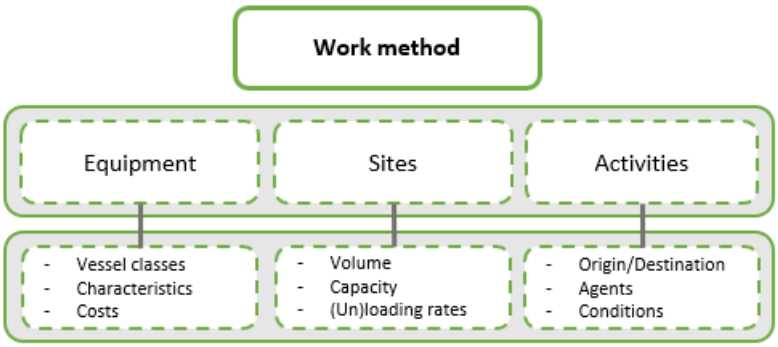

Figure 3.2: The work method and its components

The performance of the network can be expressed by transported cargo in time or time required to transport a set amount of cargo. Moreover, the costs made for transporting cargo and for not being able to meet the demand are a practical way of expressing the network performance. In this research the network performance is indicated by the transported cargo in time. This is supported qualitatively by the costs that follow from post-processing of the model results.

3.1.3. Model structure

The outline of the network performance model can be found in Figure 3.3. The LSM provides water depths as input. On one hand, these depths determine what vessel classes should be active. On the other hand, the water depths also define the load factor with which these vessels can be loaded. The load factor is directly linked to the vessel price. From a combination of the active vessel classes and the load factor, the model determines the required number of trips. With a high load factor, this number is governed by the demand. With low load factors, all available vessels are put into operation so that the number of trips is governed by the fleet size. The product of the vessel capacity, the load factor and the active fleet size give the transport capacity of the IWT network. When this is sufficient to meet the demand, no additional costs for insufficient supply are posed. The active fleet then is large enough and will not have to increase. In case the transport capacity is insufficient, costs for delayed cargo are posed and the active fleet will increase if possible. The product of the performed number of trips and the vessel price per trip results in the vessel costs. Together with the delay costs, these make up the total transport costs of the IWT system.

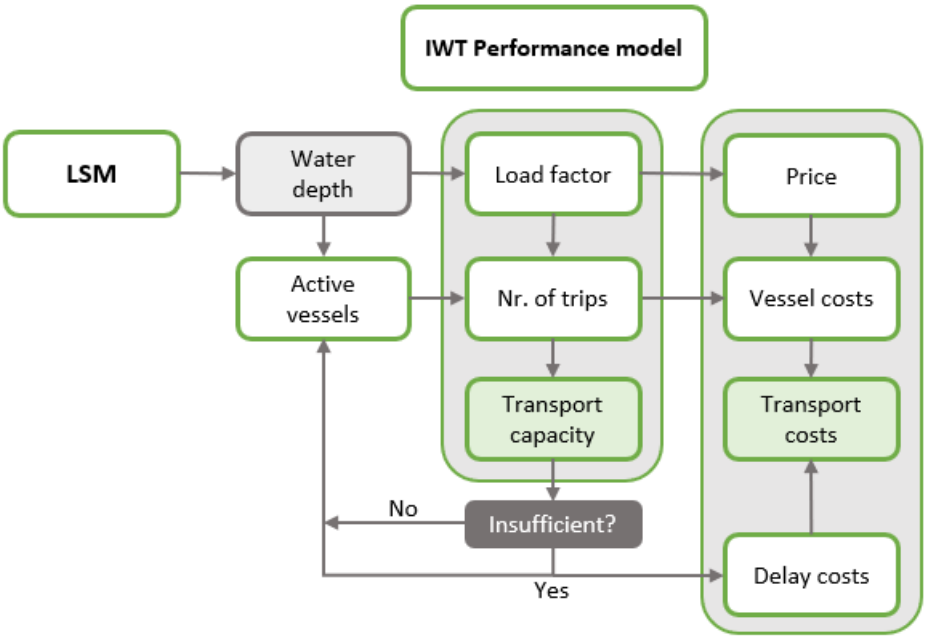

Figure 3.3: Outline of the IWT performance model; the grey block denotes input, the green blocks denote output

3.1.4. Model assumptions

Several simplifications set the context in which the model has been developed. The model outcome should thus be interpreted while keeping these simplifications in mind. The following assumptions have been made in the model development:

- The full capacity of a convoy is used when sufficient water depth is present.
- The demand for cargo is constant and does not vary over the simulation time.
- The load factor is assumed to be constant between the origin location and destination. This means that the convoy makes no stops to (un)load at inland ports.
- This research concerns the one-way transport from the Port of Rotterdam to Duisport. It is for that reason assumed that vessels sail back empty.

3.2. Input data

The input data of the model is classified into equipment, sites, and activities. Each component is described in a separate sub-section which concludes with an overview of the required input data that must be specified to lead to successful model output. This section is based on previously published thesis work (den Uijl, 2018, Van Der Bilt, 2019).

3.2.1. Equipment

The various steps in the transport cycle are carried out by equipment. As followed from Section 2.3, the equipment used for the transport of dry bulk consists of dumb barges that are pushed in convoys of 6 by pusher boats. In times of drought, the fleet mix changes so that smaller convoys first become active, with further decreasing water depths followed by Rhine vessels and coupled barges. This fleet determines the conditions regarding the sailing stages of the transport. The loading and unloading stages are governed by the equipment at the origin and destination site.

The input data concerning the equipment describes the constant and variable characteristics of the fleet and of the site equipment. These characteristics are discussed below.

Vessel capacity
Each convoy has a maximum capacity in tons cargo. With the active sailing equipment changing, also the capacity varies. This capacity largely influences the duration of all events in the transport cycle. The true transported cargo per convoy is the product of the convoy capacity and the actual load factor, induced by the draught and the actual water depth.

Draught and safety margin
The load factor linearly depends on the draught of the used equipment. A loaded draught and an empty draught are required as input for each vessel type. The actual minimum local water depth that follows from the LSM is decreased by the required safety margin and is compared to these draughts to find the possible draught and thereby the maximum load factor.

Fleet size
The fleet size describes the number of vessels present in the IWT system. With a sufficient load factor, vessels can transport enough cargo to meet the demand. Consequently, not all vessels present in the system are active so that part of the fleet is idle. The transport capacity, being a product of the load factor, the vessel capacity, and the number of active vessels, in that case satisfies the network demand. In contrast, when the load factor becomes insufficient to transport with the active equipment, a larger share of the fleet becomes active until all vessels are in operation. The fleet size poses a boundary to the maximum number of vessels of a certain fleet type that can be active within the system.

Sailing speed
The sailing speed of a vessel varies between the limits of sailing loaded and sailing empty. These limits correspond with a load factor of 100% and of 10% respectively. The sailing speed determines the time required for the sailing stages of the transport cycle.

Costs
The price of a transport convoy varies with the load factor. The regular convoy price per day is required as input. In times of drought, the principle of supply and demand heightens the need for barges and, as such, increases the price.

The characteristics of the convoy equipment that are required as input data are given in an overview in Table 3.1.

Equipment - Convoy	
Vessel name	[*string*]
Vessel capacity	[*tons*]
Vessel draught empty	[*m*]
Vessel draught full	[*m*]
Under keel clearance	[*m*]
Fleet size	[*convoys*]
Sailing speed loaded	[*m/s*]
Sailing speed empty	[*m/s*]
Convoy price	[*€/day*]

Table 3.1: The required input data for each type of vessel

(Un)loading rate
The loading and unloading stages of the transport are determined by the (un)loading rates. It is assumed that site equipment governs the events of (un)loading. For that reason, berths are included in the model at which cargo can be transferred. Both a loading and an unloading rate are required as input.

Number of resources
Every berth has limited places for the (un)loading of vessels. The number of resources denotes the number of handling places that are available at a berth. It therefore corresponds to the number of vessels that can be

handled simultaneously at a berth.

The characteristics of the berth equipment that are required as input data are given in an overview in Table 3.2.

Equipment - Berths	
Berth name	[*string*]
Nr. of resources	[*handling places*]
Loading rate	[*tons/sec*]
Unloading rate	[*tons/sec*]

Table 3.2: The required input data for the berth equipment

3.2.2. Sites

The transport of cargo is bound at two sides by the origin and the destination. These have to be defined in the model as sites. Moreover, other sites can be defined on the transport path to represent en route transfer of cargo. Every site requires a predefined list of input data. The sites require information on their geographical location, a capacity and an initial cargo volume. The required input data is listed in Table 3.3.

Sites	
Site name	[*string*]
Location	[*coordinates*]
Capacity	[*tons*]
Initial volume	[*tons*]

Table 3.3: The required input data for the sites

3.2.3. Activities

The equipment and the sites are connected by activities. For an activity to be successfully executed, it requires two sites and equipment. The activity will begin as soon as the predefined start event is fulfilled and it will stop when the stop event is met. These activities describe the actual transport processes in the IWT system. The transport processes in this research include loading, sailing loaded, unloading and sailing empty. This cycle is repeated for every vessel from the moment the start event has been met, until the stop event is approved. Moreover, multiple cycles can run simultaneously, as long as they meet the limit posed by the number of resources. In case this limit is reached, waiting is induced as a fifth component of the transport process. The cycle consisting of the transport processes is given in Figure 3.4.

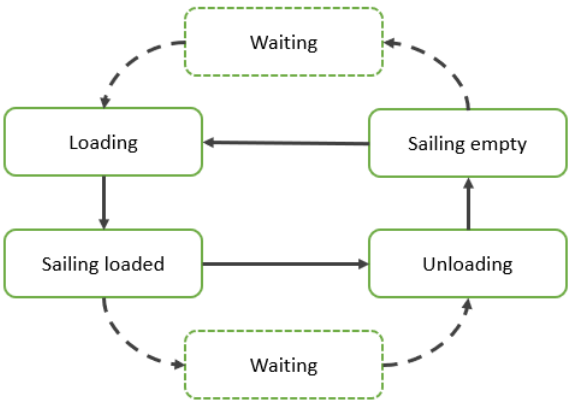

Figure 3.4: The schematized transport cycle

For a basic simulation, the required input data is given in Table 3.4.

Activities	
Activity name	[*string*]
Origin	[*site*]
Destination	[*site*]
Loader agent	[*berth*]
Mover agent	[*convoy*]
Unloader agent	[*berth*]
Start event	[*condition*]
Stop event	[*condition*]

Table 3.4: The required input data for the activities

3.3. Output data

When given the correct input, the simulation can run and be used to provide output. The concept of a simulation is shown in Figure 3.5. For various time steps, this figure provides an overview of the processes that occur in the simulation. For time $T = 0$, the overview shows a full stockpile in the origin, an empty stockpile in the destination and the first agent that is at this time unloaded. As the simulation commences, the first agent is loaded, thereby reducing the volume of the stockpile in the origin. After being loaded, this agent will set sail and will create space for a consecutive agent, as is shown for time $T = 2$. The following time steps consist of multiple processes that occur simultaneously: vessels are being loaded at the origin, sail the route towards the destination and are unloaded once they arrive. This corresponds to a continuous reduction of the stockpile volume at the origin and an on-going filling of the stockpile volume at the destination. Depending on the stop condition that was given to the activities, the simulation stops after the simulation time has passed or when the last cargo has been transported and there is no cargo left to transport in the origin. By post-processing of the simulation results, the outcome parameters that describe the network performance can be obtained per unit of time or after the simulation (i.e. at time $T = n$).

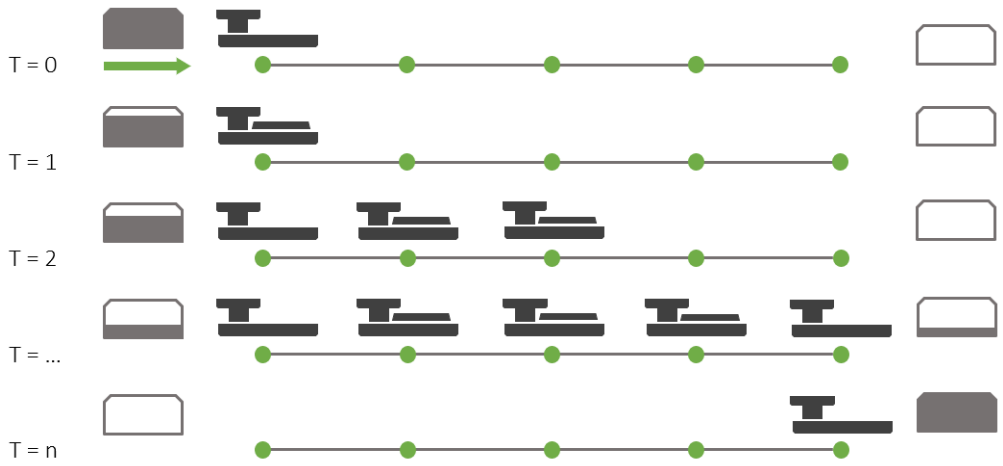

Figure 3.5: Concept of simulation of the IWT performance model

The output of the network performance model can be used to evaluate the responses of transport parameters to a varying load factor. These parameters concern the number of trips, the transported cargo and the transport costs, as are given in Table 3.5. These can be studied individually or be combined to study the change of the complete system. The model can provide output on the ability to transport in a restricted period of simulation time, or on the time required for transporting a predefined amount of cargo. Moreover, with this information, the user is able to use the model for application, e.g. decide on the effectiveness of additional measures or to determine the size of the optimal stockpile. The transported cargo and the transport costs are seen as the key performance indicators. These are used to conclude on the performance of the IWT system

in times of low water depths.

Output	
Nr. of trips	[*# trips*]
Transported cargo	[*tons*]
Vessel costs	[€]
Delay costs	[€]
Transport costs	[€]

Table 3.5: The provided output data

3.4. Conclusion

A model was developed to simulate the performance of an IWT network to varying discharges. The objective of this IWT performance model is to express the performance of the IWT system in key performance indicators, describing the transported cargo and the costs of transport. In this research, the network performance is indicated by the transported cargo in time. This is supported qualitatively by the transport costs. By doing so, this chapter has addressed the following sub-question:

What parameters indicate the performance of an IWT network?

The projected discharge following from the literature study was used to compute future water depths. To this end, use was made of the Landelijk Sobek Model. Moreover, this model provides a network and waterway cross-sections as input for the IWT performance model. The chosen model concept OpenCLSim is available at the GitHub of the TU Delft Hydraulic Engineering department. This model concept is set up as a combination of Discrete Event Simulation (DES) and Agent-Based Simulation (ABS) and is developed in a simulation environment in Python. The simulation uses a *work method* which consists of *equipment* to carry out events, *sites* between which the events take place, and *activities* that describe the actual processes. These describe the discrete events that represent the logistical chain of IWT.

The model provides output on various transport parameters in a predefined simulation time. It delivers values for the performance indicators. As such, the model has successfully addressed the objective of the IWT performance model. Moreover, with this information,the user is able to use the model for application, e.g. decide on the effectiveness of adaptation measures or to determine the size of the optimal stockpile.

4

Validation and calibration

This chapter presents the validation and calibration of the IWT performance model. Model validation consists of three phases (Truong et al., 2014). These phases are depicted in Figure 4.1. First, the internal validation is carried out to show that the model functions correctly. This phase is intended to find whether the model was built right. Consequently, in the calibration phase the model output is adjusted to find to what extent the model is able to represent reality. "The calibration is the fine-tuning of the output of a simulation model by a change in values of parameters" (Truong et al., 2014, p. 5). This chapter thereby intends to address the second section of the answer to the following research question:

How can the performance of an inland waterway network, as a result of low water depths, be simulated?

This chapter answers the following sub-question:

Can the performance indicators be reproduced for a reference period of low water depths?

Ideally, the internal validation and calibration would be extended with a external validation phase in which the calibrated model would be tested against a different data set or other data from the same data-set.

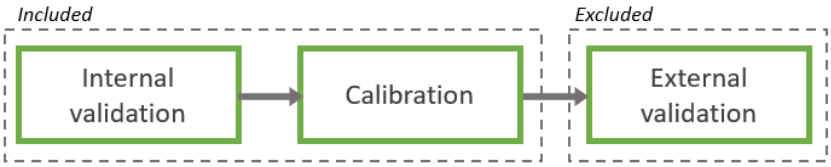

Figure 4.1: The three phases of model validation

The first step in the validation process is to test the functioning of the model by evaluating the behaviour of model parameters. It follows from predefined tests whether the model simulating the transport logistics functions the way it is supposed to. This is considered the internal validation and can be found in Section 4.1. In the next phase, the numbers produced by the model are calibrated against a data set provided by Rijkswaterstaat. This is the calibration phase which can be found in Section 4.2. As all data will be used in the calibration, no data set is available for external validation. For that reason, no external validation has been carried out. The model validation thus only consists of the internal validation and calibration. This chapter concludes on the success of the modeling effort of Chapter 3.

4.1. Internal validation

4.1.1. Internal validation method

The model is tested on several aspects that are independent of each other. Only the fourth test follows from post-processing and is therefore dependent on the model output. This way, the functioning of the model can be tested on multiple stages of the simulation. A case of vessels travelling a simple path is designed, see Figure 4.2a. The effects of drought have not been included in this simplified case. In this case, the water depth

is varied over a year to resemble river discharge seasonality. Usually, in the Dutch Rhine system, the lowest water levels occur around September and the highest water levels occur in March. Effects of drought can last for several months. In order to have the effects of drought within a one-year period, this step-wise trend has been shifted two months forward. The water level in the design case is shown in Figure 4.2b. The same four vessel classes as are seen in reality are used. The input characteristics can be found in Appendix D.

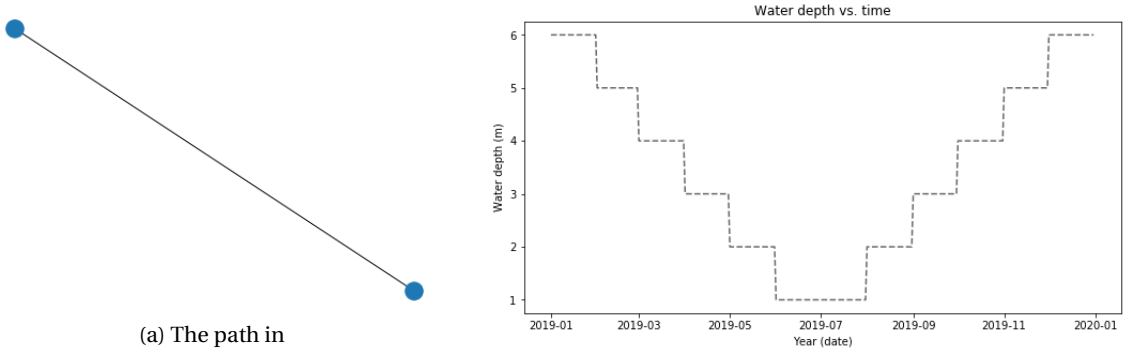

(a) The path in the design case

(b) The water depth varies over a year

Figure 4.2: Used model components in validation

The tests to which the model will be subjected are listed below. They concern the equipment and activities.

1. Load factor and vessel types vary with varying water depth
2. The number of trips varies with varying water depth
3. Compensating effect in the weekly transport after drought
4. Vessel price is inversely related to the water depth

Test 1: Load factor and vessel types vary with varying water depth
This test is performed to check if the load factor adjusts to the water depth. This is necessary for the agents in the model to adapt their activities to. The test succeeds when the same step-wise trend in the load factor as in the water depth can be discerned and the steps take place on the same moment in time. The exact results should follow the linear relation between the draught and the load factor. This relation is given by Equation 4.1. A load factor of 5% is taken for the agents sailing empty, and a load factor of 100% is understood for the agents sailing loaded. Depending on the draught when empty or loaded, and on the available water depth, the following load factors are expected:

$$Load\ factor = \frac{1.0 - 0.05}{Draught_{loaded} - Draught_{empty}} * (Water\ depth - Draught_{empty}) + 0.05 \quad (4.1)$$

	Jan '19	**Feb '19**	**Mar '19**	**Apr '19**	**May '19**	**Jun '19**
Load factor (-)	1.0	1.0	0.94	0.87	0.37	0.08
	Jul '19	**Aug '19**	**Sep '19**	**Oct '19**	**Nov '19**	**Dec '19**
Load factor (-)	0.08	0.37	0.87	0.94	1.0	1.0

Table 4.1: The expected maximum load factor

In Figure 4.3, the result of the test can be seen. For each vessel type, the load factor is given. When a vessel type is inactive, its load factor is set to 0. Keeping that in mind, the step-wise trend can clearly be distinguished. The exact values of each load factor do correspond to the expected load factors for each vessel class. Only for the 6-barge push convoys, the load factor in March 2019 does give a value of 0.80 instead of the expected 0.94. This follows from the load factor being computed as an average of the trips undertaken in a time period. In

that particular case, four convoys sail with a load factor of 0.94, leaving so little cargo for the fifth push-barge convoy that its load factor becomes 0.24. The average of those five convoys then results in a load factor of 0.80. The test result does not show an exactly symmetrical pattern. This is due to the fact that sailing stages of each cycle do take up several days and as such, adjusting of the network to a new load factor takes several days. Moreover, with water depths varying, the vessel types can be seen to switch between operation and inactivity. Seeing the different trends of the load factor, it can be concluded that the test is passed successfully.

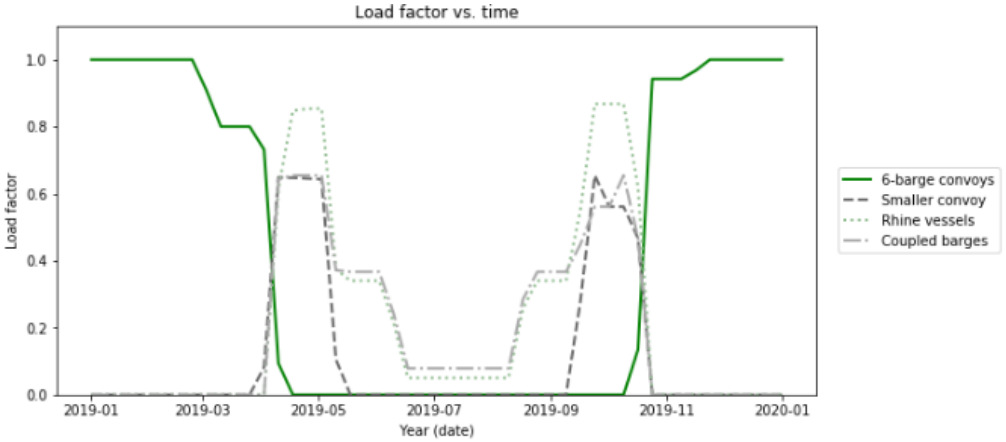

Figure 4.3: The load factor varies over a year

Test 2: The number of trips varies with varying water depth
Variations in load factor cause changes in the nr. of trips required to retain the transport capacity of the network. As each individual vessel can transport less, more vessels become necessary to persist in meeting the demand. This leads to more trips undertaken. Moreover, variations in the load factor affect the sailing speed, loading rate and unloading rate of convoys. As such, the network becomes a dynamic play of active agents.

This test is performed to see whether the model reflects this dynamic behaviour in the nr. of trips. The test is expected to show dynamic variations in the nr. of trips with an underlying step-wise trend, as it is driven by variations in the load factor. The number of trips is limited by the cycle time and the fleet size per vessel class. Moreover, it is limited by the supply of cargo when the transport capacity still meets the demand. The algorithm from which the number of trips follow is given by Equation 4.2. The expected results for the total number of trips are given in Table 4.2. The numbers presented follow from the sum of the individual vessel classes.

$$Nr.\,of\ trips = 7 * \min\left(\frac{Fleet\ size}{Cycle\ time}; \frac{Demand}{Vessel\ capacity * Load\ factor}\right) \tag{4.2}$$

	Jan '19	**Feb '19**	**Mar '19**	**Apr '19**	**May '19**	**Jun '19**
Trips (# per week)	28	28	35	224	331	331
	Jul '19	**Aug '19**	**Sep '19**	**Oct '19**	**Nov '19**	**Dec '19**
Trips (# per week)	331	331	331	50	50	50

Table 4.2: The expected total number of trips per week

The test result is shown in Figure 4.4. The dynamic behaviour of the system is clearly visible in the peaks that denote an irregular transport situation. Moreover, it can be seen in the curving trend in summer that the activity of both the Rhine vessels and the coupled barges increases somewhat after the smaller barge convoys stop operating. Following, the activity of both vessel types decreases once the water depth becomes sufficient again. This follows from the load factor that increases again, thereby inducing a lower sailing speed and longer loading and unloading per cycle. The number of trips performed by the 6-barge push convoys after summer is seen to be higher than before the summer. Before summer, this transport was restricted by

the supply. After summer, there is enough cargo to transport that could not be transported during summer and has piled up during these months. The 6-barge push convoys are therefore now restricted by its fleet size instead of by the supply. This effect is scrutinized further in Test 3. The number of trips are as projected beforehand. Hence, this aspect of the model is validated to function well.

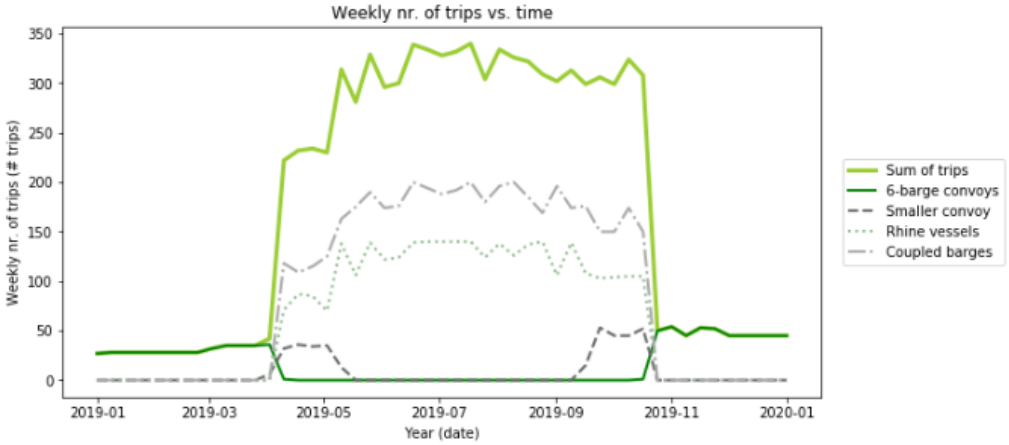

Figure 4.4: The weekly nr. of trips over a year

Test 3: Compensating effect in the weekly transport after drought
It is assumed that all cargo that cannot be transported during a drought is added to the stockpile and is transported when the network capacity recovers. As such, after the water depth has recovered, the 6-barge push fleet is expected to remain active to compensate for the earlier lack of transport. After the demand has been brought back to its original level also the active fleet, and consequently the nr. of trips performed, can return to its original size. This test is performed to show the functioning of the daily transport demand. A successful test should show a compensating effect in the period following a period where the demand could not be met. Moreover, this effect should again show a step-wise trend following the load factor. The expected transported cargo per week is given in Table 4.3. The values follow from the relation that is given by Equation 4.3.

$$Transported\ cargo = Nr.\ of\ trips * Vessel\ capacity * Load\ factor \tag{4.3}$$

	Jan '19	**Feb '19**	**Mar '19**	**Apr '19**	**May '19**	**Jun '19**
Transported cargo (tons per week)	7,000	7,000	7,000	7,000	4,042	624
	Jul '19	**Aug '19**	**Sep '19**	**Oct '19**	**Nov '19**	**Dec '19**
Transported cargo (tons per week)	624	4,024	10,115	11,750	12,500	12,500

Table 4.3: The expected transported cargo per week

The results of the test are presented in Figure 4.5. Both the decrease and increase in the sum of the transported cargo show the step-wise trend that is expected. Furthermore, the compensating effect follows from the fact that the transport with 6-barge push convoys after a drought surpasses the daily demand. Hence, the test was successful and it can be concluded that this aspect of the model functions well.

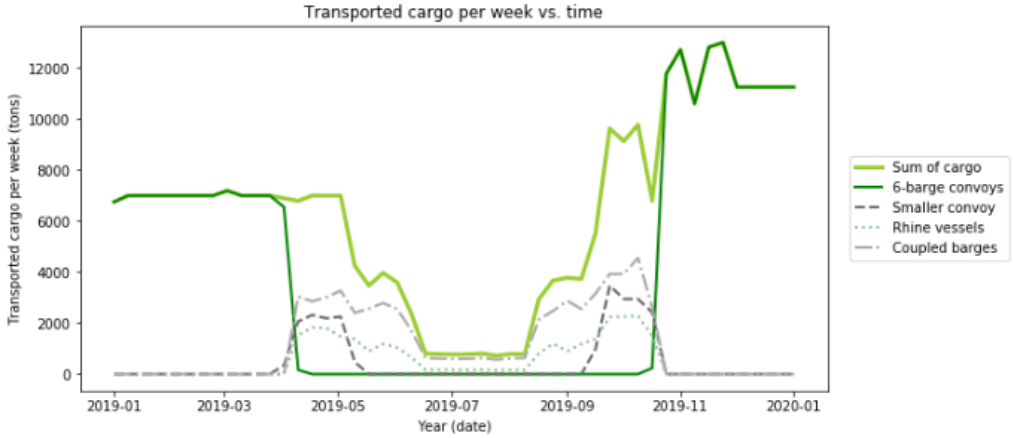

Figure 4.5: The weekly transported cargo over a year

Test 4: Vessel price is inversely related to the water depth
The weekly transport costs follow directly from the sum of the vessel costs and the costs for insufficient supply. The vessel costs are defined as the product of the number of trips per day, and the trip costs. A combined effect should therefore show both the irregular variations in the weekly nr. of trips and the step-wise trend corresponding to the weekly vessel price. As more vessels are required for transport, the demand for vessels increases. By simple means of supply and demand, this results in a higher dayrate for vessels. As a result, the costs of a trip during drought increase, contributing to a significant growth of costs in this period. These trip costs are defined as the product of the dayrate and the time required for transport in days. The higher dayrate is triggered by the load factor undershooting several limits. Moreover, as the sailing speed becomes higher for unloaded vessels, the required time for transport is expected to be least in the dry season. The weekly vessel price therefore is expected to decreasingly follow the step-wise behaviour of the water depth.

$$Vessel\ costs = Dayrate * \frac{Nr.\ of\ trips}{Sailing\ time} \tag{4.4}$$

The costs for insufficient supply follow from a deficit in the weekly transported cargo and the price for this deficit per ton. As the supply deficit is largest when water depths are lowest, the highest costs are expected during the summer months. The costs for insufficient supply follow from the product of the deficit in transported cargo and the price of insufficient supply, as can be seen in Equation 4.5. The expected transport costs are presented in Table 4.4. These result from the sum of the vessel costs and the costs for insufficient supply, as is given by Equation 4.6.

$$Costs\ of\ insufficient\ supply = Costs\ of\ insufficient\ supply\ per\ ton * (Weekly\ demand - Transported\ cargo) \tag{4.5}$$

$$Transport\ costs = Vessel\ costs + Costs\ of\ insufficient\ supply \tag{4.6}$$

	Jan '19	**Feb '19**	**Mar '19**	**Apr '19**	**May '19**	**Jun '19**
Transport costs (€)	105,000	105,000	199,500	453,740	1,118,000	1,418,000
	Jul '19	**Aug '19**	**Sep '19**	**Oct '19**	**Nov '19**	**Dec '19**
Transport costs (€)	1,418,000	1,118,000	491,240	491,240	150,000	150,000

Table 4.4: The expected transport costs per week

Figure 4.6 presents the results of this test for the daily total costs. For the lowest water depths, a reduction of vessel costs is observed. With the lowest water depth, the vessels' load factor is restricted most, thereby inducing a high sailing speed. The reduction is explained by this high velocities that vessels can sail with. Due

to the short sailing time and no further increase in price, this results in a decrease of costs. The highest costs for delay are seen during summer, as was expected. The sum of the vessel costs and the costs for insufficient supply thus gives a maximum in the period of low water depths. For April and September, the model does give different results than were expected. This could the result of longer waiting times, and hence cycle times, induced by the high number of trips undertaken in this period. Concluding, it is stated that the test is passed and that the network performance model gives a good indication of the costs.

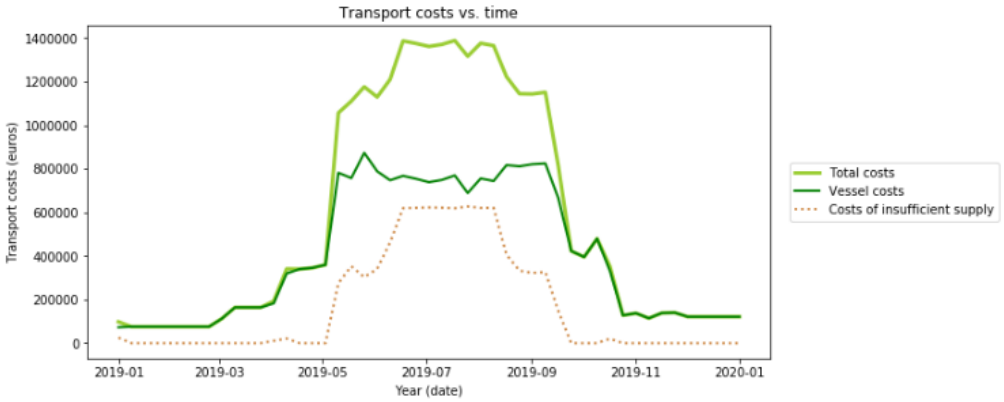

Figure 4.6: The weekly transport costs over a year

4.1.2. Conclusion of internal validation

The model has passed all four tests. The internal validation has thus been carried out successfully and the functionality of the different model components has been proven. For that reason, the qualitative and quantitative results of the model are correct and the model is able to simulate network performance in terms of transport parameters.

4.2. Calibration

In Section 4.1, the qualitative functionality of the model has been proven. Different model components were successfully tested on their ability to simulate IWT network performance. This section will consider the quantitative side of the model output. Model parameters are compared to a real data-set. Their inter-dependence and the size of their effects can then be calibrated to assure that the model results correspond with reality. In Section 4.2.1, the used data-set is described. Moreover, this section presents the calibration method. The calibration is carried out in Sections 4.2.2, 4.2.3 and 4.2.4. Deviations between the model results and the data-set are explained in Section 4.2.5. The calibration section ends with a conclusion on the two model parameters that are calibrated.

4.2.1. Calibration method

The obtained data-set consists of IVS-90 data (Informatie en Volgsysteem Scheepvaart (1990)) [1]. There are hundreds of IVS stations in the Netherlands. These collect data regarding the characteristics and shipped cargo of vessels passing those stations. Moreover, they include the type of vessel and the origin/destination in the Netherlands of each trip. As such, selecting a dry year from this historical data-set shows the effect of a dry season on the number of trips, which is directly related to the active fleet size, for each vessel class used for dry bulk transport. As other data-sets appeared incomplete or were not at disposal, the IVS-90 data-set for the dry year of 2018 is used to calibrate the model results with. From this data-set, weekly averages of the nr. of trips and the transported weight have been extracted. Unwanted peaks and measurement errors have thus been leveled out. An accuracy of a week-scale is assumed sufficient to calibrate this macro-scale model.

The calibration is carried out for two parameters: the manoeuvring time of each vessel type and the capacity per vessel type. These have been chosen as they have a large uncertainty, in combination with a significant impact on the model result, relative to other model parameters. Initial input was first used to obtain model output. This input follows partially from the transport analysis of Section 2.3. The obtained IVS-90 data considers the same IWT link so that the found numbers for the fleet and the demand can be used. This

[1] Open website of Rijkswaterstaat accessed on 25-09-2019; https://bivas.chartasoftware.com/Scenarios

set of input data is further completed by values concerning the (un)loading equipment at the EECV terminal (Ertsoverslagbedrijf Europoort CV, 2018). These values are assumed for the terminal in Duisburg as well. For the manoeuvring time, no values were found so that an estimation was required. Due to this uncertainty, the manoeuvring time is calibrated in Section 4.2.3. Ultimately, the sailing speed on the Waal was obtained from an example calculation (Backer van Ommeren, 2011). The initial conditions can be found in Table 4.5. Expectations are that the initial errors can be decreased by calibrating the manoeuvring time of each vessel type and the capacity per vessel type.

	Unit	**Value**
General		
Transport demand	[tons/year]	32 mln
Safety margin	[m]	0.75
Sailing speed unloaded downstream	[m/s]	4.50
Sailing speed loaded upstream	[m/s]	2.25
6-barge push convoys		
Convoy capacity	[tons]	16,000
Barge draught empty	[m]	0.65
Barge draught full	[m]	3.95
Fleet size	[pusher boats]	10
Manoeuvring time	[hours]	1
Smaller push-barge convoys		
Convoy capacity	[tons]	7,500
Barge draught empty	[m]	0.65
Barge draught full	[m]	3.95
Fleet size	[pusher boats]	10
Manoeuvring time	[hours]	2
Rhine vessels		
Rhine vessel capacity	[tons]	2,000
Rhine vessel draught empty	[m]	1.20
Rhine vessel draught full	[m]	3.0
Fleet size	[Rhine vessels]	15
Manoeuvring time	[hours]	3
Coupled barges		
Coupled barge capacity	[tons]	4,000
Barge draught empty	[m]	0.65
Barge draught full	[m]	3.95
Fleet size	[coupled barges]	20
Manoeuvring time	[hours]	3
Site equipment		
Nr. of resources	[berths]	6
Loading rate	[ton/s]	1.25
Unloading rate	[ton/s]	0.75

Table 4.5: Initial conditions for calibration (Backer van Ommeren, 2011, Ertsoverslagbedrijf Europoort CV, 2018)

The discharge data at Lobith of 2018 has been obtained, including the downstream LSM boundary conditions. This is used to run the LSM so that the IWT performance model can be fed with accurate water depths. These water depths can be found in Appendix C.

The results following from the model output will be compared to those following from the IVS-90 data-set by means of a statistical method. The trends for dry bulk vessels that are discerned from the data-set can be seen in Figures 4.8 and 4.9. First, a check between the calculated load factor and the observed load factor is carried out to ensure that comparable load factors count for both sets. The model results are then compared to the data-set on two aspects: (i) the transported cargo per vessel type and (ii) the nr. of trips per vessel type.

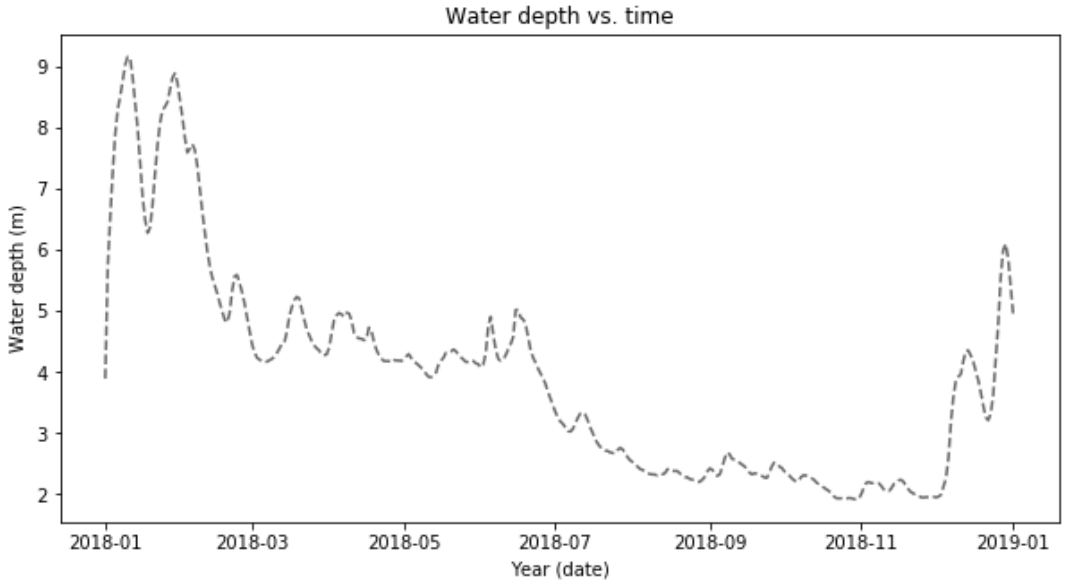

Figure 4.7: The critical water depth at Millingerwaard in 2018, computed with data from Rijkswaterstaat Waterinfo

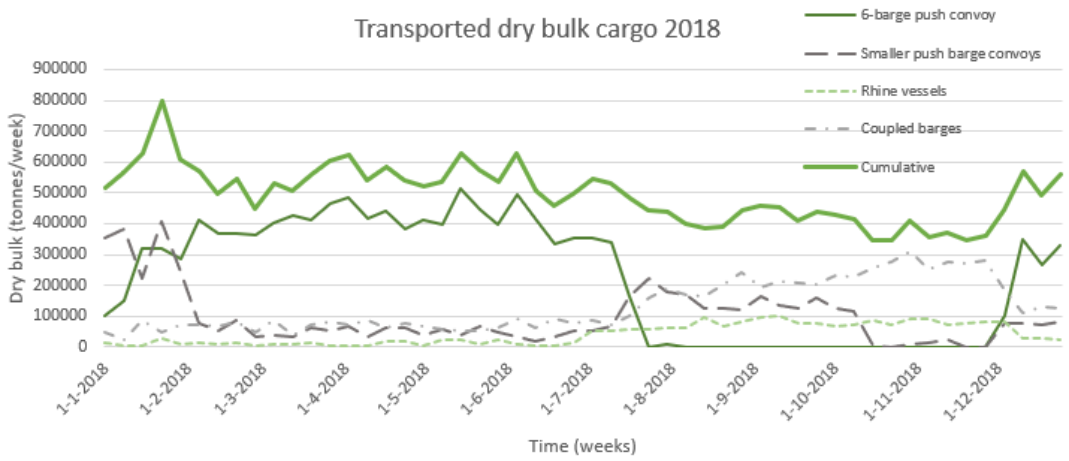

Figure 4.8: The observed weekly transported cargo in 2018 by the different vessel classes (Rijkswaterstaat, 2019a)

	Jan '18	**Feb '18**	**Mar '18**	**Apr '18**	**May '18**	**Jun '18**
Transported weight (tons)	3,112,836	2,060,585	2,196,631	2,807,329	2,268,096	2,088,863
	Jul '18	**Aug '18**	**Sep '18**	**Oct '18**	**Nov '18**	**Dec '18**
Transported weight (tons)	2,437,758	1,617,626	1,758,568	1,941,039	1,438,854	2,061,598

Table 4.6: The observed transported weight in 2018 per month

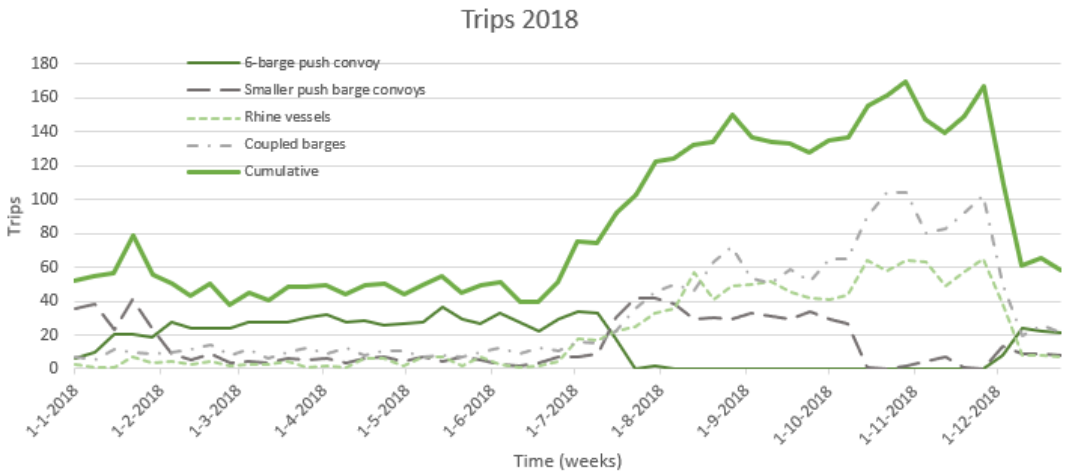

Figure 4.9: The observed weekly nr. of trips of transport vessel classes in 2018 (Rijkswaterstaat, 2019a)

	Jan '18	**Feb '18**	**Mar '18**	**Apr '18**	**May '18**	**Jun '18**
Number of trips (# trips)	297	182	182	237	198	181
	Jul '18	**Aug '18**	**Sep '18**	**Oct '18**	**Nov '18**	**Dec '18**
Number of trips (# trips)	466	540	531	758	602	293

Table 4.7: The observed nr. of trips in 2018 per month

	Unit	**Value**
Sum of transported weight	[tons]	25,789,784
Sum of trips	[trips]	4,468

Table 4.8: Sum of observations 2018

Several statistical methods can be considered to make this comparison. An often used method to measure the similarity between two data-sets is the Root Mean Squared Error (RMSE) (Truong et al., 2014). This method uses the deviations between simulation outputs and observations from reality to find the fit of the model predictions. As such, it concludes on the correctness of the model output. It can be stated that the closer to 0 the value of the RMSE is, the better the fit of the model to the measured data. The mathematical expression of the RMSE can be seen in Equation 4.7.

$$RMSE = \sqrt{\frac{\Sigma_{i=1}^{n}(\hat{y}_i - y_i)^2}{n}} \tag{4.7}$$

where:

$$\begin{aligned} \text{n} &= \text{length of data-set} \\ \hat{y}_i &= \text{value from model} \\ y_i &= \text{value from data-set} \end{aligned}$$

The RMSE follows from the absolute error between two values and does not take into account the size of those values. In other words, a model result of 105 on a measured value of 100 ($RMSE_i = \sqrt{\frac{25}{n}}$) gives a higher RMSE than a model result of 12 on a measured value of 10 ($RMSE_i = \sqrt{\frac{4}{n}}$) but has a smaller relative error ($\frac{105}{100} < \frac{12}{10}$). This can be accounted for by using the coefficient of variation (CV(RMSE)). The CV(RMSE) is determined by dividing the RMSE by the mean of the measured values and provides the size of the error relative to the mean of the observations (Van der Does De Willebois, 2019). The deviation of the model results

from the measured trend can now be expressed in a generic value that can be compared to one another. Following the RMSE, a value of the CV(RMSE) closer to 0 means a better fit of the model. A coefficient of variation below 1 is generally considered to predict low variance between the model results and the reference data-set. Coefficients of variation above 1 are said to indicate high variance in the predicted values. The network represented in the macro-scale model developed in this research is expected to know many external influences. As these contribute to a large variation, a CV below 1 is adopted in this study as low variance which denotes accurate model results. The mathematical expression of the CV(RMSE) is given in Equation 4.8.

$$CV(RMSE) = \frac{\sqrt{\frac{\Sigma_{i=1}^{n}(\hat{y}_i - y_i)^2}{n}}}{\bar{y}} \tag{4.8}$$

where:

n	=	length of data-set
$\hat{y}_i$	=	value from model
y_i	=	value from data-set
$\bar{y}$	=	mean of the data-set

Due to the use of the mean, the CV(RMSE) should not be applied when negative values are expected in the data-set. As nr. of trips and transported cargo are always positive values, this is no issue. In addition, the effect of each error on the outcome of the RMSE and CV(RMSE) is proportional to the size of the error. As such, outliers, giving large errors, have a significant effect on the value of the RMSE and CV(RMSE). This is undesired. In this case, however, the data-sets and model results used are averaged over a week and, as such, are expected to have limited outliers. The proposed method is therefore assumed to hold.

The CV(RMSE) gives a value to the error between observations and model results but it does not provide information on the correlation between these sets. To this end, the Pearson Correlation Coefficient (PCC) r_{xy} is used. This correlation coefficient is widely used to show the linear correlation between two variables (Zhou et al., 2016). The mathematical expression of the PCC is given by the division of the covariance of two variables by the product of the standard deviations of these variables, and can be found in Equation 4.9.

$$r_{xy} = \frac{\Sigma(x_i - \bar{x})\Sigma(y_i - \bar{y})}{\sqrt{\Sigma(x_i - \bar{x})^2}\sqrt{y_i - \bar{y})^2}} \tag{4.9}$$

where:

x_i	=	value from the observations
$\bar{x}$	=	mean of the observations
y_i	=	value from the model results
$\bar{y}$	=	mean of the model results

The range of the coefficient r_{xy} spans from -1 to 1. It is stated that the closer its absolute value is to 1, the stronger the linear relationship between the two data-sets is (Zhou et al., 2016). A PCC of zero denotes no correlation between the variables.

In this research, the PCC is used to show the fit of the model results to observations from reality graphically. Moreover, the correlation coefficient is used to show the improving accuracy through the different steps of calibration.

4.2.2. Calibration of null scenario

First, a check is carried out to see whether the load factor that results from the model is similar to what was observed in reality. This appeared to be not the case. A mismatch in the water depth of $0.25m$ was found between the results of the LSM and observations (Schulz, 2018, Van Hussen et al., 2019). It is assumed that this mismatch results from the coarse grid of the LSM. Local shallows in the waterway are not all included in the LSM results due to this grid. In order to comply with the measured IVS-90 data, 0.25 m is subtracted from the water depth. The results for all vessel types are presented in Figure 4.10. It can be seen that the

modeled load factor follows the measured load factor reasonably well in times of drought. When vessel types are inactive, their load factor does not reflect a realistic value. This does therefore not comply with the IVS-90 data-set. For that reason, the error in load factor is only considered in the dry period, approximately from mid-July to mid-December. The exact error is given by the RMSE and CV(RMSE) per vessel type in Table 4.9.

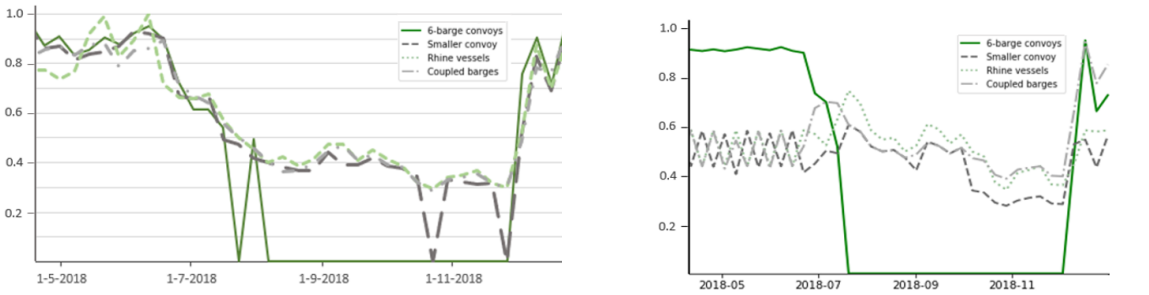

(a) The load factor during 2018 from observations

(b) The load factor during 2018 following from model

Figure 4.10: Load factors from observations and from model

	RMSE (−)	**CV(RMSE)**
6-barge push convoys	0.133	0.231
Smaller push-barge convoys	0.345	0.503
Rhine vessels	0.268	0.412
Coupled barges	0.133	0.199
Average error	0.220	0.336

Table 4.9: The error in the load factor

A calculated CV(RMSE) of 0.336 is well below the critical value of 1 so that realistic results can be expected and the calibration can be continued. Following, the initial comparison between the model output and the calibration data can be made. For all four different vessel classes, the transported weight resulting from the model and the IVS-90 data-set is given. Figure 4.11 shows the results graphically. Furthermore, the exact errors can be found in Table 4.10.

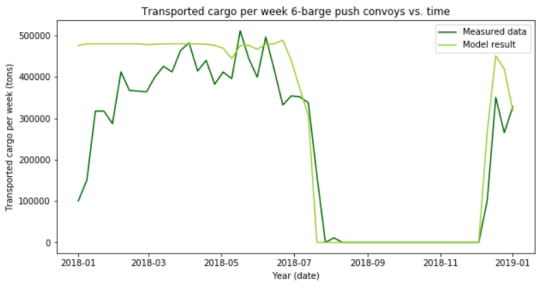

(a) 6-barge push convoys

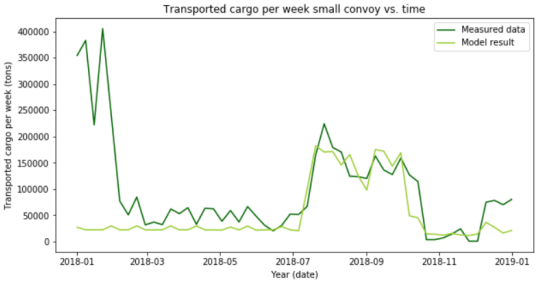

(b) Smaller push-barges

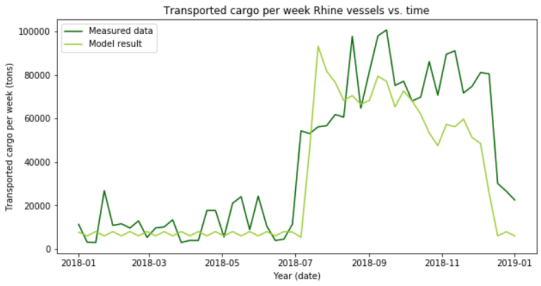

(c) Rhine vessels

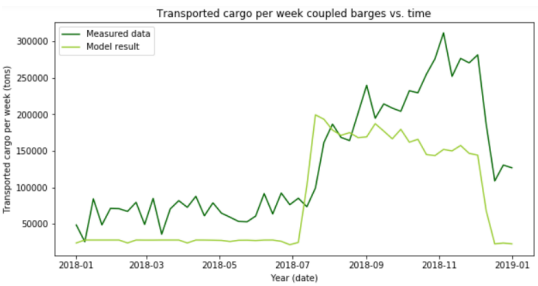

(d) Coupled barges

Figure 4.11: Observed transported cargo by different vessel types and model results before calibration

	RMSE (*tons*)	**CV(RMSE)**
6-barge push convoys	101,551.6	0.449
Smaller push-barge convoys	99,857.8	1.026
Rhine vessels	18,780.7	0.468
Coupled barges	63,195.2	0.478
Average error	70,846.3	0.605

Table 4.10: The error in transported weight in the null scenario

The number of weekly trips per vessel type, related to the weekly active fleet size, is also compared to the IVS-90 data-set. The results of this comparison are presented graphically in Figure 4.12 and exact in Table 4.11.

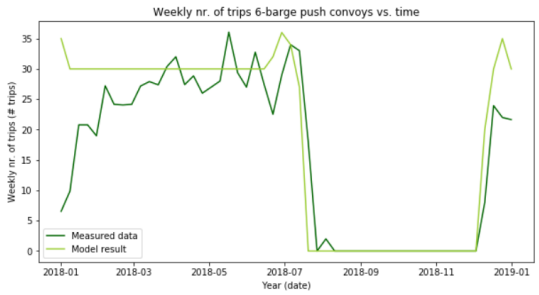

(a) 6-barge push convoys

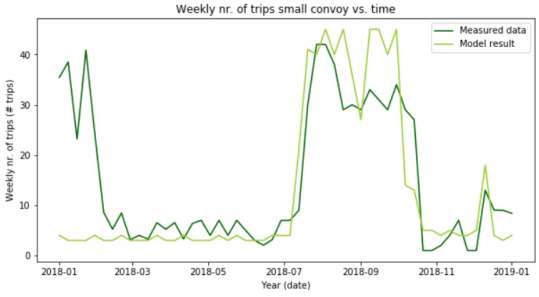

(b) Smaller convoys

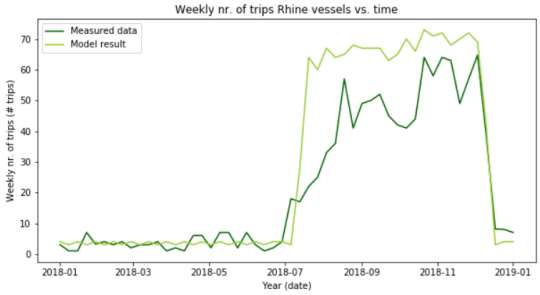

(c) Rhine vessels

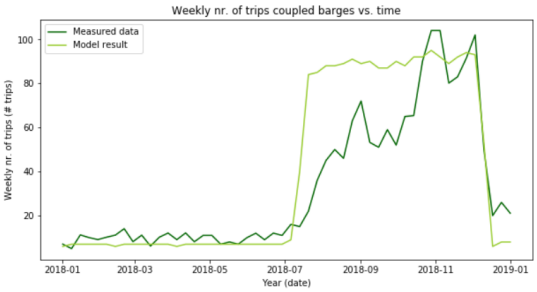

(d) Coupled barges

Figure 4.12: Observed trips by different vessel types and model results before calibration

	RMSE ($trips$)	**CV(RMSE)**
6-barge push convoys	7.138	0.449
Smaller push-barge convoys	11.098	0.752
Rhine vessels	14.077	0.641
Coupled barges	19,738	0.592
Average error	13.013	0.609

Table 4.11: The error in nr. of trips in the null scenario

The model results following from the initial conditions is called the 'null scenario'. The results of this null scenario are summarized in Table 4.12. As can be seen, the CV values for the transported weight and the nr. of trips is well below 1. This indicates that the model results have low variance and are capable of predicting actual values. Moreover, Figure 4.13 shows the correlation coefficients that have been obtained in the null scenario. For the transported cargo, a correlation coefficient of $r = 0.777$ was found, whereas for the number of trips a correlation coefficient of $r = 0.921$ was obtained.

Vessel type	**Transported weight RMSE** ($tons$)	**Transported weight CV(RMSE)**	**Trips RMSE** ($trips$)	**Trips CV(RMSE)**
6-barge push convoys	101,551.6	0.449	7.138	0.449
Smaller push-barge convoys	99,857.8	1.026	11.098	0.752
Rhine vessels	18,780.7	0.468	14.077	0.641
Coupled barges	63,195.2	0.478	19,738	0.592
Average error	70,846.3	0.605	13.013	0.609

Table 4.12: The summarized errors in transported weight and nr. of trips in the null scenario

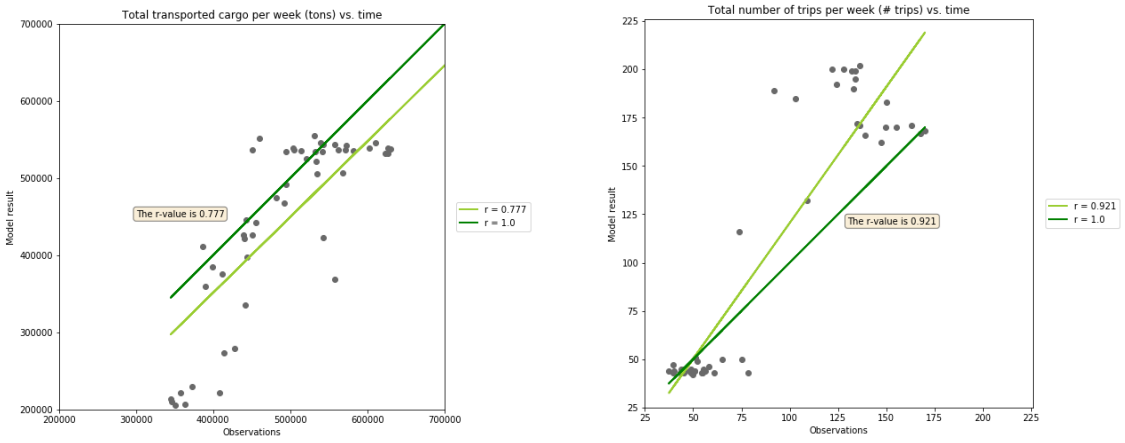

(a) Transported cargo (b) Number of trips

Figure 4.13: The correlation for the transported cargo and the number of trips in the null scenario

4.2.3. Calibration of manoeuvring time

The parameter here described as manoeuvring time does include manoeuvring time and waiting time before mooring. The manoeuvring times used in the null scenario follow from estimations based on observations and personal insight. There is a large uncertainty in this parameter, as the value does not follow from a real case. In addition, during drought, more vessels are in operation, thereby inducing more manoeuvring activities on the terminal Van Hussen et al. (2019). Beside the linear increase of manoeuvring times with the number of manoeuvres, this effect is expected to increase the waiting times significantly. The calibration thus considers an increase in average manoeuvring time per trip in a period of drought. This brings a variation between vessel types as not all vessels are active during drought. The manoeuvring time is represented in the model by an elongation of the time that a vessel spends at the port. The values from Table 4.13 are used as input for this validation.

Vessel type	**Null scenario Manoeuvring** ($hours$)	**Calibration Low** ($hours$)	**Calibration Medium** ($hours$)	**Calibration High** ($hours$)
6-barge push convoys	1.0	1.0	2.0	3.0
Smaller push-barge convoys	2.0	2.0	3.0	4.0
Rhine vessels	3.0	3.0	4.0	5.0
Coupled barges	3.0	3.0	4.0	5.0

Table 4.13: Overview of tested manoeuvring times

The results of this calibration step can be found in Tables 4.14, 4.15 and 4.16. The values in Table 4.14 correspond to the null scenario. It follows that higher manoeuvring time for every vessel class results in a more accurate prediction of the trips. The changes are significant. At the same time, the error of the transported weight improves only for the 6-barge push convoys. The model results for the transported weight become less precise for the other three vessel types. Compared to the improvements in the trips, however, these reductions in accuracy are significantly less. Nevertheless, calibration is stopped after the high-case manoeuvring times as a further reduction of accuracy of the transported weight is undesired. This is supported by the 6-barge push convoys also decreasing in accuracy when increasing its manoeuvring time further. The trends of the results is shown in Figures 4.14 and 4.15.

Vessel type	Transported weight RMSE ($tons$)	Transported weight CV(RMSE)	Trips RMSE ($trips$)	Trips CV(RMSE)
6-barge push convoys	101,551.6	0.449	7.138	0.449
Smaller push-barge convoys	99,857.8	1.026	11.098	0.752
Rhine vessels	18,780.7	0.468	14.077	0.641
Coupled barges	63,195.2	0.478	19,738	0.592
Average error	70,846.3	0.605	13.013	0.609

Table 4.14: Summarized errors with manoeuvring times for low-case

Vessel type	Transported weight RMSE ($tons$)	Transported weight CV(RMSE)	Trips RMSE ($trips$)	Trips CV(RMSE)
6-barge push convoys	92,781.5	0.410	6.614	0.417
Smaller push-barge convoys	100,233.5	1.030	10.824	0.733
Rhine vessels	20,247.4	0.504	12.750	0.580
Coupled barges	66,693.9	0.505	17.853	0.535
Average error	69,989.1	0.612	12.010	0.566

Table 4.15: Summarized errors with manoeuvring times for medium-case

Vessel type	Transported weight RMSE ($tons$)	Transported weight CV(RMSE)	Trips RMSE ($trips$)	Trips CV(RMSE)
6-barge push convoys	88,135.1	0.389	6.443	0.406
Smaller push-barge convoys	100,703.4	1.035	10.690	0.724
Rhine vessels	20,780.8	0.518	10.795	0.491
Coupled barges	69,969.5	0.529	16.246	0.487
Average error	69,897.2	0.618	11.043	0.527

Table 4.16: Summarized error with manoeuvring times for high-case

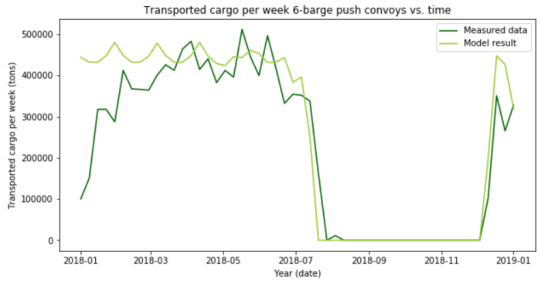

(a) 6-barge push convoys

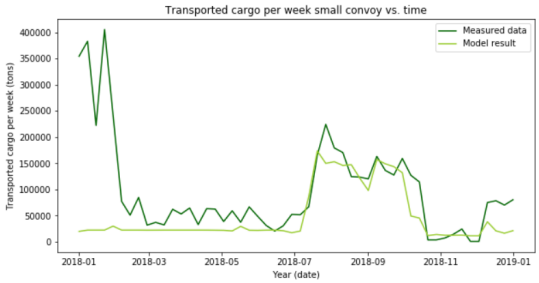

(b) Smaller push-barge convoys

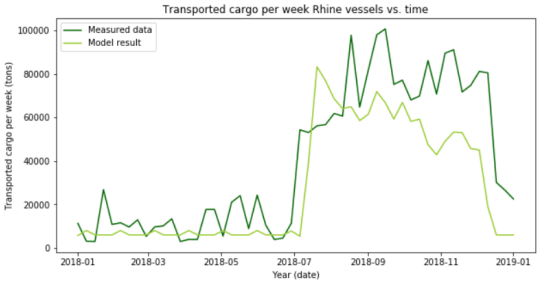

(c) Rhine vessels

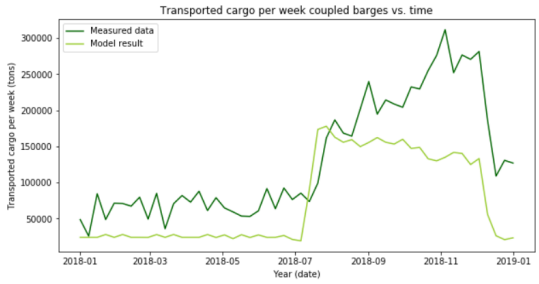

(d) Coupled barges

Figure 4.14: Observed transported cargo by different vessel types after calibration of manoeuvring time

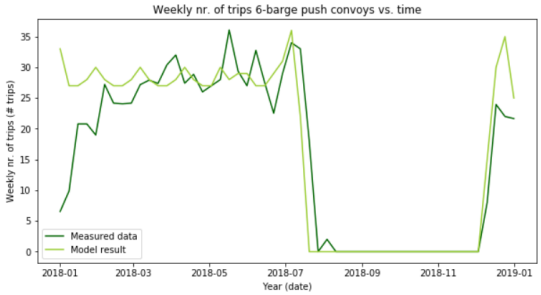

(a) 6-barge push convoys

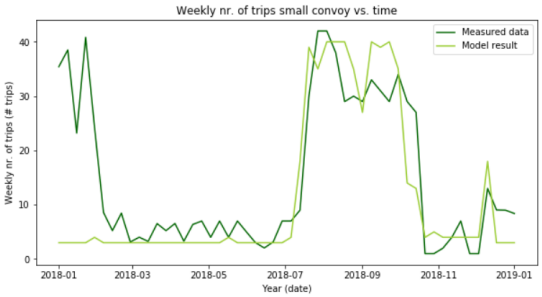

(b) Smaller convoys

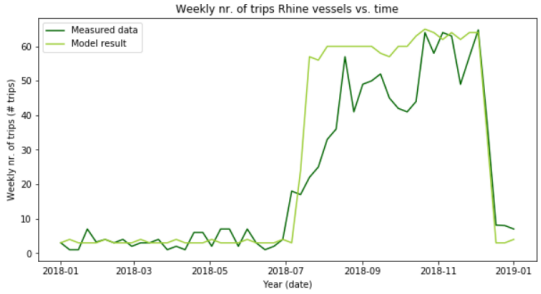

(c) Rhine vessels

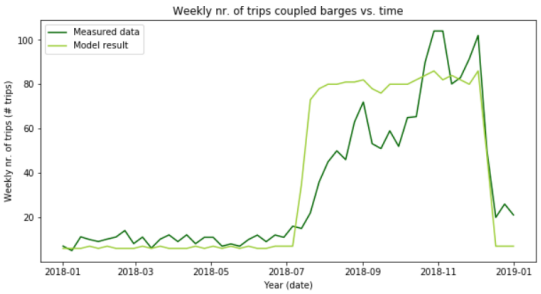

(d) Coupled barges

Figure 4.15: Observed trips by different vessel types after calibration of manoeuvring time

The correlation coefficient between the model results and observations with a calibrated manoeuvring time is seen to be higher for the transported cargo and equal for the number of trips, relative to the null scenario. Values are obtained of $r = 0.806$ for the transported cargo and $r = 0.921$ for the number of trips. These are depicted in Figures 4.16a and 4.16b. This indicates a slightly better fit of the model results to the observations after calibration of the manoeuvring time.

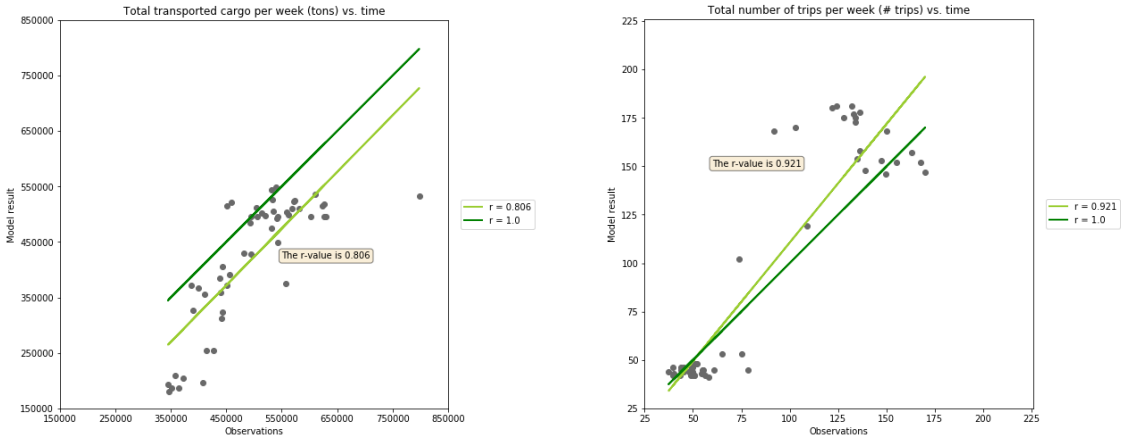

(a) Transported cargo (b) Number of trips

Figure 4.16: The correlation for the transported cargo and the number of trips after calibration of the manoeuvring time

4.2.4. Calibration of vessel type capacity

An initial estimation was done for the vessel capacity. However, both for the smaller push-barge convoys and for the coupled barges a large variation in capacity is possible. As was written, smaller push-barge combinations can sail with 1, 2 or 4 barges. As such, their capacity varies from approximately 2,700 $tons$ to 11,000 $tons$. Furthermore, the agents that account for the coupled barges vessel type can sail with 1, 2 or even 3 barges alongside, although 1 or 2 is most common. The range of capacities for each vessel type is expected to have significant effect on the network performance. An effort is therefore made to study the average capacity that best reflects the capacity of the smaller convoys and coupled barges respectively. The capacities that have been tested are given in Table 4.17.

Vessel type	**Null scenario Capacity** ($tons$)	**Calibration Low** ($tons$)	**Calibration Medium** ($tons$)	**Calibration High** ($tons$)
6-barge push convoys	16,000	16,000	16,000	16,000
Smaller push-barge convoys	7,500	6,000	7,500	9,000
Rhine vessels	2,000	1,500	2,000	2,500
Coupled barges	4,000	3,500	4,000	4,500

Table 4.17: Overview of tested vessel capacities

The results of this calibration step can be found in Tables 4.18, 4.19 and 4.20. From these, it can be concluded that the error decreases in general for both the transported weight and the trips when increasing the vessel capacity. For the Rhine vessels and the coupled barges, a higher capacity leads to a significantly reduced variance of both the transported cargo and the number of trips. For the smaller convoys, a higher capacity, however, brings a small improvement in the obtained error. It should be noted that the errors of the 6-barge push convoys vary while the capacity remains the same. This follows from the interdependency between vessels that was shown earlier. The trend of the results is shown in Figures 4.17 and 4.18. Following these values, in the obtaining of the correlation coefficients, the vessel capacity of the Rhine vessels and the coupled barges is increased to 2,500 $tons$ and 4,500 $tons$, respectively, while the capacities of the 6-barge push convoys and the smaller convoys are kept the same.

Vessel type	Transported weight RMSE ($tons$)	Transported weight CV(RMSE)	Trips RMSE ($trips$)	Trips CV(RMSE)
6-barge push convoys	102,590.8	0.453	7.138	0.450
Smaller push-barge convoys	102,798.6	1.057	11.291	0.765
Rhine vessels	24,410.6	0.608	14.241	0.648
Coupled barges	71,794.9	0.543	20.037	0.600
Average error	75,398.7	0.665	13.177	0.616

Table 4.18: Summarized error of capacity for low-case

Vessel type	Transported weight RMSE ($tons$)	Transported weight CV(RMSE)	Trips RMSE ($trips$)	Trips CV(RMSE)
6-barge push convoys	101,551.6	0.449	7.138	0.449
Smaller push-barge convoys	99,857.8	1.026	11.098	0.752
Rhine vessels	18,780.7	0.468	14.077	0.641
Coupled barges	63,195.2	0.478	19,738	0.592
Average error	70,846.3	0.605	13.013	0.609

Table 4.19: Summarized error of capacity for medium-case

Vessel type	Transported weight RMSE ($tons$)	Transported weight CV(RMSE)	Trips RMSE ($trips$)	Trips CV(RMSE)
6-barge push convoys	101,042.2	0.446	7.093	0.447
Smaller push-barge convoys	99,396.9	1.022	11.090	0.751
Rhine vessels	18,417.1	0.459	13.795	0.628
Coupled barges	56,306.8	0.426	19.572	0.587
Average error	68,790.7	0.588	12.888	0.603

Table 4.20: Summarized error of capacity for high-case

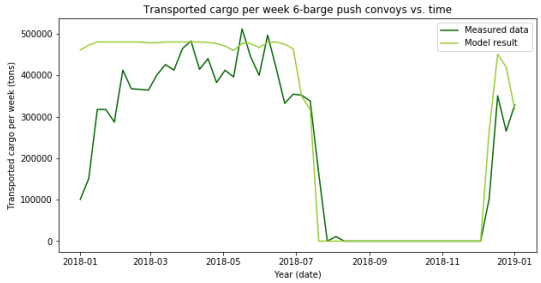

(a) 6-barge push convoys

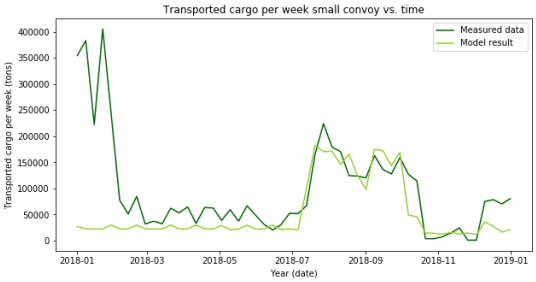

(b) Smaller push-barge convoys

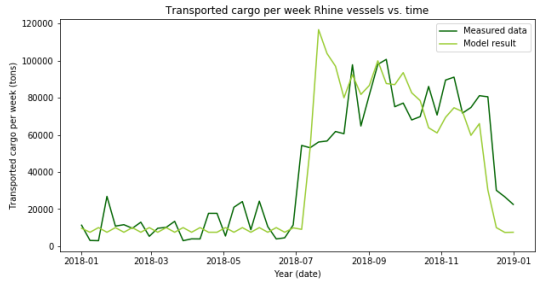

(c) Rhine vessels

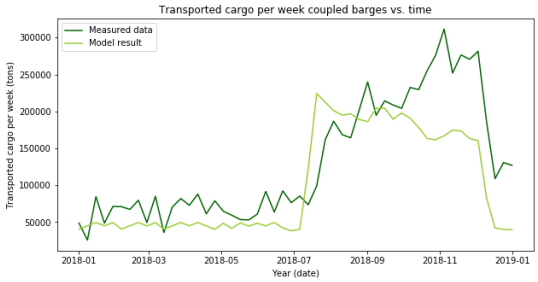

(d) Coupled barges

Figure 4.17: Observed transported cargo by different vessel types after calibration of vessel capacity

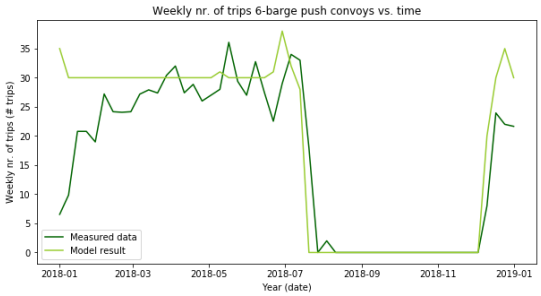

(a) 6-barge push convoys

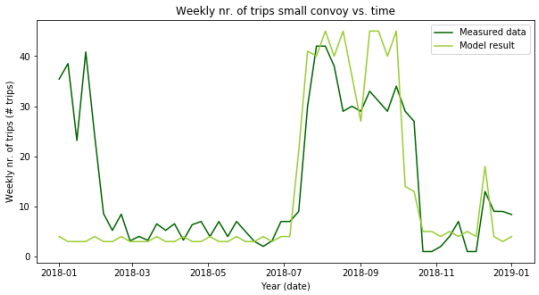

(b) Smaller convoys

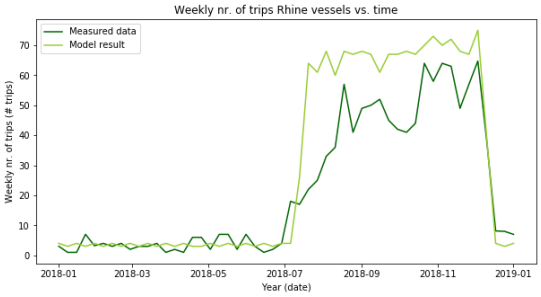

(c) Rhine vessels

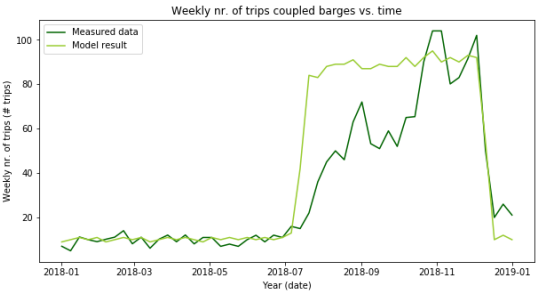

(d) Coupled barges

Figure 4.18: Observed trips by different vessel types after calibration of vessel capacity

The correlation coefficient between the model results and observations with a calibrated vessel capacity is seen to be lower for both the transported cargo and the number of trips. Values are obtained of $r = 0.758$ for the transported cargo and $r = 0.920$ for the number of trips. These are depicted in Figures 4.19a and 4.19b. Lower correlation coefficients indicate a worse fit of the model results to the observations. The decision is therefore made to only change vessel capacities that induce a significantly smaller CV(RMSE). This is the case

for the capacities of both the Rhine vessels and the coupled barges. Their capacities are thus increased to 2,500 $tons$ and 4,500 $tons$ respectively.

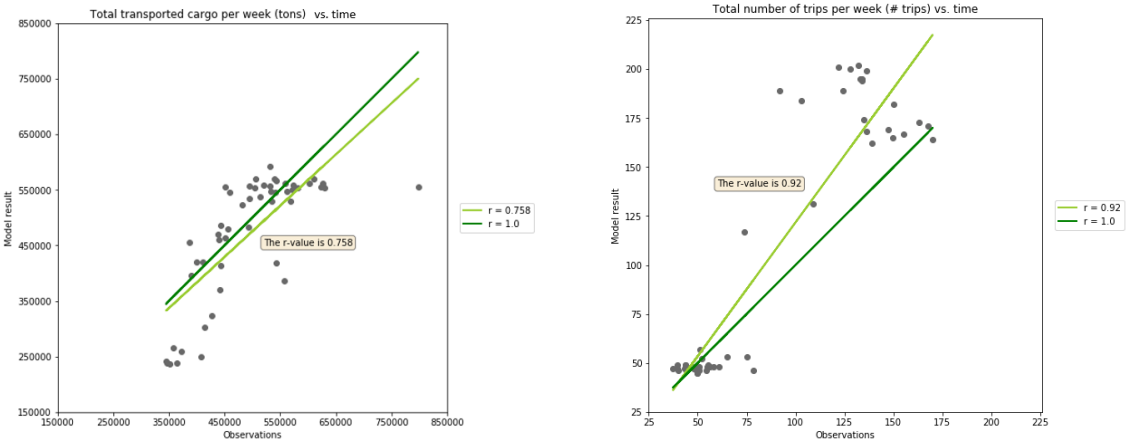

(a) Transported cargo (b) Number of trips

Figure 4.19: The correlation for the transported cargo and the number of trips after calibration of the vessel capacity

4.2.5. Uncertainties and errors

The error between the model results and reality is substantial. Following the internal validation, the model functions correctly. The error thus follows from uncertainties and simplifications made in the model. This section will scrutinize to what extent the error can be explained.

Especially the transported weight of push-barge convoys in the winter of 2018 gives relatively large errors. The model was built to simulate IWT in times of drought, usually occurring in the summer. The focus should therefore be on the last 6 months of 2018 for which the error is smaller than for the first 6 months, see Table 4.21. Figures 4.20 and 4.21 show the difference in correlation for both seasons. In summer, a correlation coefficient of $r = 0.789$ is found for the transported cargo and of $r = 0.719$ is found for the number of trips. In winter, correlation coefficients of $r = 0.312$ for the transported cargo and of $r = 0.466$ for the number of trips are found. It can be concluded that the accuracy of the model predictions for the transported weight during drought is therefore higher than for the hydrological winter. This mainly results from errors in the predictions of the 6-barge push convoys and the smaller convoys transport.

	Transported weight RMSE ($tons$)	**Transported weight CV(RMSE)**	**Trips RMSE ($trips$)**	**Trips CV(RMSE)**
Winter (wet)	71,730.8	0.760	6.599	0.673
Summer (dry)	49,719.6	0.506	12.555	0.537

Table 4.21: Errors in winter vs. summer

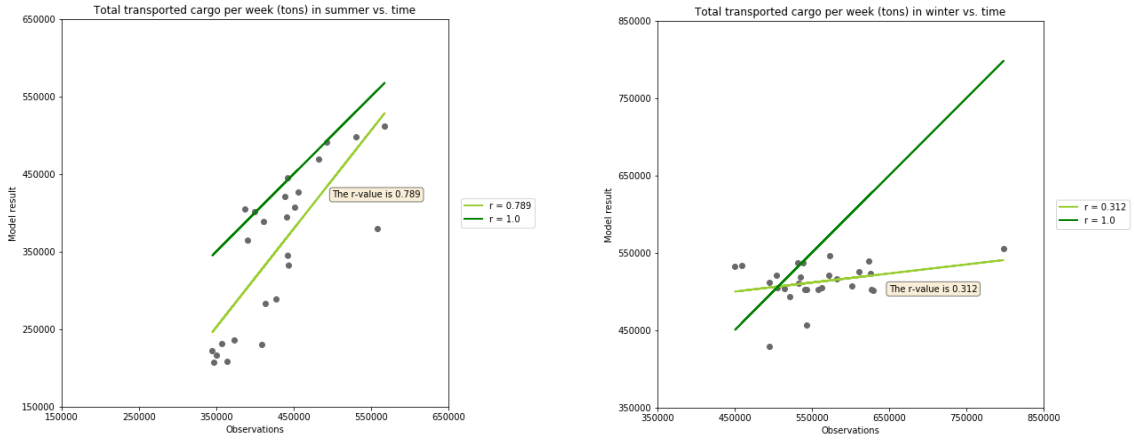

(a) Summer (b) Winter

Figure 4.20: The correlation for the transported cargo in summer and winter

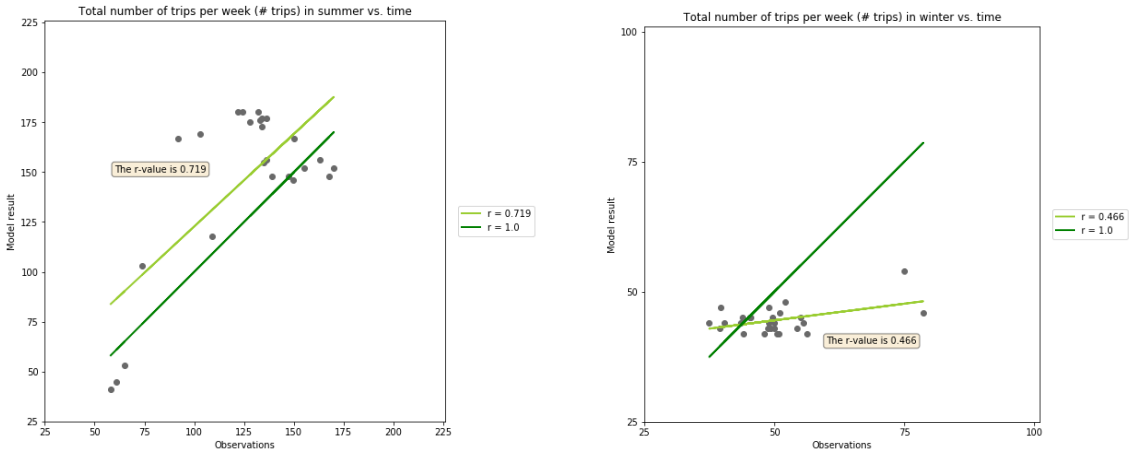

(a) Summer (b) Winter

Figure 4.21: The correlation for the number of trips in summer and winter

The model makes use of four vessel types. Each vessel type has its own characteristics and consequently its own RMSE and CV(RMSE). The vessel type with the largest error is the smaller push-barge convoys. Especially the error in predicted values of the transported cargo is significantly higher than the errors related to the other vessel types and even falls outside the boundaries of low variance. The large difference in this error can largely be explained by the high transport in the measured data in the early months of 2018. This can be a compensating effect that resulted from 2017. When excluding this period and selecting the relevant window, the errors of the smaller push-barge convoys decrease significantly, as is presented in Table 4.22.

	Transported weight RMSE $(tons)$	**Transported weight CV(RMSE)**	**Trips RMSE** $(trips)$	**Trips CV(RMSE)**
Smaller push-barge convoys	32,632.2	0.443	5.496	0.415

Table 4.22: Errors of smaller convoys excluding 2018-01 and 2018-02

An important assumption in the model is that the demand for cargo that cannot be transported will continue existing. In reality, when vessel prices go up, many parties will consider postponing the transport of their resources. The demand will thus decrease in dry times. This is not included in the model and will induce errors.

An effect that has not been included is a restriction of the transport due to the width of the river. With decreasing water depths, also the width of the waterway reduces. This can lead to the logistical restriction of

agents being allowed to sail in one direction only part of the day. In other words, the time window for sailing could be reduced, thereby limiting the transport.

Finally, some uncertainty exists in the accuracy of the data-set that can be seen in Appendix B. The sum of trips in a week at times gives a number with decimals. This cannot be physically possible as trips cannot be split. In the preparation of the calibration, special attention was given to these numbers to see whether they fit the trend. In addition to errors in the data-set, it is unknown whether all observed trips had Duisburg as their final destination. A selection was made in vessels leaving from Europoort and passing the German border at Lobith. Of these dry bulk vessels, most are expected to travel to Duisburg. Nonetheless, part of the error could result from having considered vessels that did not match the intended route.

4.2.6. Conclusion of calibration

Higher manoeuvring times than the null scenario for every vessel class result in a more accurate prediction of the trips. These changes are significant. At the same time, the CV(RMSE) for the transported weight improves only for the 6-barge push convoys. Compared to the improvements in the errors in nr. of trips, however, these reductions in accuracy are much lower. The correlation coefficient for the transported cargo increases whereas the r remains equal for the number of trips. An increase in manoeuvring time is therefore proposed for all agent types.

A higher capacity than the null scenario is seen to have a positive effect on the errors regarding the transported weight and the number of trips for all vessel classes. For smaller convoys, a variation of the capacity gave negative outcomes. For the Rhine vessels, a higher capacity, however, also results in much larger error for the trips. Only the capacity of the coupled barges is therefore adjusted to $5,000\ tons$.

From these, it can be concluded that the error decreases in general for both the transported weight and the trips when increasing the vessel capacity. For the Rhine vessels and the coupled barges, a higher capacity leads to a significantly reduced variance of both the transported cargo and the number of trips. For the smaller convoys, a higher capacity, however, brings a small improvement in the obtained error. In the obtaining of the correlation coefficients, the vessel capacity of the Rhine vessels and the coupled barges is increased to $2,500\ tons$ and $4,500\ tons$, respectively, while the capacities of the 6-barge push convoys and the smaller convoys are kept the same.

The correlation coefficient between the model results and observations with a calibrated vessel capacity is seen to be lower for both the transported cargo and the number of trips. Values are obtained of $r = 0.758$ for the transported cargo and $r = 0.920$ for the number of trips. The decision is therefore made to only change vessel capacities that induce a significantly smaller CV(RMSE) as is the case for the capacities of both the Rhine vessels and the coupled barges.

The input values that follow from the calibration are given in Table 4.23. In addition, the results of the calibration phase are given in Table 4.24. These results show CV(RSME) values well below the critical value of 1. The correlation coefficients have been increased during the calibration phase to values of $r = 0.794$ for the transported cargo and $r = 0.921$ for the number of trips. As such, it can be stated that the model results are accurate projections of reality.

	Capacity ($tons$)	**Manoeuvring time** ($hours$)
6-barge push convoys	16,000	3.0
Smaller push-barge convoys	7,500	4.0
Rhine vessels	2,500	5.0
Coupled barges	4,500	5.0

Table 4.23: Overview of input after calibration

Vessel type	Transported weight RMSE ($tons$)	Transported weight CV(RMSE)	Trips RMSE ($trips$)	Trips CV(RMSE)
6-barge push convoys	87,474.4	0.386	6.425	0.405
Smaller push-barge convoys	32,623.2	0.443	5.496	0.415
Rhine vessels	18,171.9	0.453	10.750	0.489
Coupled barges	62,374.6	0.472	15.941	0.478
Average error	50,163.3	0.439	9.653	0.445

Table 4.24: Overview of output after calibration

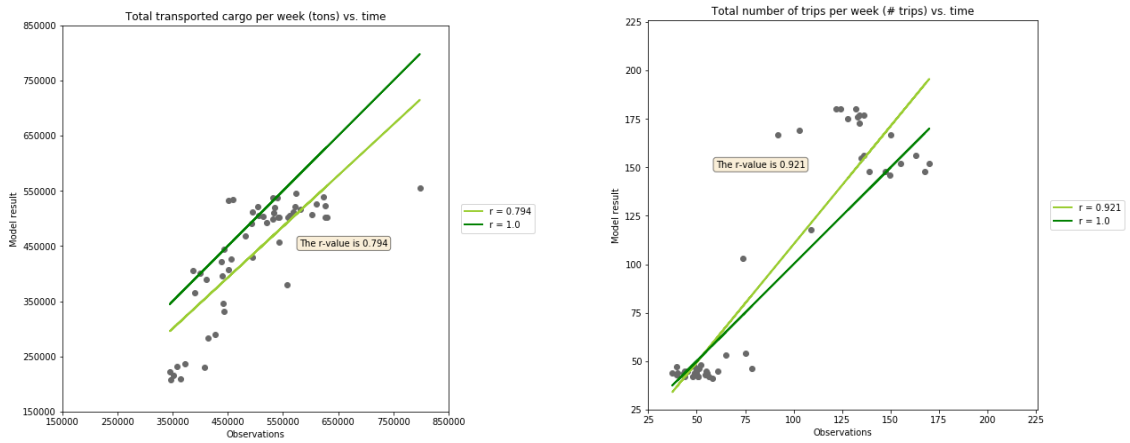

(a) Transported cargo (b) Number of trips

Figure 4.22: The correlation for the transported cargo and the number of trips after calibration

4.3. Conclusion

The results of the network performance model have been proven to be accurate with reality. As such, the model can successfully project the key indicators of the network performance. It can thus be used for further application. This chapter has thus successfully addressed the following sub-question:

Can the performance indicators be reproduced for a reference period of low water depths?

The model has passed all four tests of the internal validation. These tests concluded on the functioning of the load factor, the number of trips, the transport demand and on the vessel price. The internal validation has thus been carried out successfully and the functionality of the different model components has been proven. For that reason, the qualitative results of the model are correct and the model is able to simulate network performance in terms of transport parameters.

The model was then calibrated on two parameters that have a high uncertainty and a significant impact on the simulation; the manoeuvring time per trip and the agent capacity. For this purpose, an IVS-90 dataset was obtained that describes observations on the transported weight and the number of trips for dry bulk transport originating from Rotterdam in 2018. The calibration was thus carried out for the transported weight and the number of trips in the dry year of 2018.

It was shown that higher manoeuvring times for every vessel class result in a more accurate prediction of the nr. of trips. These changes are significant. At the same time, however, the error related to the transported weight improves only for the 6-barge push convoys. Compared to the increased accuracy of predicting the nr. of trips, however, these reductions in accuracy are much lower. An increase in manoeuvring time is therefore proposed for all vessel types.

An increase of capacity was seen to cause a reduction of the error in the transported weight for the Rhine vessels and the coupled barges. At the same time, an increase in capacity causes a larger error in the number of trips for the Rhine vessels. An increase in capacity is therefore only proposed for the coupled barges. Other vessel types showed no improvement. For that reason, the capacity of the coupled barges is increased and that of the other vessel types remains the same.

The results of the calibrated case have been plotted in Figures 4.23 and 4.24.

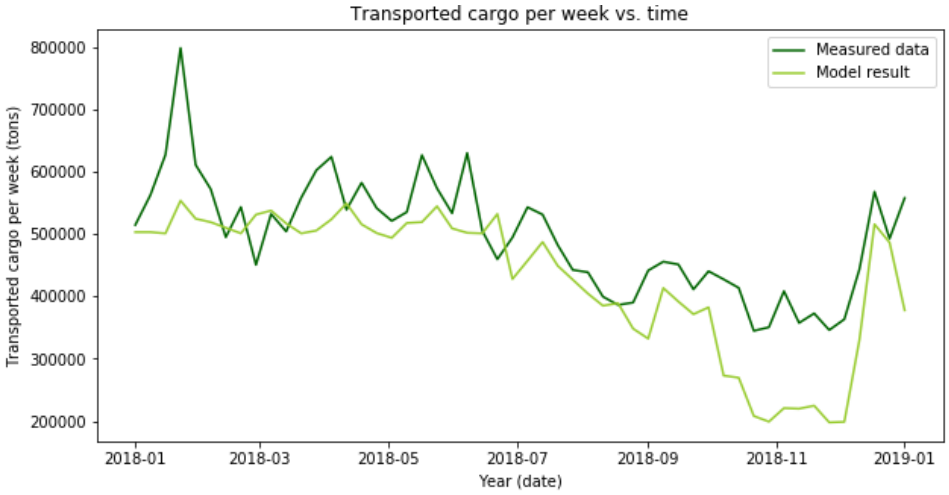

Figure 4.23: Observed weekly transported cargo and model results after calibration as sum of vessel classes

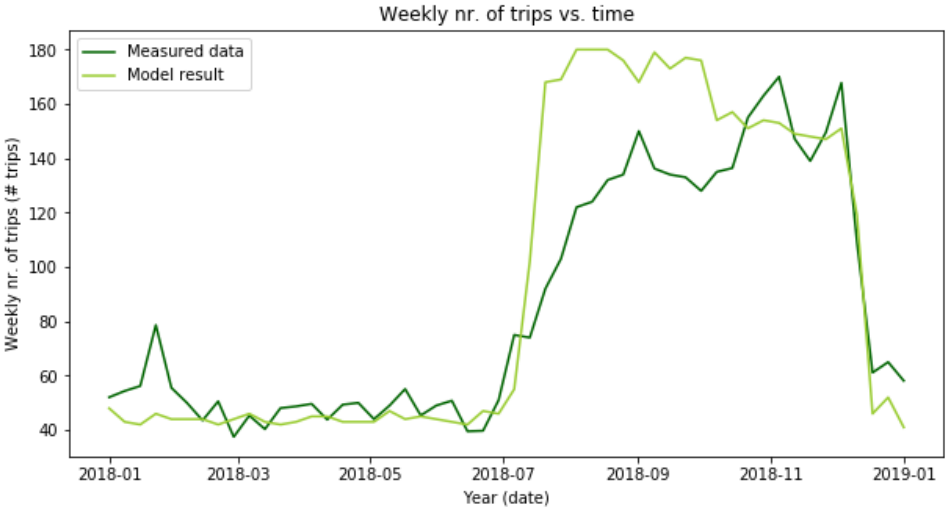

Figure 4.24: Observed weekly nr. of trips and model results after calibration as sum of vessel classes

5

Application and results

The impact of low water depths on the IWT performance is studied in this chapter. Both for the RUST- and for the STOOM-scenario, the discharge projection in 2050 is used to conclude on the performance indicators. Both cases will be compared to a base scenario which describes a discharge profile that undershoots 1020 m^3/s for the maximum allowable number of days (i.e. 5% of the year). Furthermore, the drought of 2018 is incorporated to put into perspective both the base scenario and the climate scenarios. This comparison in Sections 5.1 and 5.2 addresses the following research question:

What is the impact of periods with low discharge on the performance of the IWT network between Rotterdam and Duisburg?

The most promising measures to enhance the performance of the IWT network in times of drought have been identified in Section 2.4. The considered potential adaptations involve an equipment, an infrastructural and a site measure. These adaptation measures will be represented schematically in the model. The ideal fleet size in terms of transported weight and related transport costs has been determined for the equipment measure. For the infrastructural measure, the ideal number of river training works have been found. As this application aims to present a comparison between adaptation measures, these ideal values are used in this chapter. The determination of the ideal values is presented in Appendix F. Sections 2.4 and 5.4 address the following research question:

What adaptation measure to enhance the IWT network performance is most promising in terms of benefits and costs?

The different adaptation measures are tested in the network performance model to see the relative effect of each measure on the key performance indicators of the IWT performance. First, in Section 5.1, a base scenario is set for both considered climate projections following a case study. The results of this base scenario are presented in Section 5.2. Section 5.3 describes the way of schematically representing the adaptation measures in the model. Moreover, this section presents the results regarding the key performance indicators following from the simulations. Both the measure-effectiveness and cost-effectiveness per adaptation measure are given in Section 5.4. Ultimately in Section 5.5, an answer is provided to the addressed research question by concluding on the most promising adaptation measure.

5.1. Impact scenarios

The input values that are used per scenario are described below. First, the chosen water depth profile is elaborated on for each scenario. Consequently, the generic input values that are kept as constants throughout the model runs are given. A case study is performed to set a base scenario. The key performance indicators of this scenario can then be used to compare the model outputs of different cases with. In this manner, the relative improvement per measure can be assessed.

The base scenario is set using a discharge profile that undershoots 1020 m^3/s for the maximum allowable number of days (i.e. 5% of the year). This profile can be seen as the driest yearly discharge while meeting the agreement between Dutch authority and IWT operators. The discharge profile from the representative year 1969 has been used as this was seen to correspond with the desired base profile. The corresponding critical

water depth profile has its days of low discharge in November, as can be seen in Figure 5.1. In approximation, the return period of this water depth profile can be said to be equal to $T = 2\ years$ (de Jong, 2019).

For both the RUST-scenario and the STOOM-scenario, the discharge profile has been described in 2.1.2. The discharges of the representative year 1976 have been extrapolated to 2050 under both climate scenarios. The obtained discharge profile represents low discharges with a return period of $T = 10\ years$. Climate change is projected to change the average Rhine discharge so that a discharge with a return period of $T = 10\ years$ will describe a more extreme profile in 2050 than it will in 2019. For both climate scenarios, the obtained critical water depth profile has been given in Figure 5.1.

To put into perspective the impact of both climate scenarios, a reference scenario of 2018 is also studied. This discharge profile is seen to have a number of days of low discharge that correspond to a return period $T = 20\ years$ (Kramer et al., 2019). Moreover, the profile shows a long period of consecutive days of low discharge. The critical water depth profile for the reference scenario of 2018 is shown in Figure 5.1. The model results for this scenario follow from the IWT performance model and are therefore not the true values for the transported cargo and transport costs observed in 2018.

The significant water depths of $3.0m$ and $2.25m$, that denote the depths beneath which the 6-barge push convoys and the smaller convoys, respectively, become inactive, are depicted in Figure 5.1.

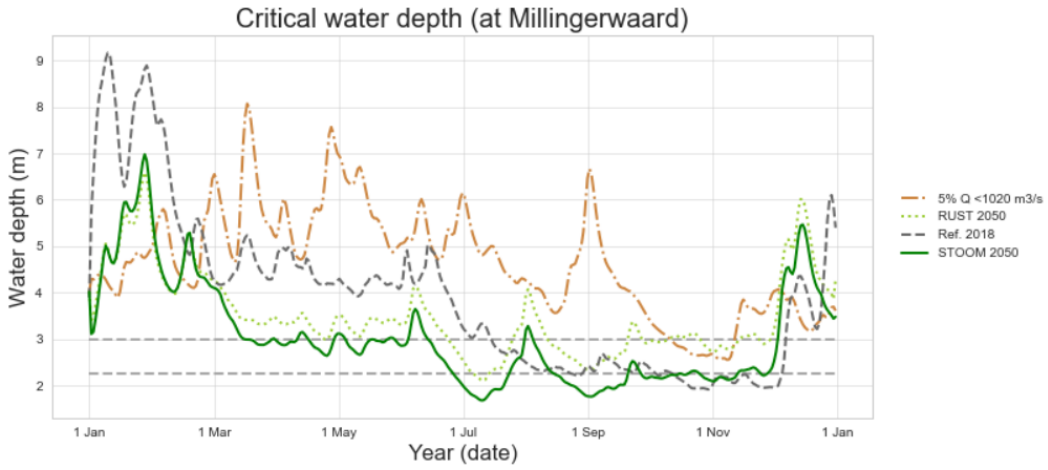

Figure 5.1: Critical water depth at Millingerwaard for all scenarios

From this figure, it appears that the critical water depth for 2018 was insufficient for unrestricted loading for over six consecutive months. Moreover, the water depth undershoots the limit of $3.0m$ for four consecutive months. It appears that the water depth profile extrapolated from 1976 to compute the water depths for the RUST- and STOOM-scenario, has a longer period in which it is insufficient for the unrestricted loading of vessels than 2018. Compared to the RUST-scenario, however, 2018 accounts for a longer period of water levels below $3.0m$. This causes the water depth profile, and correspondingly the discharge profile, of 2018 to be more severe than the RUST-scenario, but less severe than the STOOM-scenario. The studied scenarios that are used to assess the impact of low discharges are listed in Table 5.1.

Name	**Representative year**	**Days discharge below** $1020\ m^3/s$	**Return period**
Base scenario	1969	20	2
RUST scenario	1976	52	10
STOOM scenario	1976	161	10
Reference 2018	2018	126	20

Table 5.1: Scenarios used to assess impact of low discharges

The generic input values follow from the analysis of Chapter 2 on the Rhine as the Rotterdam-Duisburg corridor in the year 2050. Moreover, the values obtained in the calibration are adopted. The generic input values can be found in Table 5.2.

The simulation, that runs for a year, computes the transported cargo and the transport costs as indicators of the network performance. The size of the simulation period has been given this length as aftereffects (i.e.

	Unit	Value
General		
Transport demand	[tons/year]	32 mln
Safety margin	[m]	0.75
Sailing speed unloaded downstream	[m/s]	4.50
Sailing speed loaded upstream	[m/s]	2.25
Costs of insufficient supply (indirect)	[€/ ton]	15
6-barge push convoys		
Convoy capacity	[tons]	16,000
Barge draught empty	[m]	0.65
Barge draught full	[m]	3.95
Fleet size	[pusher boats]	10
Manoeuvring time	[hours]	3
Agent price	[€/ day]	15,000
Smaller push-barge convoys		
Convoy capacity	[tons]	7,500
Barge draught empty	[m]	0.65
Barge draught full	[m]	3.95
Fleet size	[pusher boats]	10
Manoeuvring time	[hours]	4
Agent price	[€/ day]	7,500
Rhine vessels		
Rhine vessel capacity	[tons]	2,500
Rhine vessel draught empty	[m]	1.20
Rhine vessel draught full	[m]	3.0
Fleet size	[Rhine vessels]	15
Manoeuvring time	[hours]	5
Agent price	[€/ day]	2,500
Coupled barges		
Coupled barge capacity	[tons]	4,500
Barge draught empty	[m]	0.65
Barge draught full	[m]	3.95
Fleet size	[coupled barges]	20
Manoeuvring time	[hours]	5
Agent price	[€/ day]	7,000
Site equipment		
Nr. of resources	[berths]	6
Loading rate	[ton/s]	1.25
Unloading rate	[ton/s]	0.75

Table 5.2: Input values from Rotterdam-Duisburg corridor (Backer van Ommeren, 2011, Ertsoverslagbedrijf Europoort CV, 2018, NEA, 2015, Van Hussen et al., 2019)

in a following year) of reduced network performance appeared to be absent, both in the data-set used for calibration and in the initial model results. The transported weight has been calibrated and should thus be given most weight to. The vessel prices and costs of insufficient supply follow from several studies on the economics of IWT (NEA, 2015, Van Hussen et al., 2019). Van Hussen et al. (2019) use costs between €15,– to €20,– per ton of transport deficit for the indirect impact of insufficient supply. This includes the effects of a temporary modal shift and the costs of stockpiling. Due to the relative ease with which iron ore and coal can be stockpiled, costs of €15,– per ton of transport deficit are adopted in this research. Following from economic studies, the transport costs are expected to represent reality well. The transport costs have, however, not been calibrated and should thus be seen as an indicator that can be used to compare different scenarios. The key performance indicators can be considered both weekly and cumulative. Both options

provide a break-down in different vessel types to provide a clear image of the contributors to the network performance.

5.2. Impact of low discharges

The exact output of the model executions of the various scenarios is given in Table 5.3.

	Unit	Value Base	Value RUST	Value STOOM	Value 2018
Number of trips					
Nr. of trips	[trips]	2,985	4,780	6,541	4,844
Nr. of trips June - November	[trips]	1,822	3,454	4,000	3,617
Nr. of trips January - May and December	[trips]	1,163	1,326	2,541	1,227
Trips 6-barge push convoys	[trips]	1,360	1,036	485	900
Trips smaller convoys	[trips]	342	794	858	595
Trips Rhine vessels	[trips]	436	1,168	2,184	1,367
Trips coupled barges	[trips]	847	1,782	3,014	1,982
Transported weight					
Transported weight	[tons]	26,048,467	24,303,059	20,580,313	22,650,078
Transport June - November	[tons]	12,845,937	11,683,432	7,709,564	9,520,063
Transport January - May and December	[tons]	13,202,529	12,619,627	12,870,749	13,130,014
Transport 6-barge push convoys	[tons]	20,426,582	13,609,034	6,833,572	13,530,192
Transport smaller convoys	[tons]	1,854,590	3,652,075	3,755,252	2,544,450
Transport Rhine vessels	[tons]	856,937	2,082,329	3,017,463	1,902,022
Transport coupled barges	[tons]	2,910,358	4,959,620	6,974,027	4,773,415
Transport costs					
Total costs	[€]	62,180,575	105,909,552	181,282,691	137,055,621
Costs June - November	[€]	38,138,345	71,257,903	142,234,702	116,333,499
Costs January - May and December	[€]	24,042,230	34,651,649	39,047,989	20,722,122
Costs of insufficient supply	[€]	10,724,354	28,990,508	83,504,660	55,552,704
Costs 6-barge push convoys	[€]	33,346,873	27,135,248	10,273,291	22,482,460
Costs smaller convoys	[€]	4,911,093	13,722,204	14,756,583	10,945,683
Costs Rhine vessels	[€]	1,704,487	5,575,611	13,882,030	9,446,753
Costs coupled barges	[€]	12,409,482	30,939,198	59,510,979	39,043,468

Table 5.3: Model output for scenarios on the Rotterdam-Duisburg corridor

From the output values of the scenarios, the impact of low discharges on the network performance becomes clear. The impact of both the RUST-scenario and the STOOM-scenario is compared to the base scenario. To put into perspective the outcomes of such a comparison, the reference scenario of 2018 is then included in the comparison. For the RUST-scenario, the impact on the performance indicators is given in Table 5.4.

	Unit	Absolute difference	Difference [%]
Transported weight	[tons]	−1,745,408	−6.7
Total costs	[€]	+43,728,977	+70.3

Table 5.4: Impact of RUST-scenario compared to base scenario

The results of the base scenario for the RUST projection are shown in Figures 5.2, 5.3 and 5.4. A clear distinction can be seen between the nr. of trips in the hydrological winter and summer. In the RUST-scenario, the difference in transported weight is not so evident, as the active vessels show near sufficient capacity to meet the transport demand. Nevertheless, the trend in cost shows a steeper increase during summer as a combined result of the higher number of trips and higher vessel prices.

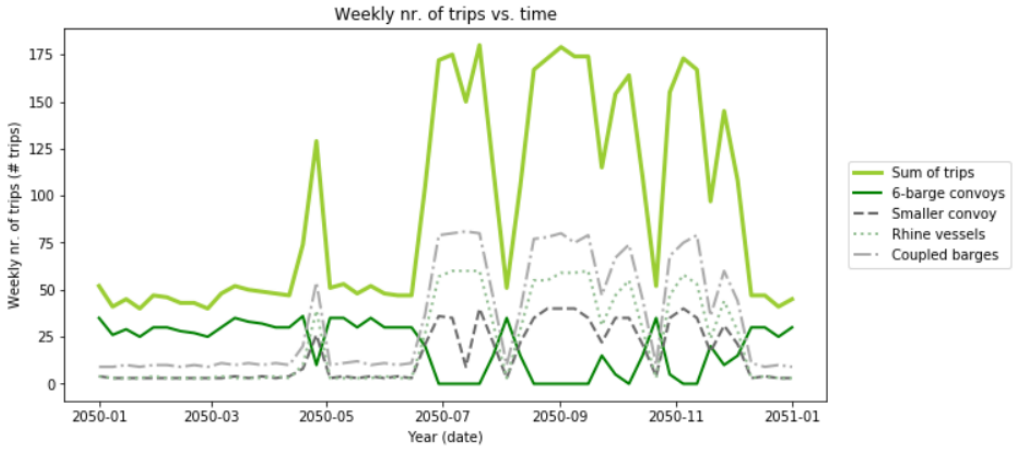

Figure 5.2: Number of trips in RUST-scenario

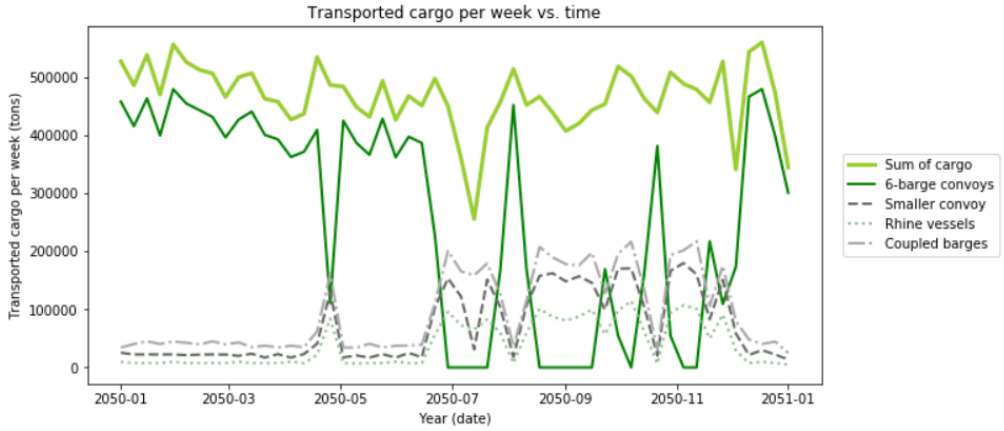

Figure 5.3: Transported cargo in RUST-scenario

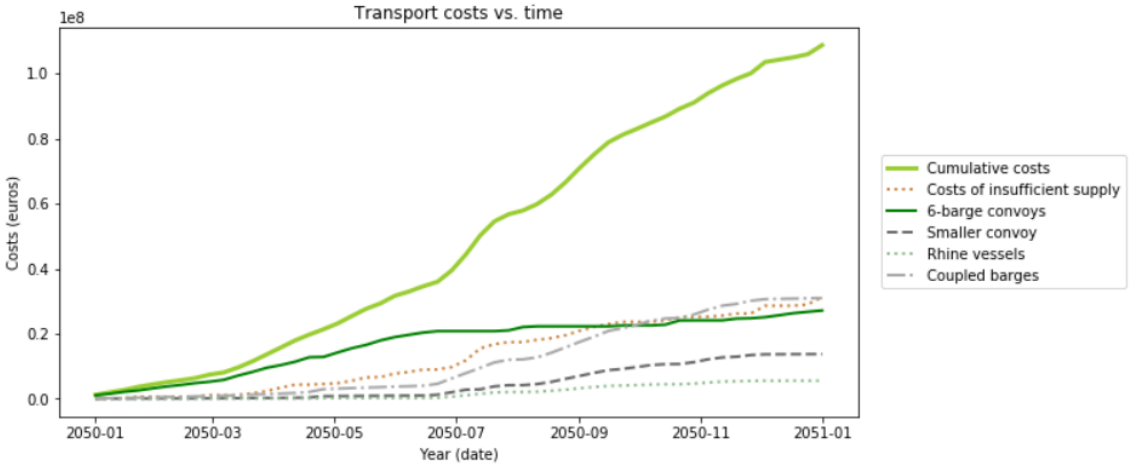

Figure 5.4: Transport costs in RUST-scenario

For the STOOM-scenario. the impact on the performance indicators is given in Table 5.5.

	Unit	Absolute difference	Difference [%]
Transported weight	[tons]	−5,468,154	−21.0
Total costs	[€]	+119,102,116	+191.5

Table 5.5: Impact of STOOM-scenario compared to base scenario

For the STOOM projection, the results of the base scenario are shown in Figures 5.5, 5.6 and 5.7. Besides the higher number of trips, a clear dip in transported cargo during the dry months can be distinguished in the STOOM-scenario. A steeper increase than for the RUST-scenario is seen for the transport costs, mainly due to the costs for not meeting the demand and the costs for the use of coupled barges.

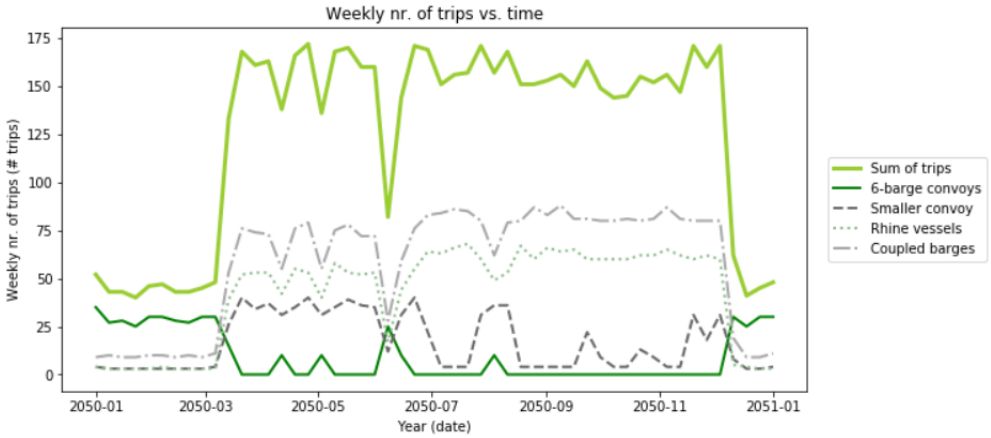

Figure 5.5: Number of trips in STOOM-scenario

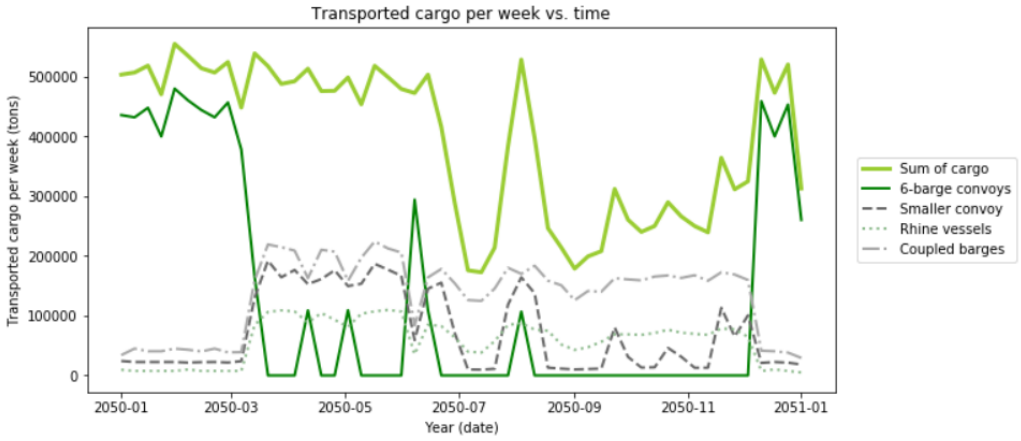

Figure 5.6: Transported cargo in STOOM-scenario

Figure 5.7: Transport costs in STOOM-scenario

Now that the impact of both climate scenarios relative to the base scenario has been computed, their relative impacts can be compared to the reference scenario of 2018. From the analysis of the water depth profiles, it was expected that 2018 would have an impact on the network performance that would be more severe than the RUST-scenario, but less severe than the STOOM-scenario. The impact of the various scenarios on the performance indicators after a simulation are given in Table 5.6. Moreover, Figures 5.8 and 5.9 show the trend of the transported cargo and the transport costs for the various scenarios throughout the simulation.

	Unit	**Base scenario**	**RUST [%]**	**STOOM [%]**	**Ref. 2018 [%]**
Transported weight	$[tons]$	26,048,467	−6.7	−21.0	−13.0
Total costs	[€]	62,180,575	+70.3	+191.5	+120.4

Table 5.6: Relative impact of climate scenarios and reference 2018

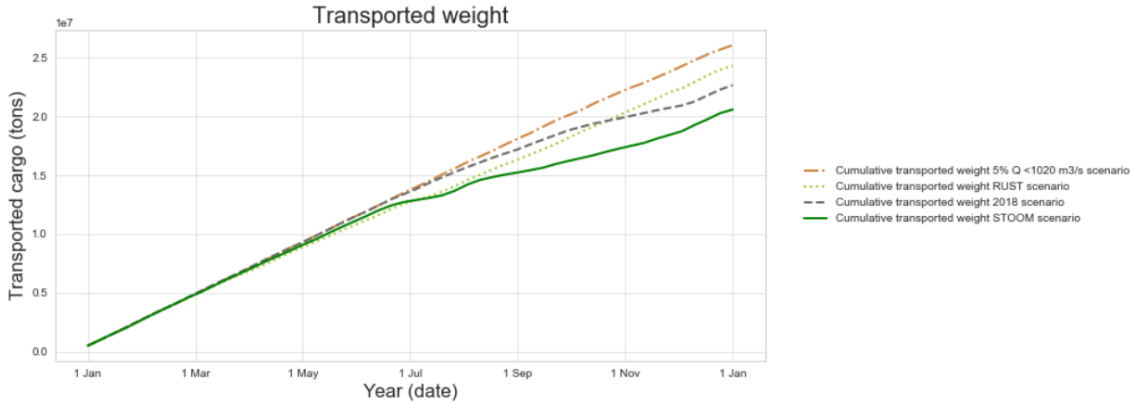

Figure 5.8: Cumulative transported weight in impact scenarios

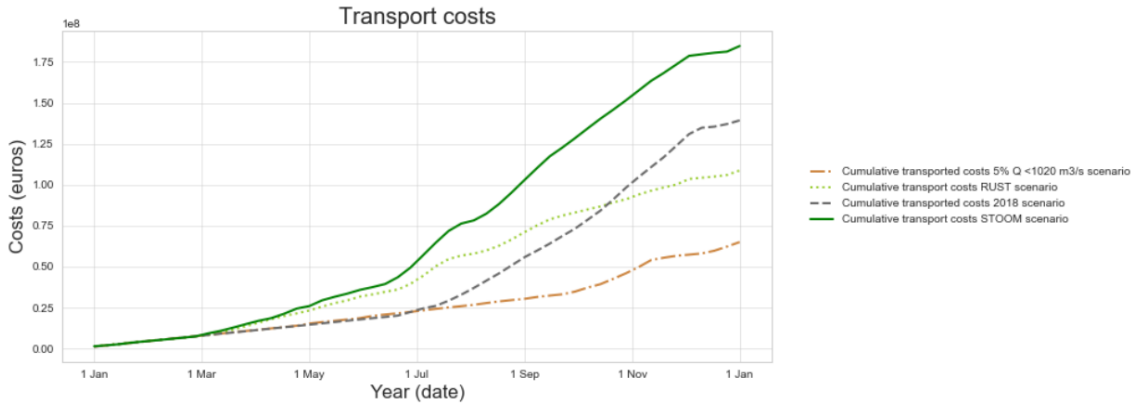

Figure 5.9: Cumulative transport costs in impact scenarios

From these trends, it becomes clear that the water depth profile used in both climate scenarios gives a lower critical depth earlier in the year, as both for the RUST-scenario and for the STOOM-scenario the transported weight shows a decrease and the transport costs show a steeper increase compared to the reference scenario of 2018. From the beginning of July, however, the 2018 scenario starts showing a steeper decline of transported weight and a steeper growth of transport costs than both climate scenarios. This corresponds to the moment that the water depths of the 2018 scenario drops below $3.0m$ and those of the climate scenarios show peaks. From this moment on, the water depths in the 2018 reference scenario undershoot the water depths of the RUST-scenario. This is seen in Figures 5.8 and 5.9 by the trend of 2018 surpassing the RUST-scenario in the reduction of the transported weight and in the growth of transport costs. As expected from the water depth profiles, the STOOM-scenario gives more extreme results than the reference scenario of 2018. The STOOM-scenario and the 2018-scenario show critical water depths in the same range for the last months of the simulation. Their trends therefore follow similar paths.

It can be concluded now that the critical water depth profile, and correspondingly the discharge profile, of 2018 which has a return period of $T = 20\ years$ is more extreme than the RUST-scenario for the year 2050 with a return period of $T = 10\ years$. The critical water depth profile of the STOOM-scenario in 2050 with a return period of $T = 10\ years$, however, is expected to be more extreme than the reference scenario of 2018 by predicting values for the transported weight and the transport costs that exceed the model results of 2018 by approximately 50%.

5.3. Adaptation measures

For each of the three adaptation measures considered in this chapter, this section holds a detailed description of the implementation in the IWT performance model. By simplifying each measure, model input can be generated that represents the effect of a measure on the various logistic processes. Following the determination of the input, results are produced. With these results, it then becomes possible to describe the measure-effectiveness by comparing performance indicators to the base scenario for the three considered measures. The adaptation measures that have been identified to be the most promising in terms of ease of implementation and estimated economic feasibility can be listed as follows:

1. Smaller (and lighter) barges
2. River training
3. Increased storage in destination

In the summer of 2019, the decision was made to start solving the depth-related problems occurring in the bend of Nijmegen (CBRB, 2019). It is expected that the critical river section will then shift to one of the other locations found in Section 2.2.1. All measures listed below are therefore considered to give no problems at Nijmegen in the future. A correction is applied to the water depths in this bend so that the critical point moves to a different section.

5.3.1. Modeling the equipment measure

Smaller and hence lighter barges are modeled by adjusting the vessel characteristics. Due to their lower capacity, the barges have a loaded draught that is less than the original barges and thus can remain sailing. As a reference, two smaller barges with a loaded draught of $3.35m$ and $3.43m$ and a capacity of approximately $2,250\ tons$ were selected [1]. A new barge is assumed to have an equal capacity, a loaded draught of $3.35m$ and an empty draught is $0.60m$. A new vessel class is added to the model, including the characteristics of this new fleet. These characteristics are listed in Table 5.7.

	Unit	Value
Empty draught	[m]	0.60
Loaded draught	[m]	3.35
Barge capacity	[tons]	2,250
Fleet size	[barges]	20
Convoy capacity	[tons]	4,500
Fleet size	[convoys]	10
Convoy price	[€/day]	4,500

Table 5.7: Characteristics of new barges

These barges are deployed in times of drought. These convoys serve to fill the gap in transport capacity that occurs after the smaller push-barge convoys have stopped operation. Due to the restricted width of the waterway, the new convoys are assumed to sail with only two barges. As was seen in Chapter 4.2, there are only ten pusher boats available for the discerned transport link. When considering the possible investment, costs related to the construction of pusher boats should also be taken into account. The costs related to this measure are the product of the construction costs per vessel and the fleet size which follows from the input values. An estimation of the construction costs per barge or pusher boat is found by a high-level search at ship brokers [2]. A conservative estimation of €750,000 for the price of a new push barge and €2,500,000 for the price of a new pusher boat is done. Moreover, additional barges have yearly recurring costs in fuel costs and maintenance. Following from expert judgement, a value of 10% of the investment costs is used in the computation. These costs can be seen in Table 5.8.

	Unit	Value
Barge construction costs	[€/ barge]	750,000
Pusher boat construction costs	[€/ pusher boat]	2,500,000
Yearly recurring costs	[€/ barge / year]	75,000

Table 5.8: Costs of vessel construction

Inland waterway vessels have an expected lifetime of a 40-50 years (Duursma, 2014). A design lifetime of 50 years is assumed. This is used in the following section to determine the present value of the future risk of damage. With the ideal fleet size determined in Appendix F, the costs for the implementation of smaller barges are given in Table 5.9.

	Unit	Total
Measure costs	[€]	18,750,000

Table 5.9: Costs of equipment measure

5.3.2. Modeling the infrastructural measure

River engineering measures are represented in the network performance model by adjusting the water depth at bottleneck locations. The depth of a river section after intervention is assumed to meet the depth require-

[1] Navin 88, https://www.rederijdejong.nl/wp-content/uploads/2014/04/Navin-88.pdf; RES-3, https://www.rederijdejong.nl/wp-content/uploads/2014/04/RES-3.pdf

[2] RensenDriessen, https://www.rensendriessen.com/ship-brokers/; GSK Brokers, http://www.gskbrokers.eu/nl/; Concordia DAMEN, https://www.concordiadamen.com/scheepsaanbod

ment of the Waal at any time. The characteristics that are used as input in the IWT performance model are listed in Table 5.10.

	Unit	Value
Depth improvement	[m]	0.25
Number of works carried out	[# works]	4

Table 5.10: Characteristics of river training works

River engineering measures are costly, relative to other measures. The measure that is carried out in the bend of Nijmegen is used as a reference project. This measure has a budget of €7.7 mln (CBRB, 2019). Average project costs of €7.5 mln per infrastructural measure are therefore assumed.

River training works in the Netherlands are usually designed for a lifetime of 80-100 years (Tosserams, 2014). An average design lifetime of 90 years is therefore assumed. This will be used in the following section to determine the potential investment based on the present value of the risk of future damage. The costs for the ideal value of infrastructural measures are given in Table 5.11.

	Unit	Total
Measure costs	[€]	30,000,000

Table 5.11: Costs of infrastructural measure

The exact locations of the bottlenecks follow from the LSM. These locations are given in Table 5.12 in the order of which they impact the navigable water depth.

Order	Location	Rhine kilometer
1	Millingerwaard	870.12
2	Nijmegen	883.71
3	Wolferen	894.84
4	Ewijk	893.31

Table 5.12: Order and location of bottlenecks on the Waal

5.3.3. Modeling the site measure

Increased storage in the destination results in higher resilience of the IWT network. This measure can be implemented in the model by including a periodic consumption to which a stockpile can be tested. The storage is deemed sufficient if this consumption can continue at the same level throughout the simulation time, even in times of drought. The optimal storage is defined as being as small as possible while being sufficient. By iteratively testing, this optimal storage can be found. Currently, there is a small storage in the Duisburg terminal as the transport makes use of the JIT principle. This storage will be subtracted of the computed optimal storage to find the required additional storage space. This can then be used to find the costs. The characteristics of the stockpile measure can be found in Table 5.13. The present stockpile is seen to meet the consumption of approximately a half week.

	Unit	Value
Weekly consumption	[tons]	500,000
Current stockpile	[tons]	283,750

Table 5.13: Characteristics of stockpile (Burgers, 2005)

The costs related to the storage area follow from the costs of land use and acquisition. These numbers are provided by RoyalHaskoningDHV. To comply with the euro as unit of costs throughout this research, the exchange rate of 24-10-2019 is used [3]. The costs can be seen in Table 5.14.

[3] Exchange rate from https://www.xe.com/currencyconverter/, accessed on 24-10-2019

	Unit	Value	Unit	Value
Land acquisition	[$ / m^2]	300	[€/ m^2]	270
Land preparation and equipment	[$ / m^2]	200	[€/ m^2]	180

Table 5.14: Costs of stockpile

The design lifetime of the storage area is estimated in order to determine the costs related to one drought. The purpose of a terminal is expected to be determined for several decades. Therefore, for port infrastructure as a storage area, a design lifetime of 50 years is assumed. This is used in the consecutive section to determine the potential costs of an increased stockpile on.

5.4. Effectiveness

This section addresses the effectiveness of the different measures regarding the performance in terms of transported cargo and costs. It does so by comparing the measure effectiveness that follows from Equation 5.1. This equation can be modified to compute the relative change, see Equation 5.2. Moreover, the present value of the reduction of expected damage is calculated to evaluate the possible investment in measures. As a result, both outcomes on the measure effectiveness and on the potential investment can be used in order to conclude on the most promising adaptation measure. The (relative) measure effectiveness follows from:

$$Measure\ effectiveness = \Sigma_{i=1}^{n}(Transported\ cargo_{New,\,i} - Transported\ cargo_{Old,\,i}) \tag{5.1}$$

$$Relative\ measure\ eff. = \frac{\Sigma_{i=1}^{n}(Transported\ cargo_{New,\,i} - Transported\ cargo_{Old,\,i})}{Transported\ cargo_{Old}} \tag{5.2}$$

where:

Transported cargo$_{New}$	[*tons*]	Transported cargo in the scenario with measure
Transported cargo$_{Old}$	[*tons*]	Transported cargo in the base scenario

To evaluate whether the implementation costs per measure are acceptable for the calculated risk, use is made of the value of expected yearly damage (EYD) and the present value of expected yearly damage (PVEYD). Using these expressions, the future damage can be translated to the present value of that damage. This can therefore be used to make a benefits-costs analysis between the potential yearly savings and the implementation costs of a measure. This benefit-cost analysis is shown by a benefit-cost ratio (BCR) between the PVEYD and the implementation costs. A ratio lower than 1 signifies a measure that is infeasible, a value between 1 and 5 requires additional benefits in order to become feasible and a value above 5 is deemed feasible. This will help justify the investment that is required for implementing a measure. The EYD, PVEYD and the BCR are presented by Equations 5.3, 5.4, and 5.5.

$$EYD = (Transport\ costs_{Old} - Transport\ costs_{New}) * \frac{1}{10} \tag{5.3}$$

$$PVEYD = EYD * \frac{1-(1-(r-g))^{n}}{r-g} \tag{5.4}$$

$$BCR = \frac{PVEYD}{Implementation\ costs} \tag{5.5}$$

where:

Transport costs$_{Old}$	[€]	Transport costs in the base scenario
Transport costs$_{New}$	[€]	Transport costs in the scenario with measure
r	[%]	Discount rate of 5.5% (Werkgroep Discontovoet, 2015)
g	[%]	Economic growth rate, 1.0% in RUST, 2.5% in STOOM (Wolters et al., 2018)
n	[years]	Design lifetime of measure
Implementation costs	[€]	The costs for implementation of the measure

A complete overview of the results of each adaptation measure, both exact values and figures, can be found in Appendix F. The following sections will consider the differences between the scenarios found for RUST and STOOM in Section 5.2 with and without measure and hence scrutinize the effectiveness. The climate scenarios without measure will further be referenced to as the original impact scenarios.

5.4.1. Effectiveness of equipment measure

The results of the simulation including the equipment measure are given below. For the RUST-scenario, the outcomes are shown in Figures 5.10 and 5.11. Hardly any difference is notable between the original impact scenario and the case with equipment measure. In the RUST-scenario, the water depths do only once become low enough for the new barges to come into operation. In July 2050, the considered case with additional barges overshoots the transported cargo of the original impact scenario. The measure therefore causes a little improvement in the transported cargo. Due to this improved transported cargo, less costs follow from insufficient supply. At the same moment in time, the case with new barges therefore shows a lower trend than the original scenario. A small reduction of the costs is therefore found.

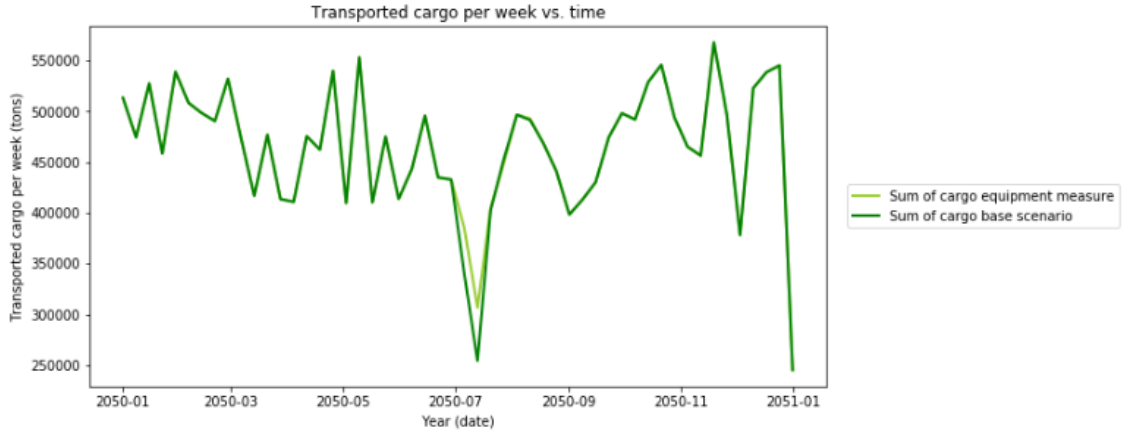

Figure 5.10: Differences in weekly transport with and without equipment measure in the RUST-scenario

Figure 5.11: Differences in weekly costs with and without equipment measure in the RUST-scenario

The model results of the equipment measure in the STOOM-scenario are depicted in Figures 5.12 and 5.13. During the period of low discharge, the smaller barges remain in operation. For that reason, transport can continue at a higher level, which is depicted by the scenario with new barges overshooting the original impact scenario in terms of transported cargo. The equipment measure therefore results in a substantial improvement of the transport.

When looking at the difference in transport costs, it can be noted that due to the smaller barges continuing their operations, less costs for insufficient supply are generated. This follows from Figure 5.13, in which

the case with equipment measure undershoots the original impact scenario in terms of transport costs. A significant reduction of the transport costs is thus caused by the equipment measure.

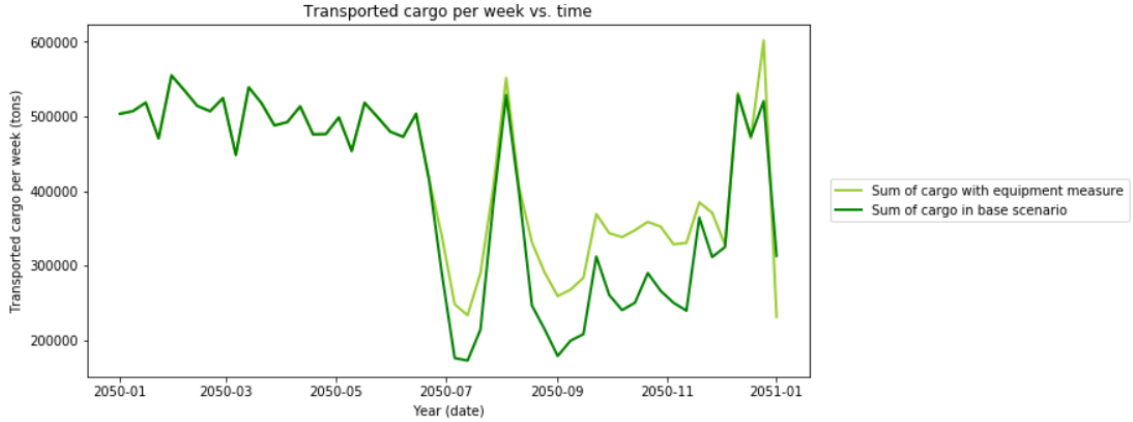

Figure 5.12: Differences in weekly transport with and without equipment measure in the STOOM-scenario

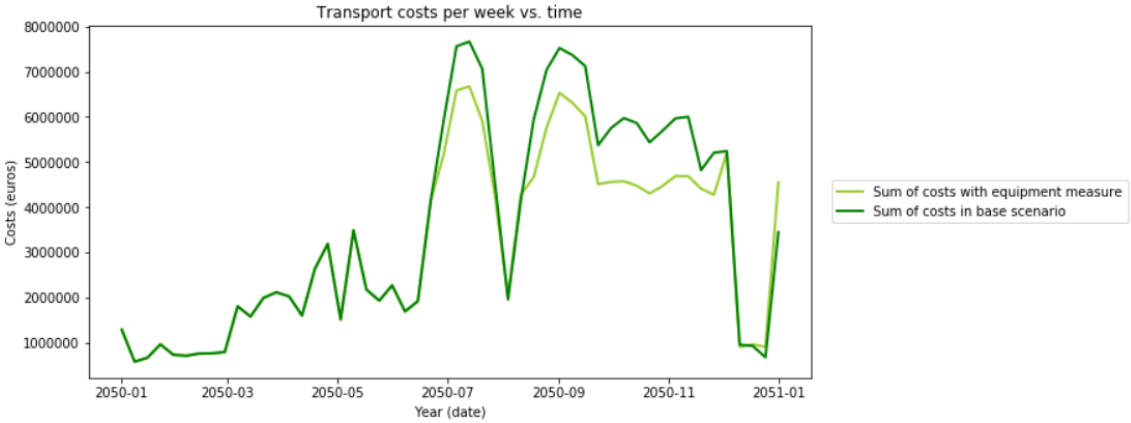

Figure 5.13: Differences in weekly costs with and without equipment measure in the STOOM-scenario

The bandwidths, indicating the transported cargo and the transport costs for both the original impact scenario and the scenario with smaller barges, for the RUST-scenario and the STOOM-scenario are depicted in Figures 5.14 and 5.15. These bandwidths help to show the benefit of the equipment measure. For the transported cargo, the considered adaptation measure is seen to make the bandwidth of the impact smaller by increasing the lower reach (for the STOOM-scenario). For the transport costs, the case with smaller barges projects lower costs for the STOOM-scenario while keeping approximately the same value for the RUST-scenario.

The exact values of the model results are given in Table 5.15. These values are computed relative to the original impact scenario. The equipment measure predicts a positive effect on the transported cargo for both the RUST-scenario and the STOOM-scenario. The improvement is, however, minor for the RUST-scenario with a value of 0.4%. The improvement is more substantial with a value of 7% for the STOOM-scenario.

The feasibility of the measure largely depends on the costs and benefits. As is seen in Figure 5.15, lower transport costs are projected for the considered case in the STOOM-scenario. This decrease in expected damage is translated to the present value. A comparison with the implementation costs then gives the feasibility. The results are given in Table 5.16. For the STOOM-scenario, the BCR is 2.7. This is well above the critical value of 1, which indicates that the benefits would be equal to the costs. The ratio, however, is lower than 5 which signifies that additional benefits, e.g. societal or environmental, are required. The implementation of smaller barges does not offer obvious additional benefits. The BCR therefore is maintained at 2.7. For the RUST-scenario, no improvement of the transport costs is projected. Including the costs for implementation,

this results in a low BCR. A value of 0.2 is found, which is well below 1. It can thus be concluded that the implementation of twenty new barges is an infeasible adaptation measure in the RUST-scenario and an adaptation measure that only becomes feasible in the STOOM-scenario when additional benefits are found.

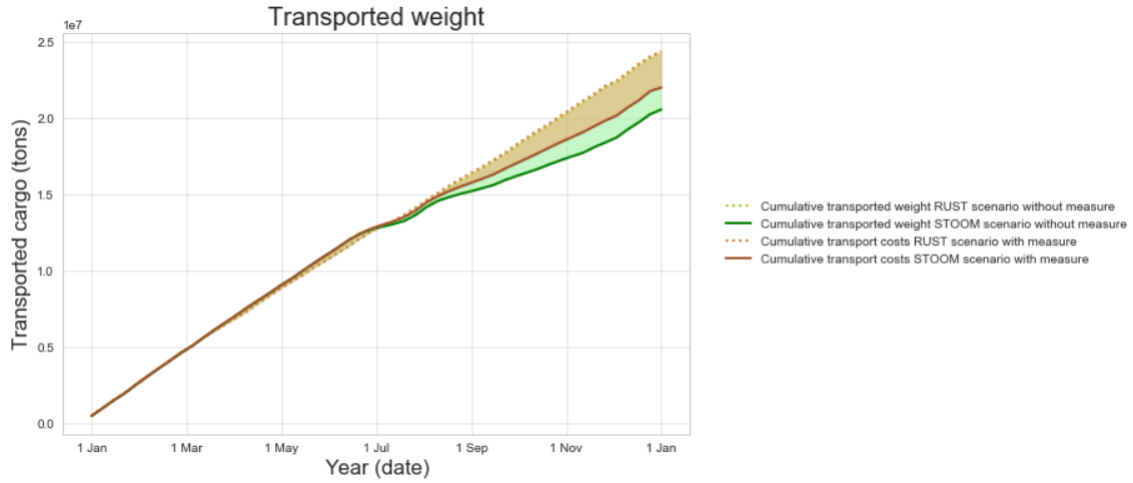

Figure 5.14: Bandwidths for the impact of low discharges on the transported cargo with and without equipment measure

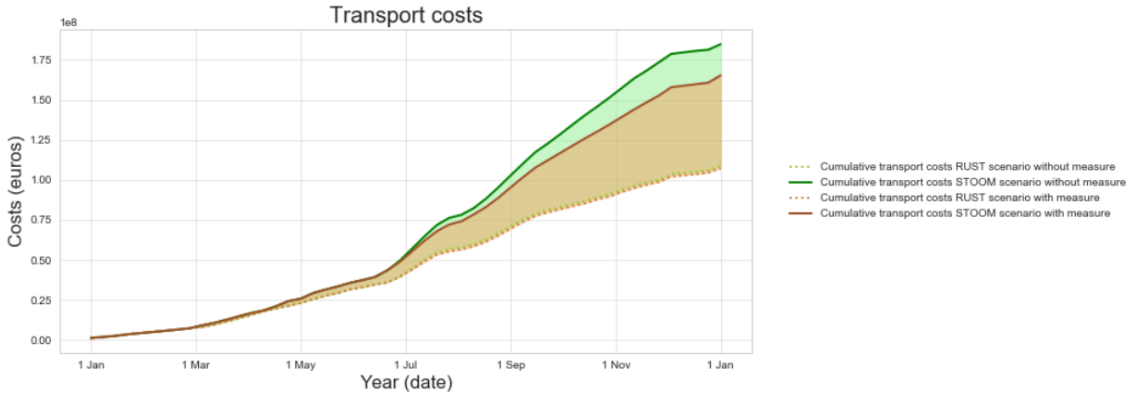

Figure 5.15: Bandwidths for the impact of low discharges on the transport costs with and without equipment measure

		Absolute difference		Relative difference [%]	
	Unit	**RUST**	**STOOM**	**RUST**	**STOOM**
Measure effectiveness	[-]	+96,823	+1,437,020	+0.4	+7.0

Table 5.15: Effectiveness of smaller barges

	Unit	**RUST**	**STOOM**
BCR	[-]	0.2	2.7

Table 5.16: BCR of smaller barges

5.4.2. Effectiveness of infrastructural measure

The results of the simulations including the infrastructural measure are given below. For the RUST-scenario, the differences with the original impact scenario are shown in Figures 5.16 and 5.17. Looking at the transported cargo per week, the case with river training works both undershoots and overshoots the original im-

pact scenario. No clear trend can thus be distinguished. This results from the fact that a transport deficit develops when the small push barge convoys stop operation. In the RUST-scenario, this occurs once and has a very short duration (i.e. in July 2050). The demand can thus be met most of the year in the original scenario. The case with infrastructural measures does therefore not show a significant improvement.

When looking at the transport costs, the differences between the case with river training works and the original case are more clear during the dry period. Again, during the hydrological winter, no clear trend can be distinguished. During the summer, however, the case with infrastructural measures remains below the original impact scenario when water depths are low (i.e. peaks in the costs). This follows directly from the fewer trips undertaken by smaller, and relatively more expensive, vessels (i.e. Rhine vessels and coupled barges). These come into operation later and stop operation earlier due to the water levels that allow for the push-barge convoys to continue operation longer. Moreover, the smaller vessels can sail with a higher load factor. This results in higher vessel prices to be triggered in a later stage. A combination of these effects contributes to a substantial improvement of the transport costs in the case with river training works.

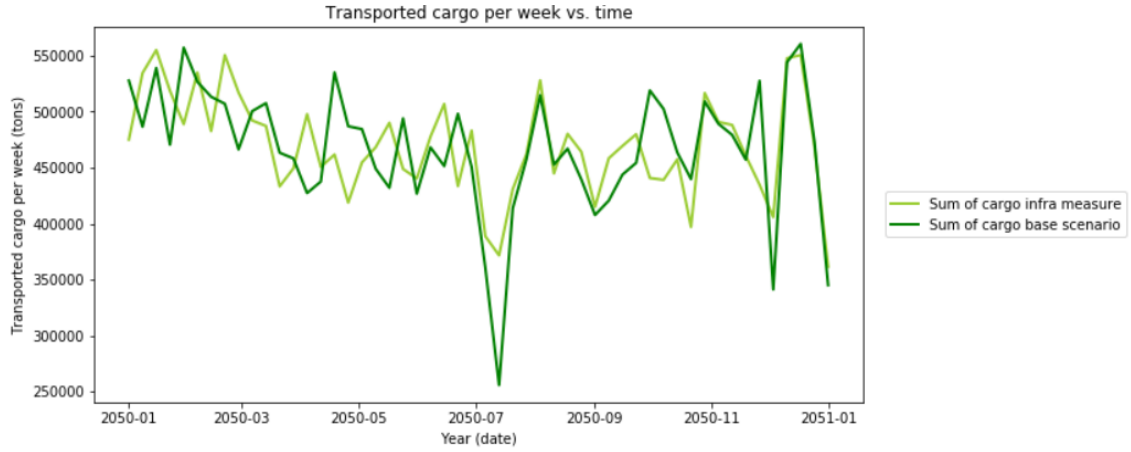

Figure 5.16: Differences in weekly transport with and without infrastructural measure in the RUST-scenario

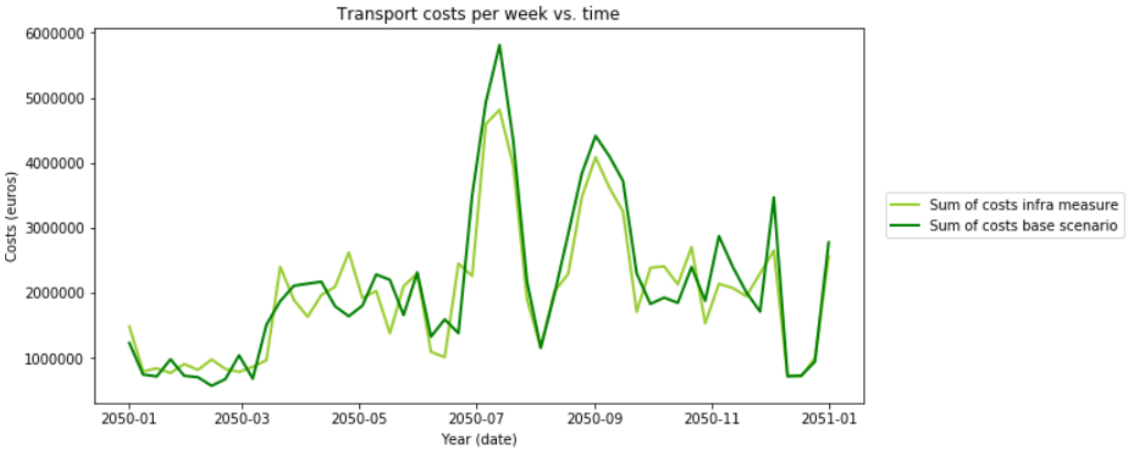

Figure 5.17: Differences in weekly costs with and without infrastructural measure in the RUST-scenario

The results of the model run of the STOOM-scenario with the infrastructural measure are presented in Figures 5.18 and 5.19. These figures show the differences in transported cargo and transport costs between the case with infrastructural measure and the original impact scenario. In the hydrological winter, no clear improvement is found for the transported cargo as the case with river training works both undershoots and overshoots the original scenario. In the hydrological summer this changes, as the considered case consistently overshoots the original impact scenario from July 2050 to December 2050. This results from transport

deficit in both cases during this period. In the case with infrastructural measures, however, the maximum load factor is just higher than for the original impact scenario, leading to more transported cargo. The applied measure therefore results in an improvement of the transported cargo in the STOOM-scenario.

When looking at the transport costs, the considered case provides lower values for most of the simulation period. This results from a combination of less trips by smaller, and relatively more expensive, vessels, a higher maximum load factor during the period of low water depths and lower costs for insufficient supply due to the increased transported cargo. In October 2050, the transport costs for the considered case are much lower than for the original impact scenario. This is the result of a vessel class (in this case the smaller push-barge convoys) having to stop operation in the original scenario while this vessel class can continue operation in the case with river training works. This induces higher costs for insufficient supply in the original impact scenario whereas these are not triggered in the considered case. This leads to a large improvement of the transport costs in the case with infrastructural measures with respect to the original impact scenario.

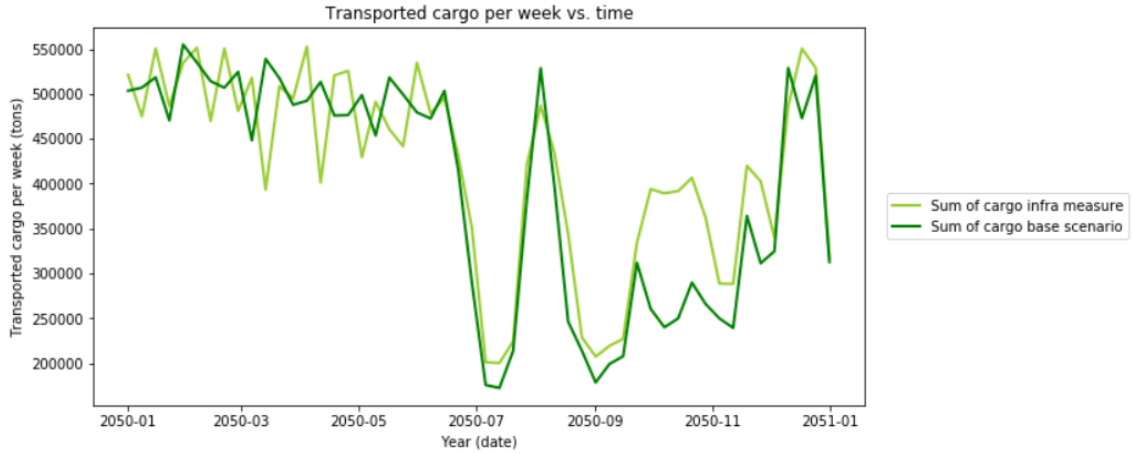

Figure 5.18: Differences in weekly transport with and without infrastructural measure in the STOOM-scenario

Figure 5.19: Differences in weekly costs with and without infrastructural measure in the STOOM-scenario

The bandwidths, indicating the transported cargo and the transport costs for both the original impact scenario and the scenario with river training works, for the RUST-scenario and the STOOM-scenario are depicted in Figures 5.20 and 5.21. These bandwidths help to show the benefit of the infrastructural measure. For the transported cargo, the considered adaptation measure is seen to make the bandwidth smaller by increasing the lower reach (for the STOOM-scenario). For the transport costs, the case with river training works projects lower costs for both the RUST-scenario and for the STOOM-scenario. The exact values of the model results are given in Table 5.17. These values are computed relative to the original impact scenario. The adaptation

measure is seen to have a minor positive effect of 0.4% on the transported cargo in the RUST-scenario. In the STOOM-scenario, the transported cargo is projected to increase 5.7% with regard to the original impact scenario.

As is seen in Figure 5.21, lower transport costs are projected for the case with river training works. The results for the BCR are given in Table 5.18. For the RUST-scenario, this gives a BCR of 0.4. This value is below 1, i.e. the implementation costs of the measure are larger than the present value of the expected yearly damage. For the STOOM-scenario, the BCR is 1.9. The implementation costs are nearly half of the present value of the expected yearly damage. In order to become feasible in the STOOM-scenario, this measure will have to supply additional benefits. River training works, however, often have a large impact on the river extending far upstream and/or downstream from the measure. This effect on nature is undesired. This type of measure is therefore expected to be even less feasible. It can thus be concluded that the construction of four river training works is an infeasible adaptation measure in both the RUST-scenario and the STOOM-scenario, in case no additional benefits are found.

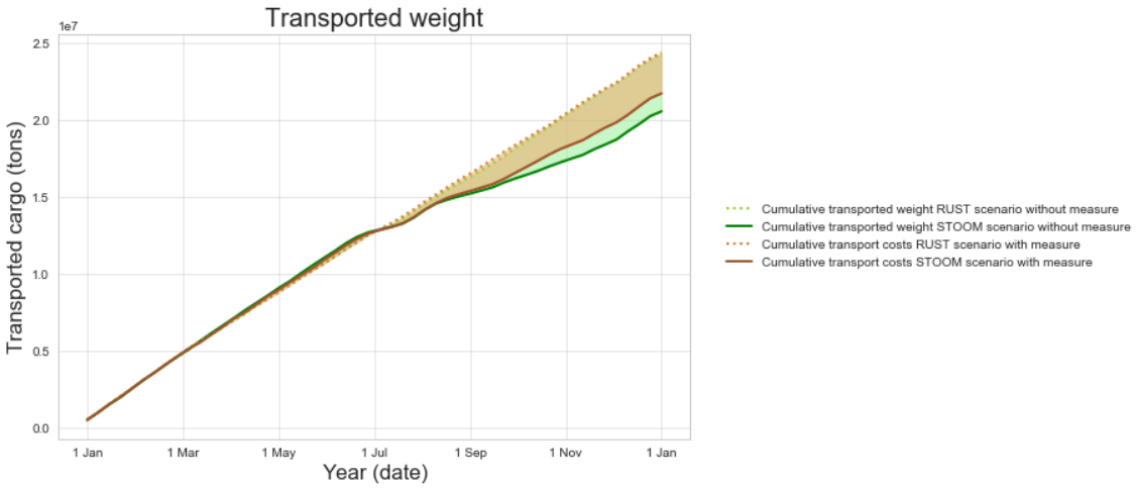

Figure 5.20: Bandwidths for the impact of low discharges on the transported cargo with and without infrastructural measure

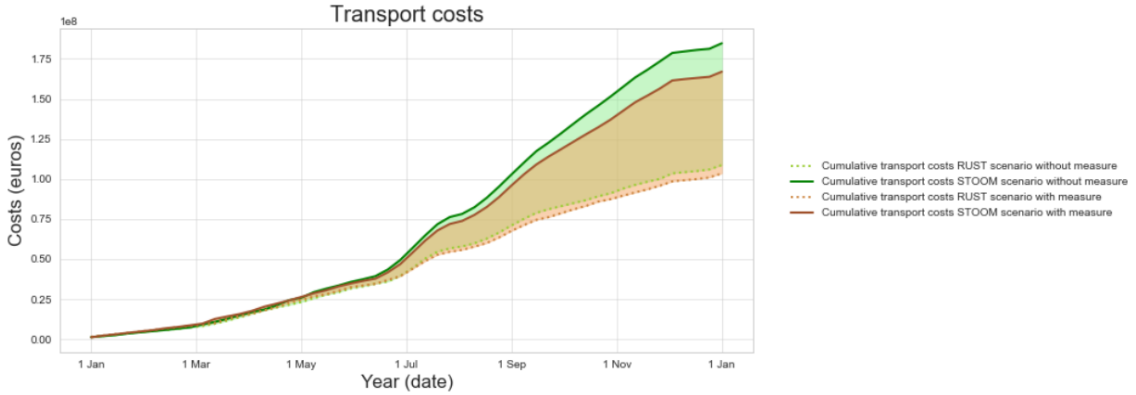

Figure 5.21: Bandwidths for the impact of low discharges on the transport costs with and without infrastructural measure

		Absolute difference		**Relative difference [%]**	
	Unit	**RUST**	**STOOM**	**RUST**	**STOOM**
Measure effectiveness	[-]	+99,845	+1,166,768	+0.4	+5.7

Table 5.17: Effectiveness of infrastructural measure

	Unit	RUST	STOOM
BCR	[-]	0.4	1.9

Table 5.18: BCR of the infrastructural measure

5.4.3. Effectiveness of site measure

It follows from the model results that a stockpile of 1,600,000 *tons* is optimal to overcome the discharge regime of the RUST-scenario in 2050. This is depicted in Figure 5.22. The oscillations show the weekly consumption. Only the dry year has been considered. For that reason, the replenishment of the stockpile in the years following drought is not included.

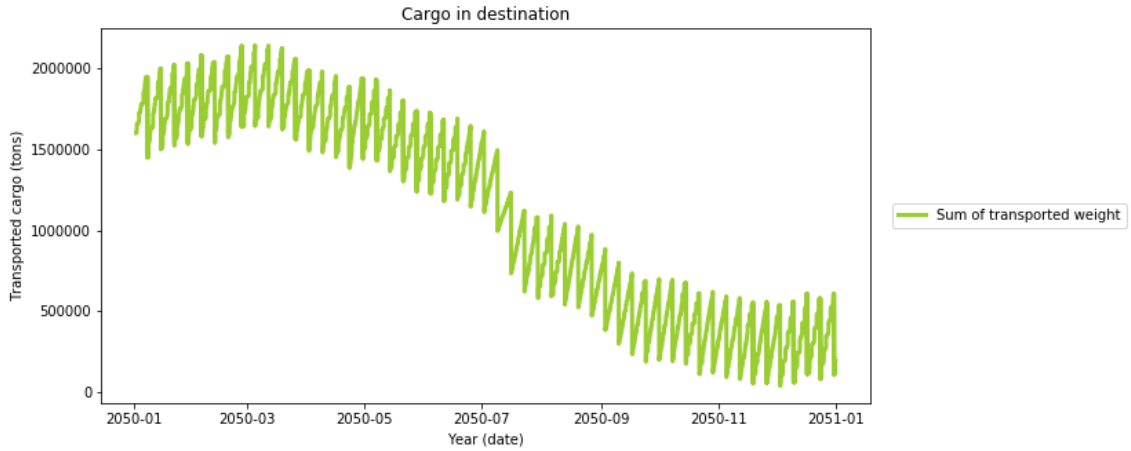

Figure 5.22: Sufficient stockpile with the site measure in RUST-scenario

For the STOOM-scenario, an optimal storage of 5,300,000 *tons* is found. The model result is plotted in Figure 5.23.

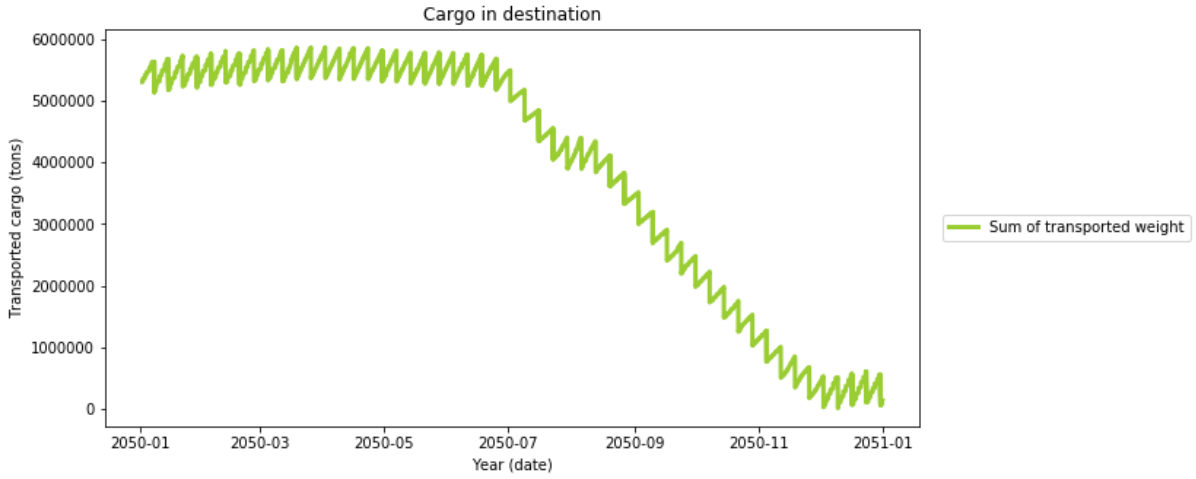

Figure 5.23: Sufficient stockpile with the site measure in STOOM-scenario

Now that the optimal storage is found for both scenarios, an estimation must be made to relate the transported weight to the required storage space. A simplification is made stating that all iron ore and coal have the same grading. The only division that has to be made therefore is between iron ore and coal. From Section 2.3.2, it follows that 75% of the weight of the yearly demand consists of iron ore and 25% of the transported weight exists of coal. This division is used in the calculation. An earlier case study was performed on the capacity of the EMO terminal by Van Huijstee (2004). Her values considering the dumping weight, the dumping angle and the height of a coal stockpile are adopted. The values used for the calculation are presented in Table 5.19.

	Unit	Value
Volume iron ore RUST	[tons]	1.2 mln
Volume coal RUST	[tons]	0.4 mln
Volume iron ore STOOM	[tons]	3.9 mln
Volume coal STOOM	[tons]	1.3 mln
Dumping weight iron ore	[tons/m^3]	2.7
Dumping weight coal	[tons/m^3]	0.9
Dumping angle iron ore	[°]	36
Dumping angle coal	[°]	38
Height coal stockpile	[m]	18

Table 5.19: Values used for stockpile calculation (Van Huijstee, 2004)

Figure 5.24 shows simplified cross-sections and top views of both the iron ore and the coal stockpile. Moreover, an assumption is made that the width of the stockpile is restricted to the reach of stacker-reclaimers used for dumping and reclaiming the cargo. This reach is estimated on 90 m, i.e. 45 m on both sides (Van Huijstee, 2004). From the fact that the dumping weight of iron ore is three times as large as the dumping weight of coal, the assumption is made that the height of the iron ore stockpile is three times as small as the height of the coal stockpile. Furthermore, the assumption is made that one track of the stockpile cannot be longer than 500 m.

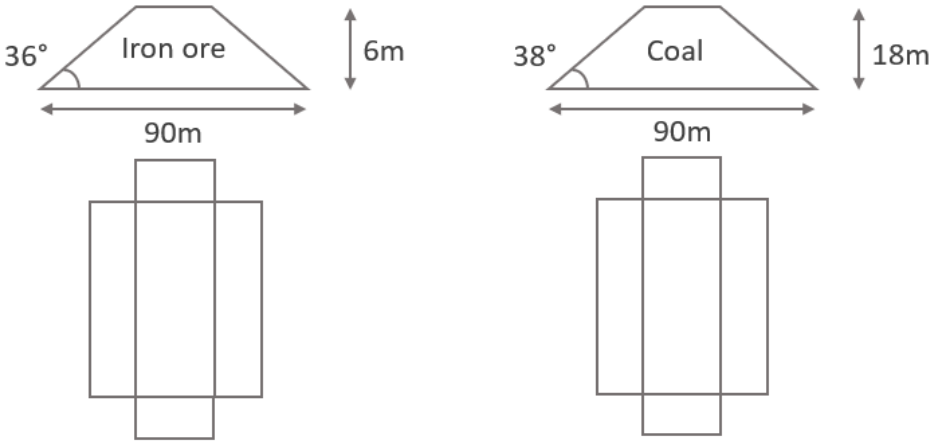

Figure 5.24: Cross-sections and top views of both stockpiles; values from Van Huijstee (2004)

The calculation of the required storage area can be found in Appendix G. The results of that calculation are presented in Table 5.20.

	Unit	Value
Storage area RUST	[m^2]	189,000
Storage area STOOM	[m^2]	545,400

Table 5.20: Required storage area for the RUST- and STOOM-scenario

After multiplication with the price per m^2, the costs for the optimal storage area in both scenarios can be found. These are presented in Table 5.21. It can be concluded that the costs for optimal storage are significant for both the RUST-scenario and the STOOM-scenario, considered to the original costs of transport. The BCR is computed by assuming that the benefit of a stockpile is equal to the costs for insufficient supply that would have occurred otherwise. The results are given in Table 5.22. Both in the RUST-scenario and in the STOOM-scenario, this ratio is above 1. This means that the implementation costs are too high and that the measure is infeasible. Many assumptions have been made in the calculation of the required storage area. The exact costs are therefore subject to interpretation. The result should therefore be seen as indicative. Nevertheless, the currently projected costs for storage are considered to be too high for implementation. It can thus be

concluded that the construction of a stockpile is an infeasible adaptation measure, both in the RUST-scenario and in the STOOM-scenario.

	Unit	RUST	STOOM
Costs	[€]	85,050,000	245,430,000

Table 5.21: Effectiveness of site measure

	Unit	RUST	STOOM
BCR	[-]	0.7	0.9

Table 5.22: BCR of the site measure

5.5. Conclusion

This chapter has shown the application of the IWT performance model in the impact assessment of low discharges on the IWT performance. A base scenario was set, corresponding to a discharge profile that undershoots 1020 m^3/s for the maximum allowable number of days (i.e. 5% of the year). The water depths encountered in the RUST-scenario and the STOOM-scenario have been compared to this base scenario in order to find the impact of projected discharge profiles. To put into perspective these impacts, a model run for the reference scenario of 2018 has been incorporated in the comparison. This provides a thorough answer to the following research question:

What is the impact of periods with low discharge on the performance of the IWT network between Rotterdam and Duisburg?

The results of the base scenario for the impact of drought are shown in Table 5.23. The RUST-scenario shows a relatively small reduction of transported weight whereas the STOOM-scenario shows a decrease of 21% compared to the base scenario. Both scenarios show large growth of the projected costs of 70% and 192%, respectively, of the costs in the base scenario.

	Unit	Absolute difference	Change [%]
RUST			
Transported weight	[tons]	−1,745,408	−6.7
Total costs	[€]	43,728,977	+70.3
STOOM			
Transported weight	[tons]	−5,468,154	−21.0
Total costs	[€]	119,102,161	+191.5
Ref. 2018			
Transported weight	[tons]	−3,398,389	−13.0
Total costs	[€]	74,875,046	+120.4

Table 5.23: Impact of low discharges in climate scenarios compared to the base scenario

It is concluded that the critical water depth profile of 2018, and correspondingly the discharge profile, which has a return period of $T = 20\ years$ is more extreme than the projections of the RUST-scenario for the year 2050 with a return period of $T = 10\ years$. The critical water depth profile of the STOOM-scenario in 2050 with a return period of $T = 10\ years$, however, is expected to be more extreme than the reference scenario of 2018 by projecting values for the transported weight and the transport costs that exceed the model results of 2018 by approximately 50%. This follows from more days in the year with a critical water depth below $2.25m$, which is the limit beneath which the smaller push-barge convoys stop operation and the transport capacity of the network becomes insufficient.

To show the application of the IWT model for practical purposes, different adaptation measures have been tested to see the relative effect of each measure on the key performance indicators of the IWT performance. Consequently, the relative improvement per adaptation measure was assessed. The transported weight has been calibrated and is thus given most weight to. This chapter has addressed the following research question:

What adaptation measure to enhance the IWT network performance is most promising in terms of benefits and costs?

The adaptation measures that have been tested are the following:

1. Smaller (and lighter) barges
2. River training
3. Increased storage in destination

Both the measure effectiveness and the cost-effectiveness have been computed for the ideal size of each measure. The measure effectiveness followed from the difference in transported weight between the original impact scenario and the case with adaptation measure applied. In order to compute the cost-effectiveness of each measure, a method was applied to compare future damages with present investments. From a comparison with the original impact scenario, the reduction in expected transport costs was calculated for each measure. This reduction in future damage was then translated to the present value of this reduction. This value was used in a benefits-costs analysis between the potential yearly savings and the implementation costs of a measure. The benefits-costs ratio (BCR) resulting from this analysis, was used to determine the feasibility of each measure. The results of the application of the IWT performance model are presented in Table 5.24. For the enlarged storage area, only the relative cost difference is given as no changes were made in the transport.

	Unit	**RUST**	**STOOM**
Smaller (and lighter) barges			
Measure effectiveness	[%]	+0.4	+7.0
BCR	[%]	0.2	2.7
River training works			
Measure effectiveness	[%]	+0.4	+5.7
BCR	[%]	0.4	1.9
Stockpile			
BCR	[%]	0.7	0.9

Table 5.24: Effectiveness and BCR of adaptation measures

Following this table, several statements can be done on the various adaptation measures:

- The differences between the two climate scenarios are significant. None of the proposed measures projects a feasible BCR in the RUST-scenario. In the STOOM-scenario, both the equipment measure and the infrastructural measure project feasible values when additional benefits of these measures are found.
- The implementation of smaller barges has a higher effect on the transported cargo than the construction of river training works, and has less implementation costs. Consequently, the equipment measure projects a higher BCR than the infrastructural measure in the STOOM-scenario.
- The result for the optimal storage area should be seen as indicative as many assumptions were made in the computation. The projected costs for storage are considered too high for implementation both in the RUST-scenario and in the STOOM-scenario.

These results largely depend on the case-specific input values. More emphasis should therefore be placed on the methodology that leads to the assessment of the impact in various situations.

6

Discussion

This chapter addresses the interpretation of the results found in Chapter 5. First, a background is sketched against which the results should be interpreted. This background is set by acknowledging the limitations to the study. This chapter does not consider an interpretation of the results following the testing of application measures as these are found to not contribute to the general conclusions of the research. These general conclusions are addressed in this chapter, supported by an analysis of how the results of this research agree or contrast with previous published work. Ultimately, different practical applications of the developed model are presented.

6.1. Discussion

The use of representative years to extrapolate the water depths for each of the studied impact scenarios provides different water depth profiles. The water depths of the RUST-scenario and the STOOM-scenario, that follow from the representative year of 1976, are seen to show a trend with more peaks during summer than the profile of 2018. Their consecutive period of insufficient water depths is therefore shorter than for 2018. When water depths recovers to become sufficient again, so does the network capacity required to compensate an arisen transport deficit. Consequently, the water depth profile induces changes in the model output that do not only follow from the critical water depth but also from the frequency of occurrence and consecutiveness of these low water depths. These changes are best seen in the cumulative trends of the transported weight and the transport costs in Section 5.2. These trends show a varying steepness throughout the year, depending on the water depth and the successiveness of low water days. It is noted that the variation in water depth profiles do impact the model output differently. The results obtained in the impact assessment of Chapter 5 should be interpreted with this in mind.

In order to comply with measurements of 2018 used for calibration, $0.25m$ was subtracted from the water depth. Although this follows actual measurements well, it is not clear what causes this discrepancy between the LSM and reality. It is assumed that the coarse grid of the LSM with data points approximately $500m$ apart does not account for local shallows. Moreover, the used LSM model dates from 2017. As such, erosion or sedimentation might have caused bed degradation or elevation. The verified reason, however, has not been found during this research. This subtraction induces lower maximum load factors and, as such, negatively affects the transport capacity of the network.

Currently, the model does include squat in a simplified way, by simple subtraction from the water depth. In this study, where depth is limited as a result of low discharge, introducing squat in more detail would impact the model results. As squat is dependent on the sailing speed, captains could pass known bottlenecks slowly and thus decrease the potential squat. This way, the ship can have a larger draught and hence could be fuller loaded. This will enhance the network performance in times of restricted loading.

In Chapter 2, a literature study has been carried out in order to find the characteristics of the IWT network between Rotterdam and Duisburg in 2050. In that sense, the chapter deals with the projections of climate change for the discharge of the Rhine in 2050. The characteristics concerning the transport, however, are determined by using present values. As such, the demand, fleet size, and vessel dimensions are assumed for the situation of 2050, thereby inducing uncertainty in the model outcome. For each of these parameters, an estimation can be made on how it will develop in the future. These estimations are scrutinized below.

In forecasts for the near future (i.e. 2030), the price of iron ore is projected to increase whereas the price of coal will likely decrease [1]. This trend is assumed to continue for the period between 2030 and 2050. It is assumed that the price of a commodity depends directly on the demand for that commodity. An estimation of the yearly demand to maintain its present value is therefore assumed to hold. In the model runs, a constant daily demand is assumed. In reality, in times of low discharge, actors will react to the resulting stress on the network, and the corresponding high costs of transport, and will postpone their usage (Van Hussen et al., 2019). The transport deficit therefore appears larger in the results than it will be reality. The extent of this effect is difficult to quantify.

The current fleet size consists of 45 vessels, excluding barges but including pusher boats. It has this size because it appears optimal for the transport in years with regular river discharge. A larger fleet size would cause overcapacity which signals that vessels would be idle a part of the time. As this directly affects the revenue that IWT operators make, overcapacity will not occur. A smaller fleet size would signify insufficient network capacity. The demand can in that case not be met, even for regular river discharge. This will therefore occur neither. The fleet size is thus expected to be directly dependent on the network demand. As the present value of the demand is assumed to hold following the reasoning above, also the present value of the fleet size is expected to hold.

A simplification has been made to divide all vessels required for dry bulk transport into four types. Within these types, all vessels are assumed to have the same characteristics. In reality, there will be variations in the specifications of vessels within vessel classes. One of these specifications is the sailing speed. In the current model, all vessels are assumed to have equal sailing speeds. In reality, however, the sailing speeds depend amongst others on engine characteristics and hull shape. Variations in the sailing speed between different vessel types could therefore induce mismatches between model results and reality. As these speeds could be higher or lower in reality, the average sailing speed is assumed to balance out the effect on the model results. Also in 2050, vessel speeds are expected to neither increase or reduce significantly so that the assumption of an average sailing speeds holds.

The model considers 168 operational hours per week. This means that no vessel can experience downtime. This is unrealistic. Captains make stops, pause more or stay nights at inland ports. The current network performance as results from the model is too high. In periods of low discharge, however, captains do sail longer hours. During drought, the assumption of 168 operational hours per week is therefore expected to approach reality.

As one of the key performance indicators, the transport costs should give accurate results. Unfortunately, no calibration data was obtained in the course of this research so that the results regarding transport costs following from the model have only been cross-referenced with literature and economical reports. In the model, all vessel types are assumed to have prices that vary with the load factor. In reality, however, some IWT operators make use of fixed contracts (Van Hussen et al., 2019). These day-rates will therefore not change in times of low discharge. It depends on the commodity to what extent fixed contracts are used.

With this context, the model results can be interpreted in the correct light. In addition to the exact values found which describe the impact of low water depth on the network performance of IWT given the predetermined input, generalizations can be made that categorize the results into key findings of this research:

- Below a critical water depth of $3.0m$ (when 6-barge push convoys are restricted), smaller convoys, Rhine vessels and coupled barges increase the number of trips by approximately 220%. Below a critical water depth of $2.25m$ (when smaller push-barge convoys have to stop operations), the number of trips reduces to an increase of the original number by 200%.
- After the smaller convoys stop operation, the temporary transport capacity decreases with 60%.
- The transported cargo is expected to reduce within a bandwidth of 7% to 21% of the original transported cargo for one year, depending on the climate scenario and a return period of $T = 10\ years$.
- The transport costs are expected to increase within a bandwidth of 70% to 192% of the original transport costs for one year, depending on the climate scenario and a return period of $T = 10\ years$.

It has appeared that the regulations on navigational restrictions are important for the performance of the IWT network; restricting push-barge convoys directly means a reduced performance in terms of transported cargo. Moreover, the Dutch IWT system appears to have insufficient vessels to continue transport at the

[1] By forecasts of the International Monetary Fund, obtained from https://knoema.com/wxgcxde/commodity-prices-forecast-2019-2030-data-and-charts; accessed on 26-11-2019

same level in a period of drought. The above presented values therefore should be interpreted for the Dutch IWT system only. The qualitative increasing or decreasing trends can, however, be understood to hold for other systems. Therefore, this model would also become appropriate for other systems to apply with simple adjustments to the input.

In literature, Beuthe et al. (2013) predicted no significant losses for IWT in 2050 on the Rhine as a result of low water levels while considering a 'dry' and a 'wet' climate scenario. It follows from this research that the potential damages are in fact large with economic losses of €44 mln and €119 mln predicted for the RUST-scenario and STOOM-scenario, respectively. It follows from this thesis that low discharges, in combination with navigational restrictions, could cause substantial losses for the IWT in 2050 in terms of transported cargo and transport costs. The restrictions to navigation posed by authorities were not included in earlier research. This has led to earlier research underestimating the potential damages of periods of low water depths. Due to its proven significance, navigational restrictions should therefore be included in future studies. Moreover, following the statements of Christodoulou and Demirel (2018), the accurate modeling of IWT includes various local effects that follow from regulations, fleet composition or waterway characteristics. This research is the first study on the impact of low water depths on the IWT performance that does not take the load factor as the only variable but that includes other network parameters as the active fleet size and the number of trips to provide a comprehensive picture of the IWT performance in periods of low discharge.

With this overview, the impact of periods of low discharge on the performance of the IWT can be studied and the effect of changes in the IWT system on different performance indicators can be tested. To show the application of the developed model, several adaptation measures have been studied on a high-level. The model can both be used to provide a first estimate of the projected benefit of adaptation measures or to provide more detailed output that assists in decision-making between possible alternatives. In addition, the application of the model has been shown in the determination of the optimal storage for upstream production facilities to overcome periods of low discharge. Furthermore, practical applications could be assessing combinations of adaptation measures, evaluating the traffic intensity on river sections to test the capacity of ship locks during drought or estimating the waiting times in ports to base terminal-investment decisions on.

7

Conclusion and recommendations

This chapter concludes on the research by addressing the main research question:

"What is the impact of climate change-induced low discharges on the network performance of inland waterway transport in the year 2050 and what adaptation measure promises to be most effective in reducing this impact?"

The objective of this study consists of several sub-questions. The answers on these questions contribute to the final conclusion on the research objective. This structure is followed in Section 7.1. In contrast to Chapter 6, this chapter does include the model results on the effectiveness of the considered adaptation measures. Consequently, Section 7.2 provides suggestions for further research.

7.1. Conclusion

The objective of this research is to provide more insight into the consequences of climate change-induced low discharges on the performance of IWT and to assist in making justified adaptation decisions. Prior research has considered the performance of the IWT system to be only dependent on the maximum load factor instead of the performance being a dynamic play of multiple network parameters. The exact role of each parameter is only slightly covered in literature while this understanding of the system is crucial for policymakers to propose the correct adaptation measures. A simulation model that includes the effects of climate change on the network parameters to study the performance of the IWT system did not exist. During this research, an IWT performance model has been developed that is capable of studying the capacity and vulnerability of the inland waterway system to low water depths, and simultaneously can be used to propose the most effective measures to strengthen the position of IWT. This research has considered a case study on the iron ore and coal transport between Rotterdam and Duisburg.

The first research question that was addressed is as follows:

What are the characteristics of the inland waterway transport network between Rotterdam and Duisburg in the year 2050?

A literature study was conducted in Chapter 2 on the current and future state of the Rhine. The seasonality in the yearly discharge is expected to enlarge as a result of the Rhine shifting from being a snow-fed river to a rain-fed river. To study the effect of climate change on the discharge, there has been chosen to make use of daily discharges from the dry year 1976, and to extrapolate these under two climate projections into a discharge for the year 2050. The RUST- and the STOOM-scenario of the Deltaprogram have been used, representing respectively moderate and rapid climate change. In this way, a time-series consisting of daily discharges at Lobith has been created that represents the discharge in the year 2050 with a return period of $T = 10\ years$. The analysis of the transport corridor between Rotterdam and Duisburg has led to several characteristics describing the fleet and navigability on the Rhine. The most promising adaptation measures have been identified in Section 2.4 based on expected impact and ease of implementation.

Following, the second research question was addressed:

How can the performance of an inland waterway network, as a result of low discharges, be simulated?

A model was developed to simulate the performance of an IWT network to varying discharges. The objective of this IWT performance model is to accurately express the performance of the IWT system in key performance indicators describing the transported cargo and the costs of transport. In this research, the network performance is indicated by the transported cargo in time. This is supported qualitatively by the transport costs.

To assess the quality of the logistic simulations, the model has been subjected to a number of validity tests related to the functioning of the load factor, the number of trips, the transport demand and the transport costs in the internal validation of Section 4.1. The expected output corresponds well with the model output. The model was then calibrated in Section 4.2 on two parameters that have a high uncertainty and a significant impact on the simulation; the manoeuvring time per trip and the vessel capacity. For this purpose, an IVS-90 data-set was obtained that describes the observed transported weight and number of trips for dry bulk transport originating from Rotterdam in 2018. For a simulation containing both a summer and a winter, the model shows a correlation coefficient for the transported cargo of $r = 0.794$ and for the number of trips of $r = 0.921$. From these values, it can be concluded that the results of the IWT performance model are relatively accurate with reality.

Consequently, the third research question was addressed:

What is the impact of periods with low discharge on the performance of the IWT network between Rotterdam and Duisburg?

A base scenario was set, corresponding to a discharge profile that undershoots the agreed limit for low discharge of 1020 m^3/s for the maximum allowable number of days, i.e. 5% of the year. The water depths encountered in the RUST-scenario and the STOOM-scenario have been compared to this base scenario in Section 5.1. To put into perspective these impacts, a model run for the reference scenario of 2018 has been incorporated in the comparison.

When assessing the impact of low discharges, a comparison of model outcomes given the set of input values is presented in Table 7.1. The RUST-scenario shows a relatively small reduction of transported weight whereas the STOOM-scenario shows a decrease of 21% compared to the base scenario. Both scenarios show large growth of the projected costs of 70% and 192% of the costs in the base scenario, respectively. It is concluded that the critical water depth profile of 2018, which has a return period of $T = 20\ years$, is more extreme than the projections of the RUST-scenario for the year 2050 with a return period of $T = 10\ years$. The critical water depth profile of the STOOM-scenario in 2050 with a return period of $T = 10\ years$, however, is expected to be more extreme than the reference scenario of 2018 by projecting values for the transported weight and the transport costs that exceed the model results of 2018 by approximately 50%. This follows from more days in the year with a critical water depth below $2.25m$, which is the limit beneath which the smaller push-barge convoys stop operation and the transport capacity of the network becomes insufficient.

	Unit	**Base scenario**	**RUST [%]**	**STOOM [%]**	**Ref. 2018 [%]**
Transported weight	$[tons]$	26,048,467	−6.7	−21.0	−13.0
Total costs	[€]	62,180,575	+70.3	+191.5	+120.4

Table 7.1: Relative impact of climate scenarios and reference 2018

Figures 7.1 and 7.2 show the trend of the transported cargo and the transport costs for the various scenarios throughout the simulation. These can also be found in Section 5.2. The use of representative years to represent the water depths in each of the studied impact scenarios provides different water depth profiles. The water depths of the RUST-scenario and the STOOM-scenario, that follow from the representative year of 1976, show a trend with more peaks during summer than the profile of 2018. Their consecutive period of insufficient water depths is therefore shorter than for 2018. When water depths recover to become sufficient again, so does the network capacity required to compensate an arisen transport deficit. Consequently, the water depth profile induces changes in the model output that do not only follow from the critical water depth but also from the frequency of occurrence and consecutiveness of these low water depths. These changes are best seen in the cumulative trends of the transported weight and the transport costs in Section 5.2. These trends show a varying steepness throughout the year, depending on the water depth and the successiveness of low water days.

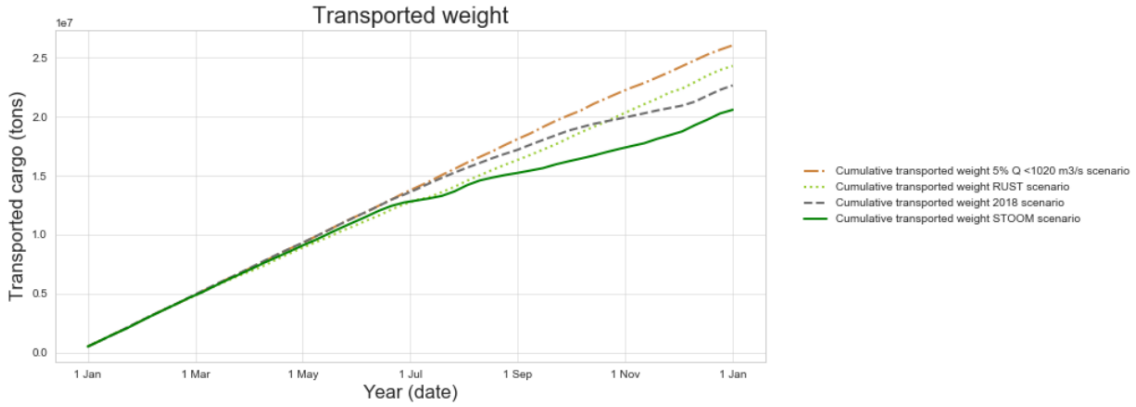

Figure 7.1: Cumulative transported weight in impact scenarios

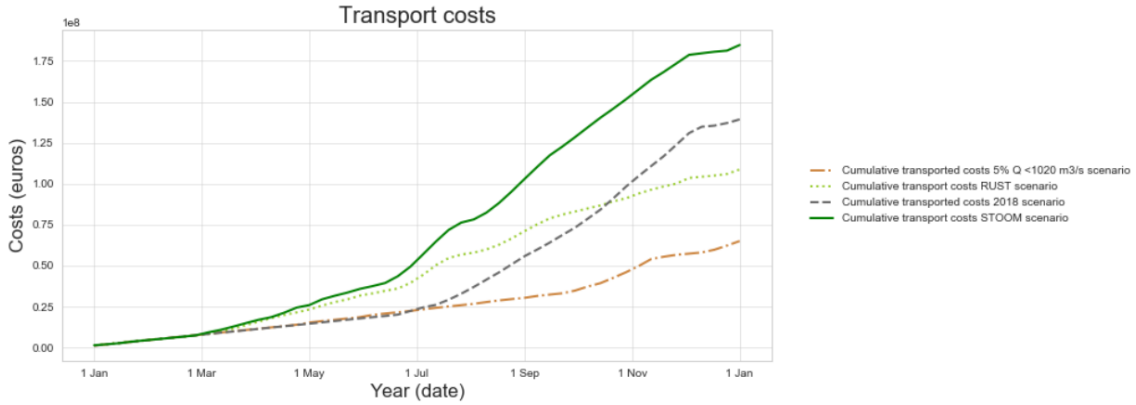

Figure 7.2: Cumulative transport costs in impact scenarios

The comparisons provide a comprehensive overview of the potential impact that low discharges bring to the IWT performance on the Rotterdam-Duisburg corridor.

This leads to the fourth and final research question:

What adaptation measure to enhance the IWT network performance is most promising in terms of benefits and costs?

To show a high-level application of the IWT model for practical purposes, different adaptation measures have been tested in Section 5.4 to see the effect of each measure on the key performance indicators of the IWT performance. The adaptation measures that have been tested are the following:

1. Smaller (and lighter) barges
2. River training
3. Increased storage in destination

The improvement per adaptation measure was assessed by a comparison with the original impact scenario, for the RUST-scenario and the STOOM-scenario, respectively. From this comparison, the differences both in transported weight and transport costs have been computed. The reduction of expected costs was translated to its present value in order to evaluate whether the investment in each adaptation measure would be justified. The feasibility of a measure was determined both by the effect of a measure on the transported cargo and by the benefit-cost ratio (BCR) between the potential saving in transport costs and the implementation costs.

It appears from this assessment that, given the current set of input values, smaller barges are most promising when considering the cost-effectiveness. Moreover, as the model has not been calibrated on costs, more weight should be given to the effect on transported cargo. On the transported cargo, smaller barges also

project a more positive effect, thereby supporting the conclusion. All assumptions done in this first application of the IWT performance model should be verified by future research and corrected if necessary in order to find the true potential of each measure.

Following from literature, the accurate modeling of IWT should include various local effects that follow from regulations, fleet composition or waterway characteristics. This research is the first study on the impact of low water depths on the IWT performance that does not take the load factor as the only variable but that includes other network parameters as the active fleet size and the number of trips to provide a comprehensive picture of the IWT performance in periods of low discharge. With this overview, the impact of periods of low discharge on the performance of the IWT can be studied and the effect of changes in the IWT system on different performance indicators can be tested for future applications.

7.2. Recommendations

This research has caused a leap forward in the comprehension of the contributing parameters in the IWT performance following from varying discharges. The developed model is the first effort in simulating the IWT performance in times of low discharge while including network parameters as the active fleet size and the number of trips. The impact of low discharges on the performance of an IWT network can now be assessed with a decent certainty. In future research, the model can be further improved and its applications can be extended. Moreover, the extended understanding of the network parameters can contribute in future decisions that deal with IWT. This section addresses the recommendations for further research.

Practical recommendations for IWT in the light of climate change

This research has shown that the performance of IWT could be impacted by low discharges resulting from climate change. Not only will the considered IWT network be able to transport less cargo, also the transport costs will increase considerably. This could impact the competitiveness of IWT with respect to other modalities. As such, these low discharges can result in a modal shift. This is undesired, as was written in Section 1.1. In order to counteract this potential effect, adaptation measures can be studied that will strengthen the performance of IWT. For example, river sections can be controlled by creating buffer reservoirs, although this is easier in regions that have an appropriate geographical situation (Fischer et al., 2015). An other measure that has been the subject of research is the canalization of the Waal. The construction, maintenance and operational costs, however, are expected to be too high for this measure to be feasible (Taekema, 2017).

The sensibility of the network performance to low water depths partially results from the trend of the last decades to increase vessel sizes, and consequently enlarge their draught (CCR, 2019). The size and design of vessels should therefore be the subject of study concerning economic feasibility, technical optimization and market implementation. It appears from this research that an adjustment to the fleet is most promising in terms of benefits and costs in a dry climate scenario. Smaller barges are able to continue transport in periods of low water depths and do therefore lower the potential damage of low discharges. In times of sufficient water depth, the smaller barges cause a lower network capacity than the conventional push barges. Care should thus be taken so that the entrance of these barges into the IWT market does not replace conventional barges, thereby decreasing the network capacity. Presently, this network capacity is limited by the number of pusher boats present in the IWT system. The construction of additional pusher boats can thereby compensate the reduction of capacity caused by the entrance of smaller barges. This would, however, bring a higher investment following the construction of additional pusher boats. The optimal way of implementing this adaptation measure (i.e. achieving minimal costs against a maximum benefit) should be the subject of future research.

River training works have been tested on a high-level by manually adjusting the water depth in the IWT performance model. In reality, river training could have effects on the water depth far upstream or downstream from the location of the measure. These could worsen or improve the water depth on potential bottleneck locations and as such, have a larger impact than has now been tested in a simplified way. In order to find the true potential of river training works on reducing the impact of low discharges, adjustments should be made to the river cross-sections in *Sobek*. The water depths, as result from this hydraulic model, could then show variations at locations upstream and downstream that should be used in the IWT performance model.

Furthermore, it results from this study that the impact of climate change on the network performance varies considerably depending on the climate scenario. This adds uncertainty to the long-term effects of cli-

mate change for IWT. This framework provides a quantification of the reduced network performance that can be used in the decision-making on adaptation measures and acceptable risk. In order to use this quantification, the bandwidth that has now been set for two extreme climate scenarios should be narrowed. In this way, the true climate change can be projected with the highest possible accuracy. This will then lead to a realistic value of the potential damages of low discharges.

Increase applicability with other types of cargo
This research has considered dry bulk as the transport of this commodity was seen to be most affected by low water depths. The model has been validated and calibrated on this type of transport. By introducing other vessels and berth equipment characteristics, this can relatively easily be extended to other types of transport such as container and liquid bulk. By considering other commodities as well, a complete overview of the impact of low discharges can be provided. This will assist in the decision-making on adaptation measures that affect all transport types as e.g. river training works. The implementation of other types of cargo in the model can be realized by addressing the following bullet points:

- *New input on berth equipment:* Other commodities are handled with different loading- and unloading-rates than dry bulk. Additional berths and berth equipment should therefore be included.
- *Additional input on vessel characteristics:* With different commodities come other dedicated vessels that have their own characteristics concerning capacity, draught and sailing speed.
- *Different navigational restrictions for other commodities:* The navigational restrictions were seen to have a major impact on the transport capacity of the IWT network for dry bulk. For other commodities, this relation should therefore be given special attention.

Expand indirect damages
In this research, the projected impact of dry periods on the transported cargo and the transport costs has been scrutinized. This impact does not yet give the complete damage-profile. Although an estimate is used for the indirect damage of insufficient supply, the indirect damages are much more complicated than this study shows. The used estimate includes the costs of a temporary modal shift and the price of stockpiling. In reality, the indirect damage consists of more components as e.g. loss of revenue as a result of a manufactural stop in production. This scrutinization of the complete damage-profile falls outside the scope of the logistic model. Nonetheless, the performance indicators in the model output can serve as input for economic models designed to study the indirect impact.

Three dominant classes of economic models are often proposed for the calculation of indirect economic losses; simultaneous equation econometric models, input-output (I/O) models and computable general equilibrium (CGE) models (Galbusera and Giannopoulos, 2018). Of these, I/O and CGE models are regarded as "most commonly used and well-documented" (Koks and Thissen, 2016). Often these models are applied on one single country or region but as waterway networks stretch across regional or country borders, it might prove more useful to look at multiregional effects, incorporated in so-called Multiregional Input-Output (MRIO) models.

The delay in transported cargo that results from the IWT performance model can serve directly as input for these MRIO models. A more complete damage-profile increases the applicability of this research in decision-making.

Extend the model with inland ports and locks
The model developed in this research focuses on the IWT network between Rotterdam and Duisburg by having been calibrated on this route, and by having its application shown by proposing measures on this path. The model scope therefore includes encountered properties such as the origin and destination and river cross-sections. Not encountered parts on this route are, however, left out of the model. For that reason, inland ports other than Duisburg have not been included. When incorporated, inland ports would result in additional manoeuvring time and possibly (un)loading time. This could also result in the cargo being transported to several locations, therewith adjusting the sailing speed and hence transport duration along the way. For other case studies, inland ports could be added to the work method. Furthermore, no ship locks are encountered on the route between Rotterdam and Duisburg. Ship locks cause a longer duration of transport and as such do influence the IWT performance. In other case studies where ship locks are present, they could be included schematically by adding a delay or could be modeled as separate agents, functioning dependent

on factors as traffic intensity, discharge etc.

Include other modalities
This research has focused on IWT. One of its objectives was to suggest adaptation measures to strengthen the position of IWT in periods of low water depths. Other modalities have, however, been left out of the scope of this research. The IWT has therefore been assumed to have a fixed demand and prices that depend on the water depth. In reality, the demand and prices are influenced by other modalities. The functionality of the model could therefore be improved by introducing dependency of IWT on other modalities. In order to keep the model as an 'IWT performance' model, other modalities could be entered on high-level. The following is a scenario of triggers that could occur in a future form of the model:

1. Water depths decrease as a result of low discharge.
2. The maximum load factor decreases, thereby increasing the demand for more IWT vessels.
3. IWT prices increase so that shippers will shift to using other modalities. The demand for IWT does not increase further.
4. The prices of road and rail transport increase. At the same time, IWT continues at a lower rate than its capacity allows.
5. Congestion causes delays in road transport and only limited space is available by rail so that the capacities of both is met.
6. The demand for IWT increases again, now disregarding the risen prices but wanting to continue transport at all costs.

High-level adaptation measures can then be applied on different modalities. Moreover, the relative effects can be seen to impact a modal shift.

Perform other case studies to further validate the model
The IWT performance model has passed the internal validation and calibration phase of model development. No external validation has been carried out. In an external validation, the developed model is provided with new input to see whether it is generally applicable and is not catered to one specific case. An external validation by performing more case studies or by extending the input on the current case, is therefore suggested. This could show the correct applicability of the model in other situations and as such increase the area of interest of this research. The external validation should be carried out for both the number of trips and the transported cargo on a week-scale for dry bulk vessels in periods of low discharges. This corresponds to the calibration that has been carried out in this research. Moreover, future case studies could be used to verify the transport costs as predicted by the model. The day-rate per vessel class and the triggers that induce higher vessel prices can be adjusted to enhance the transport costs from being estimations to being validated performance indicators. Similar to the calibrated parameters, a range of values can be used for the calibration of the transport costs. The costs for insufficient supply currently do not include costs for manufactural stop of production. These are therefore expected to cover the low-end of the range. The values in Table 7.2 are recommended:

	Unit	Low	Medium	High
Rate 6-barge push convoys	[€/ day]	13,500	15,000	16,500
Rate smaller convoys	[€/ day]	6,500	7,500	8,500
Rate Rhine vessels	[€/ day]	1,500	2,500	2,500
Rate coupled barge combinations	[€/ day]	6,000	7,000	8,000
Costs for insufficient supply	[€/ ton]	15	20	25

Table 7.2: Overview of cost ranges for future calibration

Enhance user experience
The IWT performance model requires a lot of manual input. Per site, berth, and vessel class, the model requires 5+ input parameters. The user experience can be increased by having standardised input on berth equipment and vessel classes. This would take a lot of time away from the user that would only want to use

the model to make a quick analysis. For engineers, considering adaptation measures that differ in details, the model should keep an option for manual input. The user experience can also be enhanced by splitting the model into a model core including calculations, post-processing and other general model components, and a specific part that varies for each project and which should be visible to the user. This way, the model becomes more concise which will improve the usability.

Bibliography

E. Backer van Ommeren. Globale schets gasolieverbruik binnenvaartschepen. 2011.

M. Beuthe, B. Jourquin, N. Urbain, B. Ubbels, and I. Lingemann. Climate change impacts on transport on the Rhine and Danube: A multimodal approach. *Transportation Research Part D: Transport and Environment*, 27:6–11, 2013. ISSN 13619209. doi: 10.1016/j.trd.2013.11.002. URL http://dx.doi.org/10.1016/j.trd.2013.11.002.

J. j. Burgers. ThyssenKrupp Veerhaven. Technical report, Delft University of Technology, 2005.

F. Castagnetti. Facing up the Congestion and Environmental Challenges of Europe. *Procedia - Social and Behavioral Sciences*, 48:12–20, 2012. ISSN 18770428. doi: 10.1016/j.sbspro.2012.06.983. URL http://dx.doi.org/10.1016/j.sbspro.2012.06.983.

CBRB. Blij met aanpak 'harde laag' Nijmegen, 2019. URL https://www.cbrb.nl/nieuws/nieuws/1317-aanpak-harde-laag-nijmegen.

CCR. Europese Binnenvaart Marktobservatie. Technical report, Centrale Commissie voor de Rijnvaart, 2018. URL https://www.inland-navigation-market.org/wp-content/uploads/2017/09/om16_II_nl.pdf.

CCR. Europese Binnenvaart Marktobservatie. page 96, 2019. URL https://www.inland-navigation-market.org/wp-content/uploads/2017/09/om16_II_nl.pdf.

A. Christodoulou and H. Demirel. *Impacts of climate change on transport - A focus on airports, seaports and inland waterways*, volume JRC108865. Publications Office of the European Union, Luxembourg, 2018. ISBN 978-92-79-97039-9. doi: 10.2760/378464.

M. Colin, F. Palhol, and A. Leuxe. Adaptation of Transport Infrastructures and Networks to Climate Change. *Transportation Research Procedia*, 14(0):86–95, 2016. ISSN 23521465. doi: 10.1016/j.trpro.2016.05.044. URL http://dx.doi.org/10.1016/j.trpro.2016.05.044.

F. P. Collas, A. D. Buijse, L. van den Heuvel, N. van Kessel, M. M. Schoor, H. Eerden, and R. S. Leuven. Longitudinal training dams mitigate effects of shipping on environmental conditions and fish density in the littoral zones of the river Rhine. *Science of the Total Environment*, 2018. ISSN 18791026. doi: 10.1016/j.scitotenv.2017.10.299.

J. de Jong. Beschrijving droge jaren in klimaatscenario's met stationaire afvoeren_CONCEPT_DISCUSSIEDOCUMENT. 2019.

P. W. De Langen and K. Sharypova. Intermodal connectivity as a port performance indicator. *Research in Transportation Business and Management*, 8:97–102, 2013. ISSN 22105395. doi: 10.1016/j.rtbm.2013.06.003. URL http://dx.doi.org/10.1016/j.rtbm.2013.06.003.

Deltares. D-Flow 1D Technical Reference Manual. Technical report, Deltares, 2019.

J. den Uijl. Integrating engineering knowledge in logistical optimisation. Technical report, Delft University of Technology, 2018.

G. Desquesnes, H. Nouasse, G. Lozenguez, A. Doniec, and E. Duviella. A Global Approach for Investigating Resilience in Inland Navigation Network Dealing with Climate Change Context. *Procedia Engineering*, 154:718–725, 2016. ISSN 18777058. doi: 10.1016/j.proeng.2016.07.574. URL http://dx.doi.org/10.1016/j.proeng.2016.07.574.

G. S. DiPietro, H. Scott Matthews, and C. T. Hendrickson. Estimating economic and resilience consequences of potential navigation infrastructure failures: A case study of the Monongahela River. *Transportation Research Part A: Policy and Practice*, 69:142–164, 2014. ISSN 09658564. doi: 10.1016/j.tra.2014.08.009. URL http://dx.doi.org/10.1016/j.tra.2014.08.009.

J. v. Dorsser. *Very Long Term Development of the Dutch Inland Waterway Transport System - Extended Summary Report*. PhD thesis, Delft University of Technology, 2015.

M. Duursma. Het water op, de ruimen leeg, 2014. URL https://www.nrc.nl/nieuws/2014/11/20/het-water-op-de-ruimen-leeg-1439860-a690722.

Ertsoverslagbedrijf Europoort CV. Terminal Information Book. 2018.

Eurostat. Modal split of freight transport, 2019. URL https://ec.europa.eu/eurostat/databrowser/view/t2020_rk320/default/table?lang=en.

C. B. Field, V. R. Barros, K. J. Mach, and M. D. Mastrandrea. Climate Change 2013, The Physical Science Basis Technical Summary. Technical report, International Panel on Climate Change, 2014.

H. Fischer, A. Gratzki, H. Heinrich, S. Kofalk, S. Mai, T. Maurer, A. Mehling, H. Moser, M. Schröder, B. Schubert, S. Wienhaus, and N. Winkel. Impacts of Climate Change on Waterways and Navigation in Germany. Technical report, KLIWAS, 2015.

L. Galbusera and G. Giannopoulos. On input-output economic models in disaster impact assessment. *International Journal of Disaster Risk Reduction*, 30(May):186–198, 2018. ISSN 22124209. doi: 10.1016/j.ijdrr.2018.04.030. URL https://doi.org/10.1016/j.ijdrr.2018.04.030.

H. Havinga. Visie op het rivierbeheer van de Rijn. Technical report, Rijkswaterstaat, 2016.

C. Hendrickx and T. Breemersch. The Effect of Climate Change on Inland Waterway Transport. *Procedia - Social and Behavioral Sciences*, 48:1837–1847, 2012. ISSN 18770428. doi: 10.1016/j.sbspro.2012.06.1158.

F. Henriet, S. Hallegatte, and L. Tabourier. Firm-network characteristics and economic robustness to natural disasters. *Journal of Economic Dynamics and Control*, 36(1):150–167, 2012. ISSN 01651889. doi: 10.1016/j.jedc.2011.10.001.

K. S. Hiemstra. Development of a methodology to assess functional performance of the Dutch Rhine. Technical report, Delft University of Technology, 2018.

M. Hitij. Ongoing Low Water Levels Hamper Shipping On Rhine River, 2018. URL https://www.gettyimages.nl/fotos/rhine-river?mediatype=photography&phrase=rhineriver&sort=mostpopular.

ICBR. Rijndelta. URL https://www.iksr.org/nl/themas/rijn/deelstroomgebieden/rijndelta/.

O. Jonkeren, J. v. Ommeren, and P. Rietveld. Effects of low water levels on the river Rhine on the inland waterway transport sector. *Economics and Management of Climate Change*, 41(September):53–64, 2008. doi: 10.1007/978-0-387-77353-7{_}5.

O. Jonkeren, B. Jourquin, and P. Rietveld. Modal-split effects of climate change: The effect of low water levels on the competitive position of inland waterway transport in the river Rhine area. *Transportation Research Part A: Policy and Practice*, 45(10):1007–1019, 2011. ISSN 09658564. doi: 10.1016/j.tra.2009.01.004. URL http://dx.doi.org/10.1016/j.tra.2009.01.004.

A. Jonkman. Veerhaven III (Waterbuffel). URL https://vlootschouw.nl/schepen/schip/veerhaven-iii-waterbuffel/.

S. Kallas. White Paper on transport - Roadmap to a single European transport area - Towards a competitive and resource-efficient transport system. Technical Report 2001, European Commission, 2011. URL http://eur-lex.europa.eu/LexUriServ/LexUriServ.do?uri=COM:2011:0144:FIN:EN:PDF.

S. W. Kienzle, M. W. Nemeth, J. M. Byrne, and R. J. MacDonald. Simulating the hydrological impacts of climate change in the upper North Saskatchewan River basin, Alberta, Canada. *Journal of Hydrology*, 412-413:76–89, 2012. ISSN 00221694. doi: 10.1016/j.jhydrol.2011.01.058. URL http://dx.doi.org/10.1016/j.jhydrol.2011.01.058.

E. Kirschbaum. Drought has hit Europe's Rhine river and its commerce hard: 'Everyone's hoping for rain', 2018. URL https://www.latimes.com/world/europe/la-fg-europe-germany-rhine-20181112-story.html.

A. Klein Tank, J. Beersma, J. Bessembinder, B. Van den Hurk, and G. Lenderink. KNMI'14 climate scenarios for the Netherlands; A guide for professionals in climate adaptation. Technical report, KNMI, De Bilt, The Netherlands, 2015.

C. d. Kock. Duwvaartrederij thyssenkrupp Veerhaven B.V. bestaat 50 jaar, 2017. URL https://www.portofrotterdam.com/nl/nieuws-en-persberichten/duwvaartrederij-thyssenkrupp-veerhaven-bv-bestaat-50-jaar.

O. Koedijk, A. van der Sluis, MSc, and M. Steijn. Richtlijnen Vaarwegen 2017 Kader verkeerskundig vaarwegontwerp Rijkswaterstaat. Technical report, Rijkswaterstaat; Water, Verkeer en Leefomgeving; Afdeling BNSV, 2017. URL https://staticresources.rijkswaterstaat.nl/binaries/richtlijnen-vaarwegen-2017_tcm21-127359.pdf.

M. J. Koetse and P. Rietveld. The impact of climate change and weather on transport: An overview of empirical findings. *Transportation Research Part D: Transport and Environment*, 14(3):205–221, 2009. ISSN 13619209. doi: 10.1016/j.trd.2008.12.004. URL http://dx.doi.org/10.1016/j.trd.2008.12.004.

E. E. Koks and M. Thissen. A Multiregional Impact Assessment Model for disaster analysis. *Economic Systems Research*, 28(4):429–449, 2016. ISSN 14695758. doi: 10.1080/09535314.2016.1232701. URL https://doi.org/10.1080/09535314.2016.1232701.

N. Kramer, M. D. Mens, J. K. Beersma, and N. R. Kielen. Hoe extreem was de droogte van 2018 ? *H2O*, pages 1–7, 2019.

A. Law and W. D. Kelton. *Simulation Modeling and Analysis*. Mc Graw Hill, third edition, 2000. ISBN 978-7302041320. URL https://www.amazon.com/Simulation-McGraw-Hill-Industrial-Engineering-Management/dp/0073401323.

G. Lenderink and J. Beersma. The KNMI'14 WH,dry scenario for the Rhine and Meuse basins. Technical report, Royal Netherlands Meteorological Institute, 2015.

A. Levermann. Climate economics: Make supply chains climate-smart. *Nature*, 506(7486):27–29, 2014. ISSN 0028-0836. doi: 10.1038/506027a.

M. Mens, R. Van der Wijk, N. Krame, J. Hunink, J. De Jong, B. Becker, P. Gijsbers, and C. Ten Velden. Hotspot-analyses voor het Deltaprogramma Zoetwater. Technical report, Deltares, 2018.

F. Millerd. Possible locations for adaptation to climate change by Canadian commercial navigation on the great lakes. *2006 IEEE EIC Climate Change Technology Conference, EICCCC 2006*, 30(January 2005):269–280, 2007. doi: 10.1109/EICCCC.2006.277252.

H. Nachtmann and F. Oztanriseven. Arkansas Inland Waterways and. 2014.

NEA. Model kostenkengetallen extern mei 2015, 2015.

E. S. Nugroho. Development of Climate Resilient Ports. Technical report, Delft University of Technology, 2016.

M. J. Overduin. Comparing one and two- dimensional hydraulic modelling of flow on varying spatial scales. Technical report, Delft University of Technology, 2018.

R. K. Pachauri, A. Reisinger, L. Bernstein, P. Bosch, O. Canziani, Z. Chen, R. Christ, O. Davidson, S. Huq, W. Hare, D. Karoly, V. Kattsov, Z. Kundzewicz, J. Liu, U. Lohmann, M. Manning, T. Matsuno, B. Menne, B. Metz, M. Mirza, N. Nicholls, L. Nurse, R. Pachauri, J. Palutikof, M. Parry, D. Qin, N. Ravindranath, A. Reisinger, J. Ren, K. Riahi, C. Rosenzweig, M. Rusticucci, S. Schneider, Y. Sokona, S. Solomon, P. Stott, R. Stouffer, T. Sugiyama, R. Swart, D. Tirpak, C. Vogel, and G. Yohe. Climate Change 2007; Synthesis Report. Contribution of Working Groups I, II and III to the Fourth Assessment Report of the Intergovernmental Panel on Climate Change. Technical report, IPCC, Geneva, Switzerland, 2007.

Port of Rotterdam. Coal import, export and transhipment, a. URL https://www.portofrotterdam.com/en/doing-business/logistics/cargo/dry-bulk/coal-import-export-and-transhipment.

Port of Rotterdam. Iron ore import and throughput, b. URL https://www.portofrotterdam.com/en/doing-business/logistics/cargo/dry-bulk/iron-ore-import-and-throughput.

Port of Rotterdam. Port vision 2030. (December):108, 2011. URL http://www.portofrotterdam.com/.

Port of Rotterdam. 1.000.000.000e ton overgeslagen bij EECV, 2016. URL https://www.portofrotterdam.com/nl/nieuws-en-persberichten/1000000000e-ton-overgeslagen-bij-eecv.

Port of Rotterdam. Feiten en cijfers haven van Rotterdam. 2018.

P. Quist and H. Verheij. Staat van de scheepvaart en de binnenvaartwegen in Nederland 2009. Technical report, Delft University of Technology, 2010.

Rijkswaterstaat. Rijkswaterstaat Waterinfo. URL https://waterinfo.rws.nl/#!/nav/index/.

Rijkswaterstaat. BIVAS Scenario's, 2019a. URL https://bivas.chartasoftware.com/Scenarios.

Rijkswaterstaat. Verdringingsreeks bij watertekort, 2019b. URL https://www.infomil.nl/onderwerpen/lucht-water/handboek-water/thema-s/watertekort/verdringingsreeks/.

B. Rothstein and A. Scholten. *Navigation on the Danube Limitations by low water levels and their impacts*. Number November 2016. 2017. ISBN 9789279647987. doi: 10.2788/236234.

A. Scholten, B. Rothstein, and R. Baumhauer. Criticial Parametes for Mass-Cargo Affine Industries Due to Climate Change in Germany: Impacts of Low Water Events on Industry and Possible Adaptation Measures. *Climate Change Management*, (October):267–287, 2011. doi: 10.1007/978-3-642-14776-0. URL http://www.springerlink.com/index/10.1007/978-3-642-14776-0.

A. Scholten, B. Rothstein, and R. Baumhauer. Mass-cargo-affine industries and climate change: The vulnerability of bulk cargo companies along the River Rhine to low water periods. *Climatic Change*, 122(1-2): 111–125, 2014. ISSN 01650009. doi: 10.1007/s10584-013-0968-0.

E. Schulz. Betreft: Diepgang Waal, 2018.

D. Sheppard and G. Chazan. Rhine drought leaves Europe's industry high and dry, 2018. URL https://www.ft.com/content/6356471c-d6c7-11e8-a854-33d6f82e62f8.

R. Sluijter. Jaar 2010: Koudste jaar sinds 1996, 2011. URL https://www.knmi.nl/nederland-nu/klimatologie/maand-en-seizoensoverzichten/2010/jaar.

F. Sperna Weiland, M. Hegnauer, L. Bouaziz, and J. Beersma. Implications of the KNMI'14 climate scenarios for the discharge of the Rhine and Meuse. Technical report, Deltares; Royal Netherlands Meterological Institute, 2015.

V. Stenek, J.-C. Amado, S. Wright, B. Pope, J. Hunter, J. McGregor, W. Morgan, B. Stanley, R. Washington, D. Liverman, H. Sherwin, P. Kapelus, C. Andrade, and J. D. Pabón. Climate Risk and Business: Ports. Technical report, International Finance Corporation, 2011. URL https://www.ifc.org/wps/wcm/connect/98f63a804a830f878649ff551f5e606b/ClimateRisk_Ports_Colombia_Full.pdf?MOD=AJPERES.

T. F. Stocker, D. Qin, G.-K. Plattner, M. M. Tignor, S. K. Allen, J. Boschung, A. Nauels, Y. Xia, V. Bex, and P. M. Midgley. Climate Change 2013: The Physical Science Basis. Contribution of Working Group I to the Fifth Assessment Report of the Intergovernmental Panel on Climate Change. Technical report, Intergovernmental Panel on Climate Change, Cambridge UK and New York USA, 2013.

S. Taekema. Climate change and Waal Canalization Climate change and Waal Canalization. 2017.

M. Tosserams. Vervangingsopgave Natte Kunstwerken. Technical report, Rijkswaterstaat, Water, Verkeer en Leefomgeving, 2014.

M. T. Truong, F. Amblard, B. Gaudou, and C. Sibertin-Blanc. To calibrate & validate an agent-based simulation model : An application of the combination Framework of BI solution & multi-agent platform. In *ICAART 2014 - Proceedings of the 6th International Conference on Agents and Artificial Intelligence*, volume 2, pages 172–183, 2014. ISBN 9789897580161.

D. Ullrich. Karte des Rhein, 2012. URL `https://upload.wikimedia.org/wikipedia/commons/4/47/Rhein-Karte.png`.

V. . Van Der Bilt. Assessing emission performance of dredging projects. Technical report, Delft University of Technology, 2019.

J. Van der Does De Willebois. Assessing the impact of quay-wall renovations on the nautical traffic in Amsterdam. Technical report, Delft University of Technology, 2019.

R. Van der Mark. Guest Lecture CoVadem, 2019.

B. Van der Walle. Schepen begrepen: weetjes over scheepsbouw. 2006.

S. M. Van Huijstee. Capaciteitenanalyse van een droge bulk terminal. Technical report, Delft University of Technology, 2004.

K. Van Hussen, I. Van de Velde, R. Läkamp, and S. Van der Kooij. Economische schade door droogte in 2018. Technical report, Ecorys, Rotterdam, 2019.

M. Van Koningsveld, J. Den Uyll, F. Baart, and A. Hommelberg. OpenCLSim (version 0.3.0), 2019. URL `http://doi.org/10.5281/zenodo.3251546`.

J. Van Meijeren, T. Groen, and D. Vonk Noordegraaf. Impact of Climate Change on the Competitive Position of Inland Waterways Transport and Logistic Solutions. 2011. URL `http://www.etcproceedings.org/paper/smart-card-data-for-multi-modal-network-planning-in-london-five-case-studies`.

W. Volker and M. Volker. Bevaarbaarheid van de Waal nu en in de toekomst. Technical report, 2015.

Werkgroep Discontovoet. Rapport werkgroep discontovoet 2015. Technical report, Rijkswaterstaat, 2015.

H. Wolters, J. Hunink, J. Delsman, G. De Lange, F. Schasfoort, R. Van der Mark, G. J. Van den Born, E. Dammers, B. Rijken, and S. Reinhard. Deltascenario's voor de 21 e eeuw. 2018. URL `https://media.deltares.nl/deltascenarios/Deltascenarios_actualisering2017_hoofdrapport.pdf`.

Y. Zheng and A. M. Kim. Rethinking business-as-usual: Mackenzie River freight transport in the context of climate change impacts in northern Canada. *Transportation Research Part D: Transport and Environment*, 53:276–289, 2017. ISSN 13619209. doi: 10.1016/j.trd.2017.04.023. URL `http://dx.doi.org/10.1016/j.trd.2017.04.023`.

H. Zhou, Z. Deng, Y. Xia, and M. Fu. A new sampling method in particle filter based on Pearson correlation coefficient. *Neurocomputing*, 216:208–215, 2016. ISSN 18728286. doi: 10.1016/j.neucom.2016.07.036.

Appendices

A

Landelijk Sobek Model

A.1. Theory

The LSM runs on software that has been developed within the D-Hydro Suite package by Deltares. The software is named D-Flow 1D and is best used in situations where simulation effort and robustness are considered more important than a high level of accuracy. In this 1D-model the flow computations follow the Saint Venant equations for unsteady flow which are simplified versions of the Navier-Stokes equations (Deltares, 2019). This set of equations consists of the 1D continuity equation (Equation A.1) and the 1D momentum equation (Equation A.2).
1D Continuity equation:

$$\frac{\delta A_T}{\delta t} + \frac{\delta Q}{\delta x} = q_{lat} \tag{A.1}$$

where:

A_T	Total area (sum of flow area and storage area)	$[m^2]$
Q	Discharge	$[m^3/s]$
q_{lat}	Lateral discharge per unit length	$[m^2/s]$

1D Momentum equation:

$$\frac{\delta Q}{\delta t} + \frac{\delta}{\delta x}(\frac{Q^2}{A_F}) + gA_F\frac{\delta \zeta}{\delta x} + \frac{gQ|Q|}{C^2RA_F} - w_f\frac{\tau_{wind}}{\rho_w} + gA_F\frac{\xi Q|Q|}{L_x} = 0 \tag{A.2}$$

where:

A_F	Flow area	$[m^2]$
C	Chézy value	$[m^{1/2}/s]$
ζ	Water level	$[m]$
Q	Discharge	$[m^3/s]$
R	Hydraulic radius	$[m]$

Often the Saint Venant momentum equation only consists of the first four terms, representing inertia, convection, water level gradient and the bed friction. In the D-Flow 1D software, two terms have been added to account for wind force and extra resistance respectively (Overduin, 2018).

These equations can only be used when several assumptions can be made. These assumptions are:

- "The flow is one-dimensional i.e. the velocity can be represented by a uniform flow over the cross-section and the water level can be assumed to be horizontal across the section." (Deltares, 2019, p.1)
- "The streamline curvature is small and the vertical accelerations are negligible, hence the pressure is hydrostatic." (Deltares, 2019, p.1)
- "The effects of boundary friction and turbulence can be accounted for through resistance laws analogous to those used for steady flow." (Deltares, 2019, p.1)

- "2D/3D dynamic effects in (sharp) bends are not taken into account, i.e. their effect on the global flow behavior is assumed negligible" (Overduin, 2018, p.12)

Following the reasoning that no flood waves are studied, these assumptions hold and the results are expected to be accurate enough. Moreover, the research area is stretched out over several hundred kilometers. This would result in unviable large simulation times for a more accurate, i.e. 2D/3D, model. The LSM can be therefore be considered suitable for its purpose of computing the water depths.

The water level follows directly from the discharge and is, as such, a result of the simulation. The bed level however is defined as the lowest point in the cross-section and therefore follows from each cross-section that has been specified in advance. D-Flow 1D interpolates the bathymetry between cross-sections. As such, a large number of nodes would increase the accuracy of the bathymetry and so enhance the accuracy of the water depth. The LSM is set-up to be consisting of nodes and branches that connect these nodes (Deltares, 2019). The computational grid that is used determines the water depth at each node, and determines the discharge and flow on each branch. This set-up of the network can be seen in Figure A.1 and is used in Chapter 3 to model the network performance.

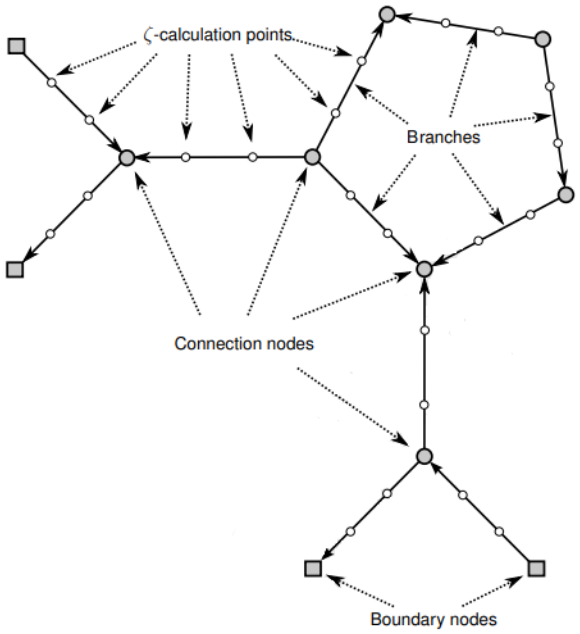

Figure A.1: Sobek network (Deltares, 2019)

A.2. Input data

The expected daily discharge that is given at the boundary condition at Lobith was found in Section 2.1.2. The time-series are depicted in Figure A.2.
On the four downstream boundary nodes, daily water levels are required. These are obtained from Rijkswaterstaat for the year 2010. This year is regarded as an average year in terms of precipitation (Sluijter, 2011).

Furthermore, the nodes in the network require a predefined cross-section. This cross-section is built-up of a certain width W corresponding to a height Z relative to a reference level. Figure A.3 shows an example of one of these cross-sections. In the received *Sobek*-model all cross-sections had been predefined so that no additional action was required.

A.3. Boundary conditions

The LSM model provides five boundary nodes, corresponding with five boundary conditions. Each boundary condition must represent the water flow, either by discharge or by water level. Of these five boundary nodes, four are located at the downstream ends of the model. The fifth is located at Lobith and represents the water flowing into the Dutch Rhine system. For that reason, the boundary condition at Lobith is defined as the expected daily discharge. The four downstream boundary nodes are located at Krimpen aan de Lek (Lek),

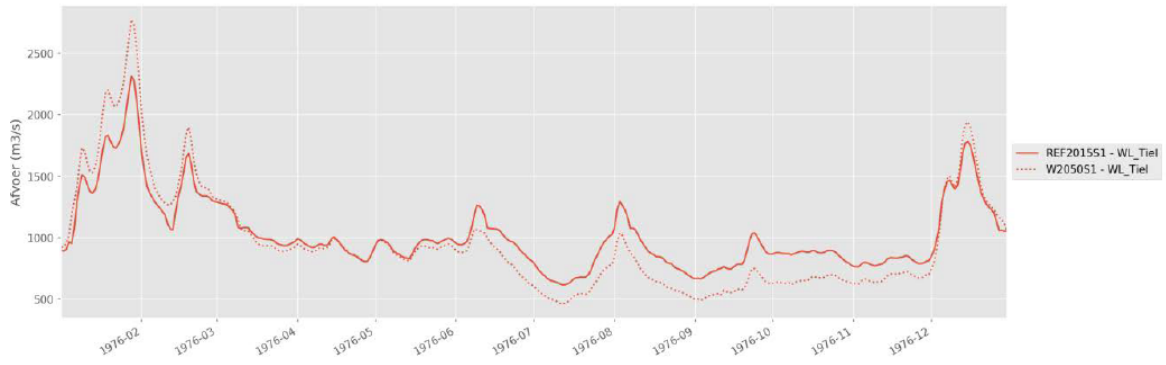

Figure A.2: Characteristic year 1976 translated to 2050 (Mens et al., 2018)

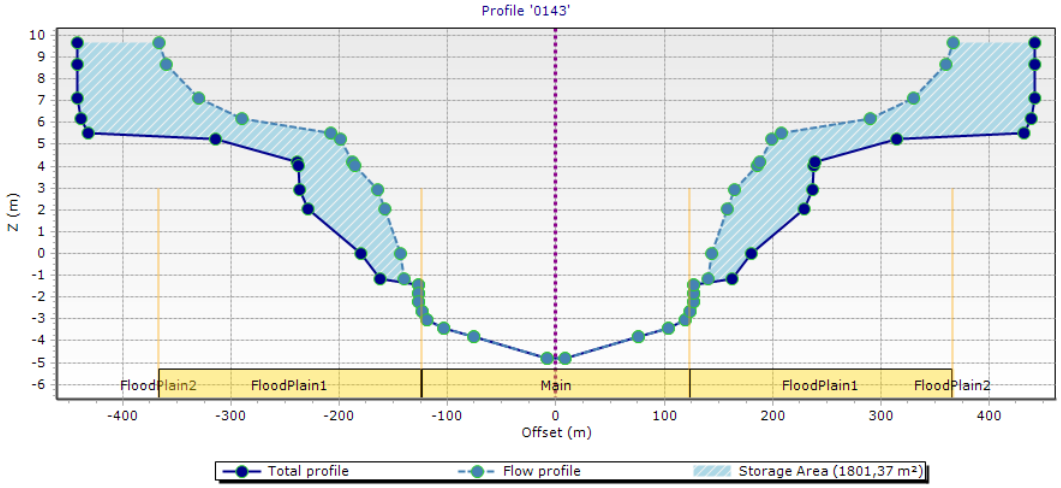

Figure A.3: Example of a cross-section in LSM

Hardinxveld (Waal), Keteldiep (IJssel) and Kattendiep (IJssel). The boundary nodes at Krimpen aan de Lek and Hardinxveld are tidally influenced and therefore follow the water level of the North Sea on the Dutch coast to some extent. The tidal effect decreases further inland so that the exact influence of increasing sea-water levels is unknown. Moreover, the North Sea water level is highly variable as it is heavily affected by variations related to wind (Klein Tank et al., 2015). As it thus remains complicated to find a realistic projection of the water levels at the boundary nodes of Krimpen aan de Lek and Hardinxveld there has been chosen to adapt the daily water levels on these locations of an average year in terms of precipitation. Both the Keteldiep and Kattendiep flow out in the IJsselmeer lake and therefore follow this water level. There is a large uncertainty however in predicting the water level of the IJsselmeer lake due to uncertainty in projections of SLR and infrastructural developments. For that reason, in accordance with the other boundary conditions, there has been chosen to adapt the daily water levels of the same average year in terms of precipitation at the boundary nodes of Keteldiep and Kattendiep. Moreover, due to the location of these two nodes outside the area of study and the relatively long distance (100+ km) to the area of study, any discrepancies between the used and the correct water levels on these locations are assumed to have a negligible effect on the outcome of the LSM.

A.4. Output data

The D-Flow 1D computations result among others in daily water levels on all nodes that are used in this research, following from the daily boundary conditions. Knowing these, subtracting the bed levels would result in the maximum local water depth for each node, every day of the year 2050. Figure A.4 shows the output of the LSM on a random day with each dot representing a node and thus a water level.
However, it is not the maximum water depth that is used for navigational purposes. In Section 2.3.4 it was seen that a minimum navigable river width of 150 m should be guaranteed under ALW conditions. As such,

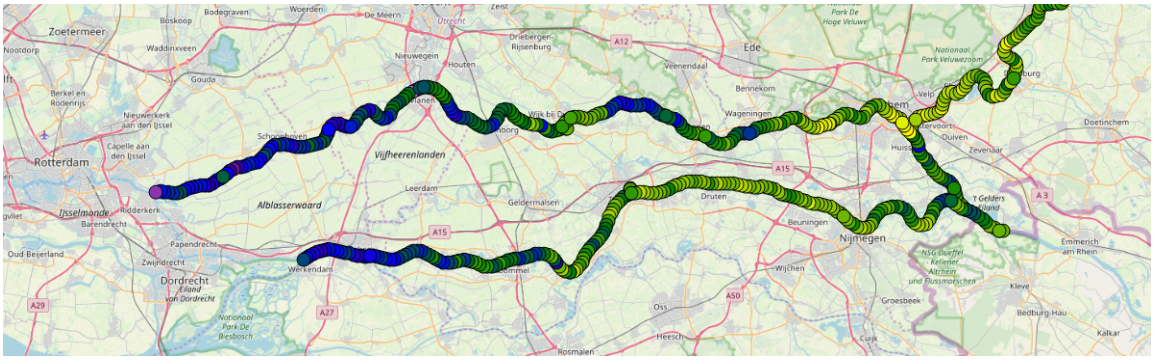

Figure A.4: Example output of LSM

the part of the bathymetry that does not meet this requirement does not agree with navigation standards and should thus not be taken into calculation of the navigable water depth. A correction is therefore proposed on all nodes. The height of the bathymetry that shows a lower width than the minimum allowable width is subtracted off the earlier computed water depth on that cross-section. This is done for all nodes on every day of the year. In Figure A.5 a schematic representation of a cross-section is given including the relevant parameters for the correction of the water depth.

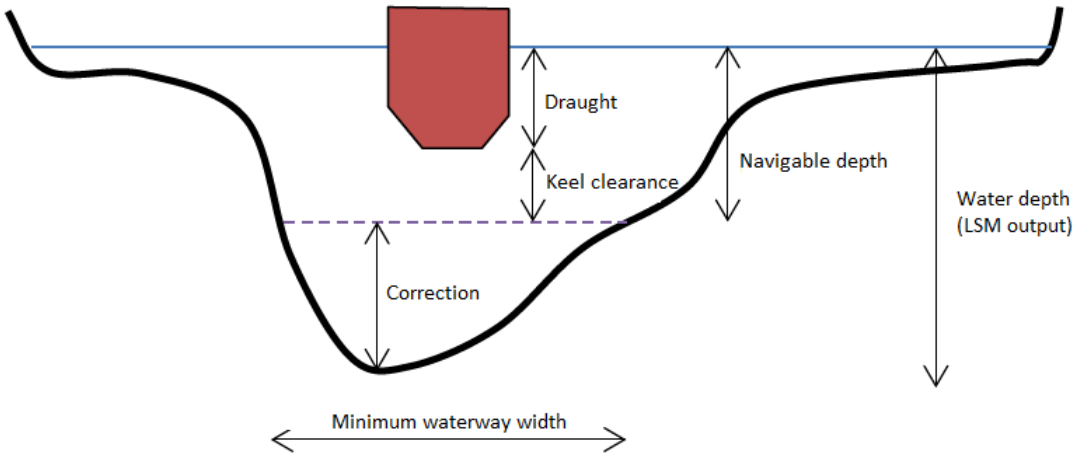

Figure A.5: Schematisation of corrected water depth (Mens et al., 2018)

Including this correction gives a daily water depth per node that can be used in determining the navigability of each river branch. Hence, this can be used to determine the network performance of the IWT system.

B

BIVAS IVS-90 Data

This chapter presents the figures that follow from the Binnenvaart Analyse Systeem (BIVAS) data-set used for model calibration. The obtained data-set consists of IVS-90 data (Informatie en Volgsysteem Scheepvaart (1990)) [1]. This web page shows various scenarios. To calibrate with the data of 2018, the scenario 'reizen 2018 IVS' has been selected. This scenario holds information on all trips performed by IWT in 2018. A filter has been applied in order to select the correct vessels. This filter denotes a classification in cargo ('Ertsen, metaalafval, geroost ijzerkies' en 'Vaste minerale brandstoffen'), the type of cargo ('Droge bulk') and the origin ('Europoort'). Per vessel type, the data-set was built up by extracting weekly totals for the trips, the transported cargo and the transport capacity. The data-set is too extensive to show in this Appendix. When interested, the author can be contacted.

B.1. 6-barge push convoys

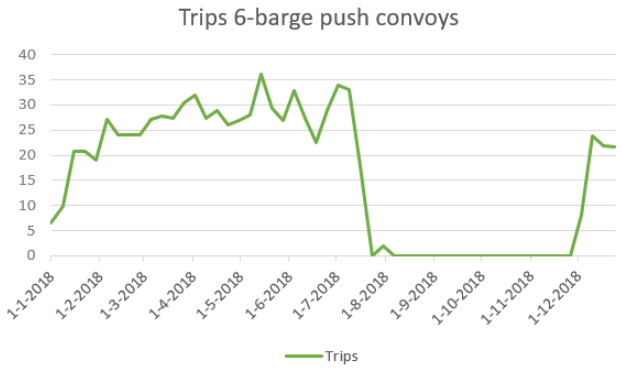

Figure B.1: Weekly trips by 6-barge push convoys in 2018

[1] Open website of Rijkswaterstaat accessed on 25-09-2019; https://bivas.chartasoftware.com/Scenarios

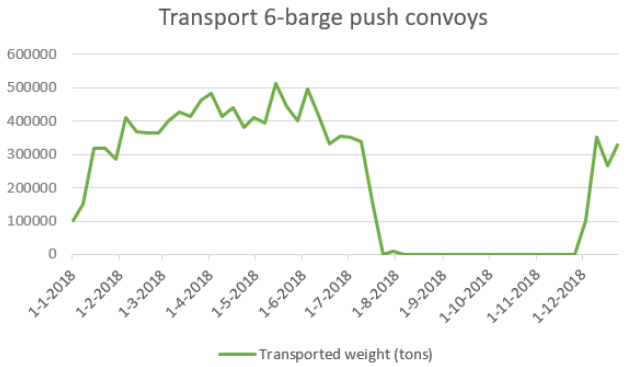

Figure B.2: Weekly transport by 6-barge push convoys in 2018

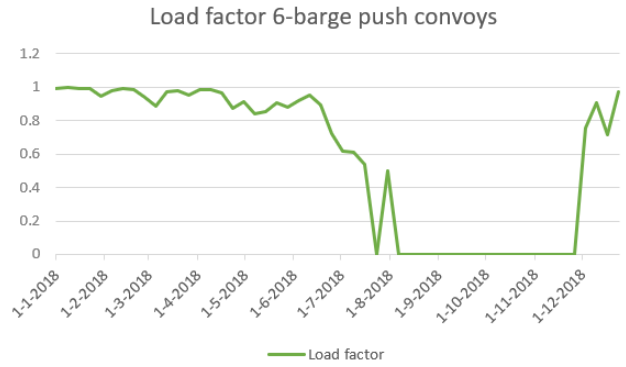

Figure B.3: Weekly average load factor by 6-barge push convoys in 2018

B.2. Smaller push-barge convoys

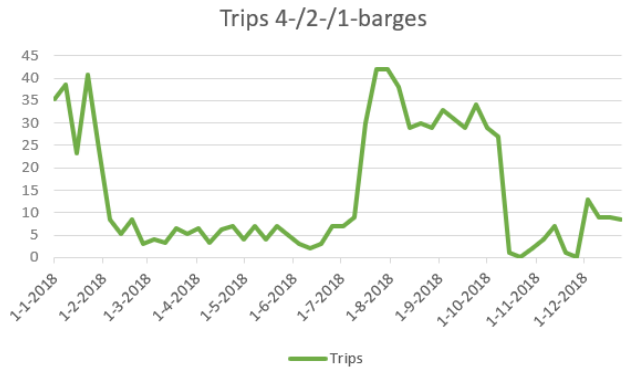

Figure B.4: Weekly trips by smaller push-barge convoys in 2018

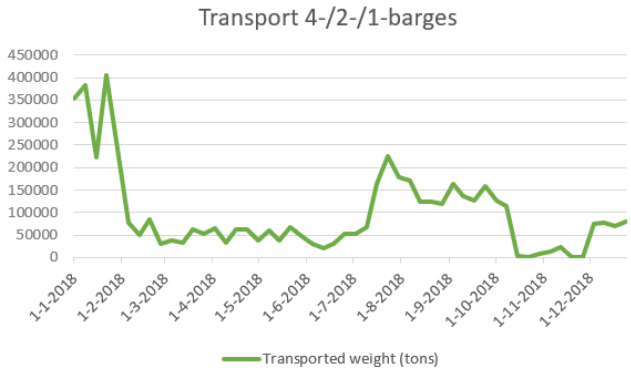

Figure B.5: Weekly transport by smaller push-barge convoys in 2018

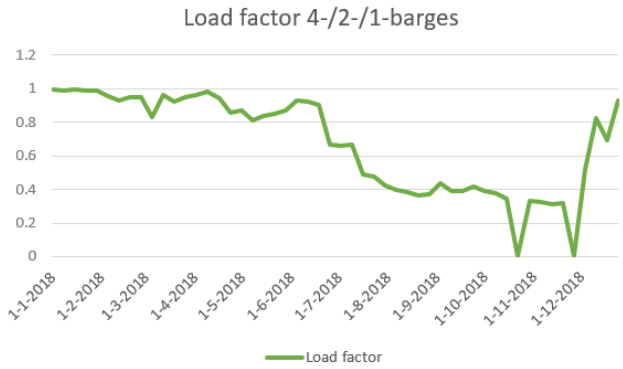

Figure B.6: Weekly average load factor by smaller push-barge convoys in 2018

B.3. Rhine vessels

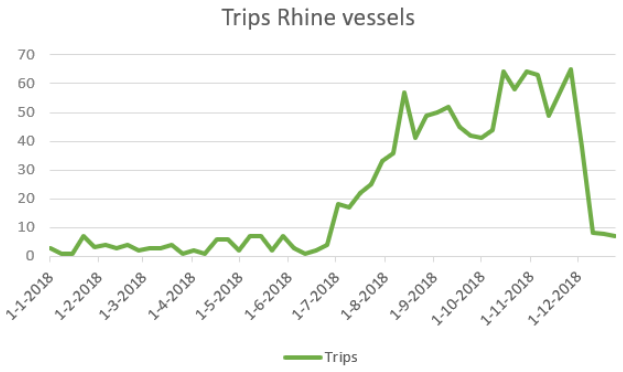

Figure B.7: Weekly trips by Rhine vessels in 2018

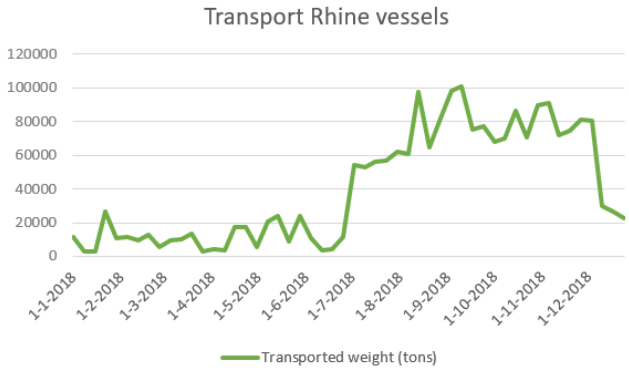

Figure B.8: Weekly transport by Rhine vessels in 2018

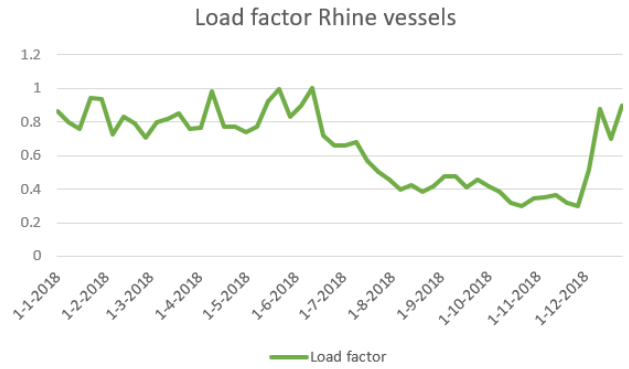

Figure B.9: Weekly average load factor by Rhine vessels in 2018

B.4. Coupled barges

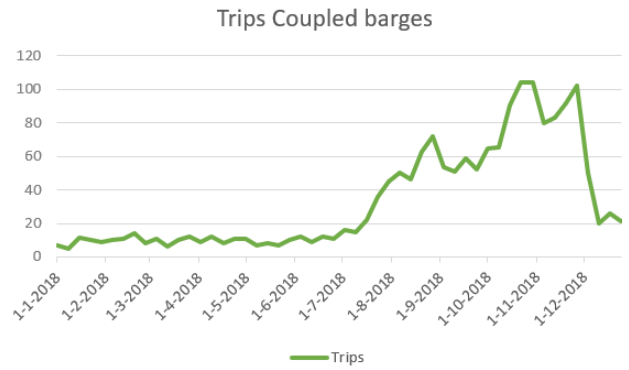

Figure B.10: Weekly trips by coupled barges in 2018

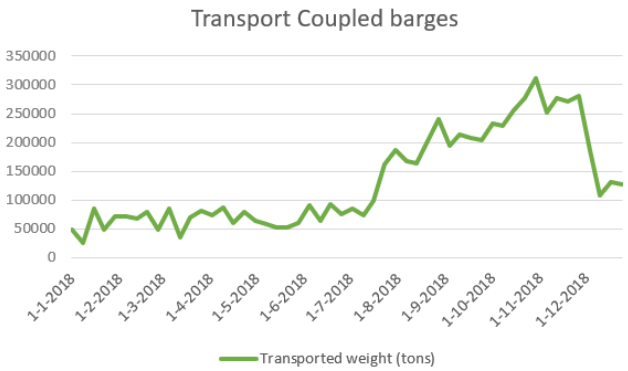

Figure B.11: Weekly transport by coupled barges in 2018

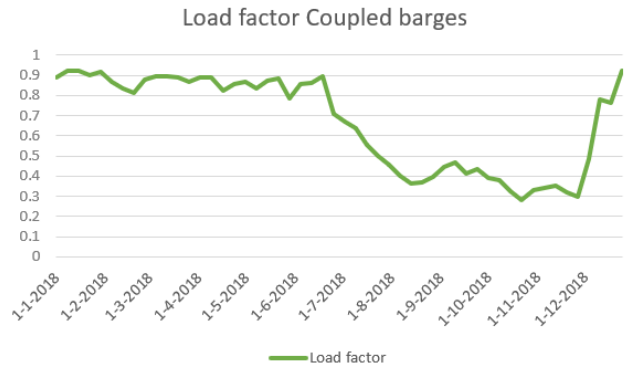

Figure B.12: Weekly average load factor by coupled barges in 2018

C

LSM Calibration Output

Due to the extensiveness of this data-set, the data has been uploaded on the repository of the Delft University of Technology.

D

Initial conditions internal validation

	Unit	Value
General		
Transport demand	[tons/year]	365,000
Safety margin	[m]	0.25
Sailing speed unloaded downstream	[m/s]	4.75
Sailing speed loaded upstream	[m/s]	2.50
Costs insufficient supply	[€/ ton]	1,000
6-barge push convoys		
Convoy capacity	[tons]	250
Barge draught empty	[m]	0.65
Barge draught full	[m]	3.95
Fleet size	[pusher boats]	15
Manoeuvring time	[hours]	0
Agent price	[€/ day]	15,000
Smaller push-barge convoys		
Convoy capacity	[tons]	100
Barge draught empty	[m]	0.65
Barge draught full	[m]	3.95
Fleet size	[pusher boats]	15
Manoeuvring time	[hours]	1
Agent price	[€/ day]	7,500
Rhine vessels		
Rhine vessel capacity	[tons]	25
Rhine vessel draught empty	[m]	1.20
Rhine vessel draught full	[m]	3.0
Fleet size	[Rhine vessels]	35
Manoeuvring time	[hours]	2
Agent price	[€/ day]	2,500
Coupled barges		
Coupled barge capacity	[tons]	40
Barge draught empty	[m]	0.65
Barge draught full	[m]	3.95
Fleet size	[coupled barges]	50
Manoeuvring time	[hours]	2
Agent price	[€/ day]	7,000
Site equipment		
Nr. of resources	[berths]	1
Loading rate	[ton/s]	0.05
Unloading rate	[ton/s]	0.05

Table D.1: Input values for internal validation

E

LSM Output Null scenario

Due to the extensiveness of this data-set, the data has been uploaded on the repository of the Delft University of Technology.

F

Results Application

This section studies the ideal size of each adaptation effect. Section F.1 addresses the ideal fleet size of new barges and pusher boats that should be implemented in order to have the optimal combination of effect on the network performance and ratio between costs and benefits. In Section F.2, this is repeated for the river training works.

F.1. Results lighter barges

The ideal fleet size is checked for barges in the range from 14 to 26 in steps of 6. For 14 and 20 barges, no additional pusher boats are required. For 26 barges, per two barges one additional pusher boat is required. These additional pusher boats merely appear in the cost evaluation. The results for each fleet size for both the RUST- and the STOOM-scenario are shown below.

	Unit	Value RUST	Value STOOM
Number of trips			
Nr. of trips	[trips]	5,156	7,126
Nr. of trips June - November	[trips]	3,813	4,513
Nr. of trips January - May and December	[trips]	1,343	2,613
Trips 6-barge push convoys	[trips]	925	435
Trips smaller convoys	[trips]	917	847
Trips new barges	[trips]	39	526
Trips Rhine vessels	[trips]	1,363	2,266
Trips coupled barges	[trips]	1,912	3,052
Transported weight			
Transported weight	[tons]	24,192,291	21,113,721
Transport June - November	[tons]	11,857,760	8,450,132
Transport January - May and December	[tons]	12,334,531	12,663,589
Transport 6-barge push convoys	[tons]	12,271,564	6,249,506
Transport smaller convoys	[tons]	4,183,948	3,694,903
Transport new barges	[tons]	71,416	1,099,304
Transport Rhine vessels	[tons]	1,939,432	2,448,187
Transport coupled barges	[tons]	5,725,931	7,621,821
Transport costs			
Total costs	[€]	110,254,403	173,246,323
Costs June - November	[€]	72,633,351	130,629,008
Costs January - May and December	[€]	37,621,052	42,617,316
Costs of insufficient supply	[€]	30,854,984	73,964,523
Costs 6-barge push convoys	[€]	23,972,622	9,579,770
Costs smaller convoys	[€]	16,047,435	14,901,334
Costs new barges	[€]	316,401	6,715,560
Costs Rhine vessels	[€]	6,521,705	14,678,411
Costs coupled barges	[€]	33,290,075	60,817,561

Table F.1: Output values with 14 barges in equipment scenario

	Unit	Value RUST	Value STOOM
Number of trips			
Nr. of trips	[trips]	4,832	7,201
Nr. of trips June - November	[trips]	3,506	4,659
Nr. of trips January - May and December	[trips]	1,326	2,542
Trips 6-barge push convoys	[trips]	1,036	485
Trips smaller convoys	[trips]	794	857
Trips new barges	[trips]	50	700
Trips Rhine vessels	[trips]	1,170	2,169
Trips coupled barges	[trips]	1,782	2,990
Transported weight			
Transported weight	[tons]	24,399,882	22,017,334
Transport June - November	[tons]	11,780,256	9,146,947
Transport January - May and December	[tons]	12,619,627	12,870,387
Transport 6-barge push convoys	[tons]	13,609,034	6,833,070
Transport smaller convoys	[tons]	3,652,075	3,748,347
Transport new barges	[tons]	91,576	1,496,966
Transport Rhine vessels	[tons]	2,087,186	3,009,552
Transport coupled barges	[tons]	4,960,011	6,929,3990
Transport costs			
Total costs	[€]	104,468,658	160,690,541
Costs June - November	[€]	69,817,009	121,379,614
Costs January - May and December	[€]	34,651,649	39,310,928
Costs of insufficient supply	[€]	27,538,034	62,325,642
Costs 6-barge push convoys	[€]	27,134,889	10,371,250
Costs smaller convoys	[€]	13,714,463	14,797,241
Costs new barges	[€]	397,656	8,763,424
Costs Rhine vessels	[€]	5,588,712	13,899,7146
Costs coupled barges	[€]	30,945,778	59,813,768

Table F.2: Output values with 20 barges in equipment scenario

	Unit	Value RUST	Value STOOM
Number of trips			
Nr. of trips	[trips]	5,191	7,524
Nr. of trips June - November	[trips]	3,850	4,912
Nr. of trips January - May and December	[trips]	1,341	2,612
Trips 6-barge push convoys	[trips]	925	435
Trips smaller convoys	[trips]	917	846
Trips new barges	[trips]	72	97
Trips Rhine vessels	[trips]	1,366	2,239
Trips coupled barges	[trips]	1,911	3,029
Transported weight			
Transported weight	[tons]	24,249,319	21,978,395
Transport June - November	[tons]	11,923,998	9,316,653
Transport January - May and December	[tons]	12,325,321	12,661,742
Transport 6-barge push convoys	[tons]	12,270,825	6,249,506
Transport smaller convoys	[tons]	4,184,994	3,690,855
Transport new barges	[tons]	131,626	2,037,437
Transport Rhine vessels	[tons]	1,944,265	2,426,518
Transport coupled barges	[tons]	5,717,608	7574,079
Transport costs			
Total costs	[€]	108,832,823	160,970,627
Costs June - November	[€]	71,862,737	118,346,664
Costs January - May and December	[€]	36,970,085	42,623,963
Costs of insufficient supply	[€]	29,332,326	60,966,702
Costs 6-barge push convoys	[€]	23,674,322	94,926,690
Costs smaller convoys	[€]	16,187,059	15,066,756
Costs new barges	[€]	584,479	12,458,426
Costs Rhine vessels	[€]	6,470,400	14,805,836
Costs coupled barges	[€]	33,469,262	61,260,101

Table F.3: Output values with 26 barges in equipment scenario

The data from these tables is used to compute the relative measure effectiveness and cost-benefit ratio for each number of equipment measures in order to determine the optimal number of measures. The results are given in Figures F.1a, F.1b, F.1c, F.1d, F.1e and F.1f. The ideal number of measures provides the highest measure effectiveness, i.e. highest growth of transported cargo, and has the lowest cost-benefit ratio, i.e. the implementation costs are less than the benefit in costs.

More vessels are seen to have a nearly linear relation with the measure effectiveness. The difference is made in the cost-benefit ratio. For the RUST-scenario, the lowest value is seen for twenty new barges. For the STOOM-scenario, a small increase is seen for 14 to 20 barges but the increase in measure effectiveness is much larger. Looking at both climate scenarios, it can be concluded that the costs of the pusher boats cause a turning point in the cost-benefit evaluation. It can thus be concluded that applying twenty new barges and no additional pusher boats is the optimal number of equipment measures.

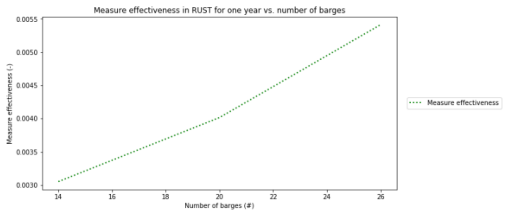

(a) Equipment measure effectiveness in RUST-scenario for one year

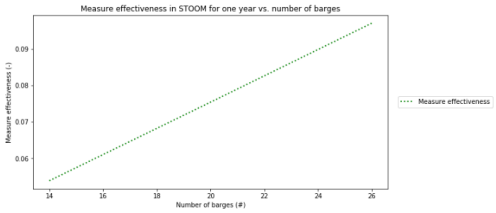

(b) Equipment measure effectiveness in STOOM-scenario for one year

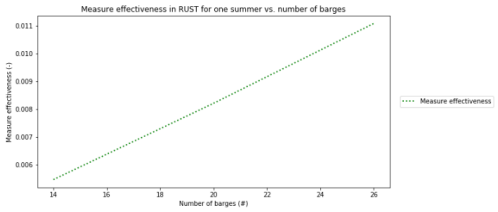

(c) Equipment measure effectiveness in RUST-scenario for one summer

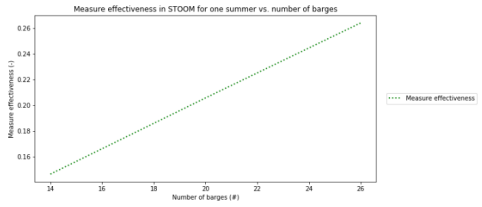

(d) Equipment measure effectiveness in STOOM-scenario for one summer

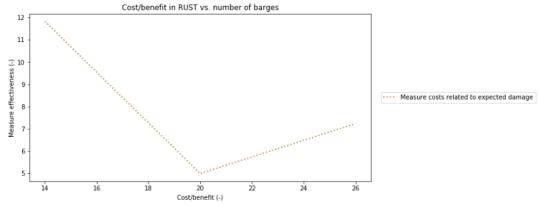

(e) Cost-benefit ratio in RUST-scenario for one year

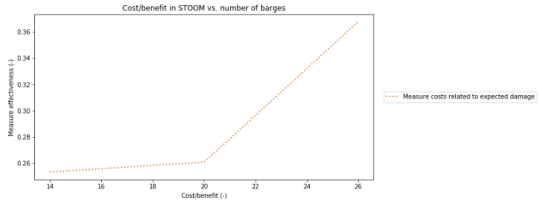

(f) Cost-benefit ratio in STOOM-scenario for one year

Figure F.1: Selection of optimal number of new vessels

The results of the simulation after adding these vessels measures are shown below for both climate scenarios.

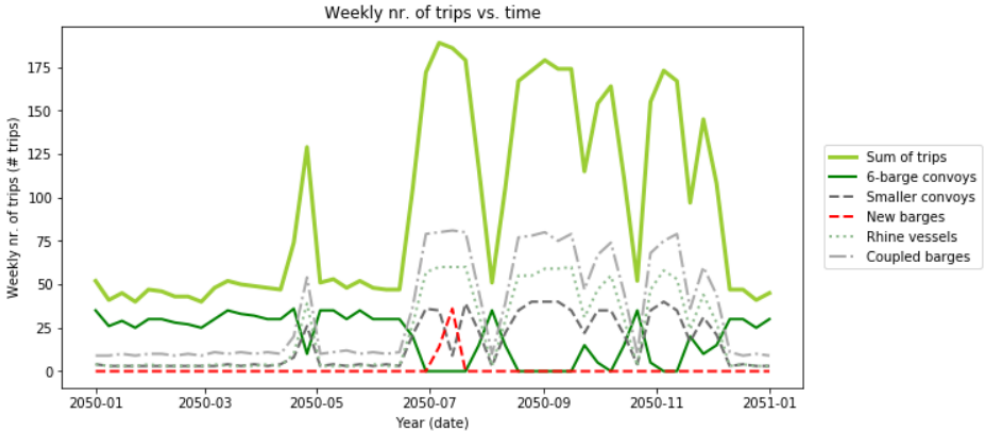

Figure F.2: Number of trips in RUST-scenario with smaller barges

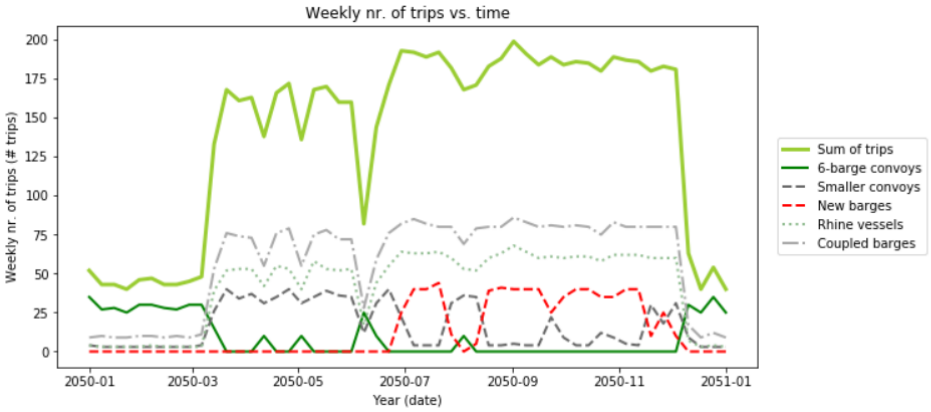

Figure F.3: Number of trips in STOOM-scenario with smaller barges

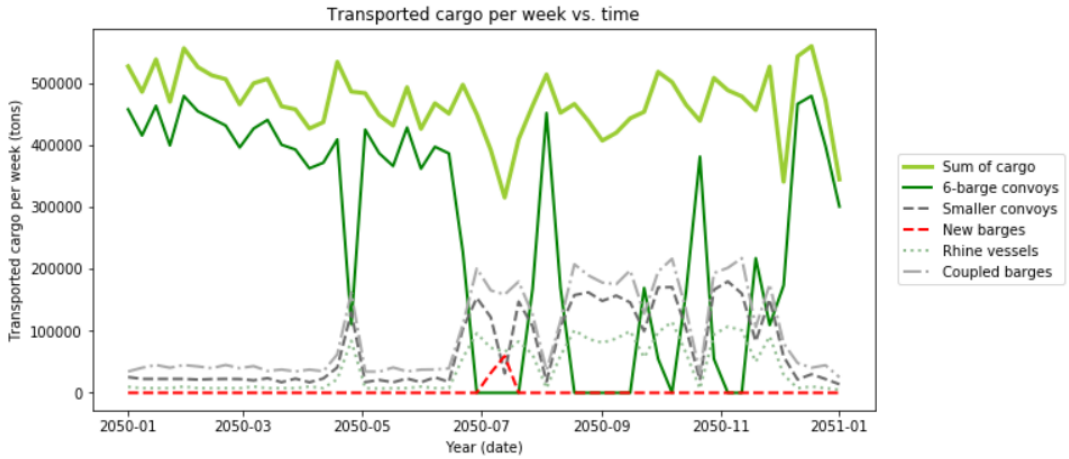

Figure F.4: Transported cargo in RUST-scenario with smaller barges

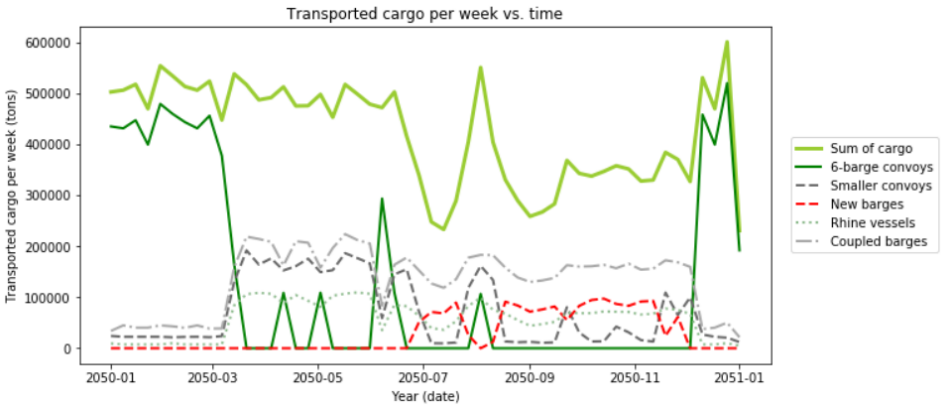

Figure F.5: Transported cargo in STOOM-scenario with smaller barges

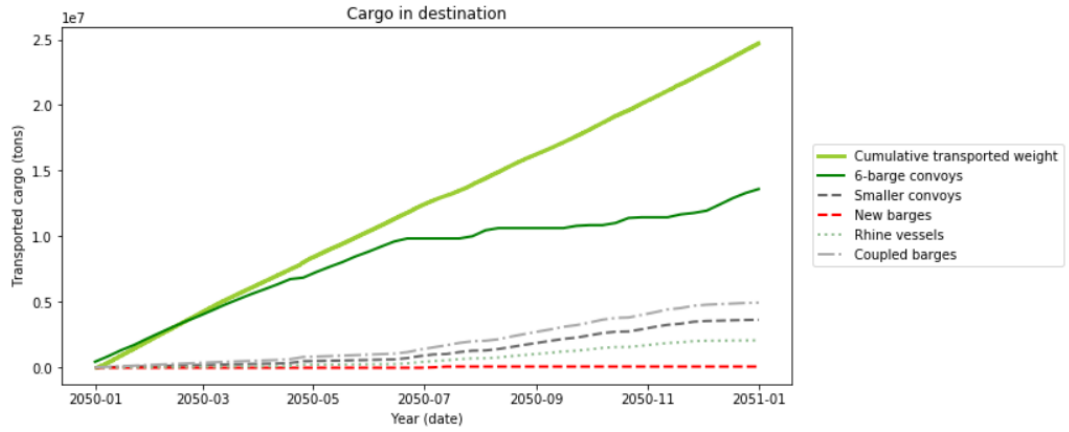

Figure F.6: Cumulative cargo in RUST-scenario with smaller barges

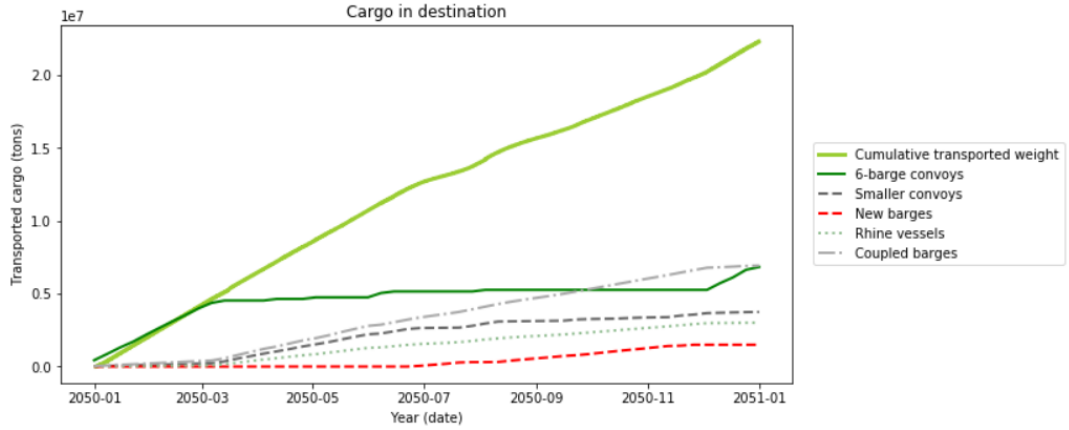

Figure F.7: Cumulative cargo in STOOM-scenario with smaller barges

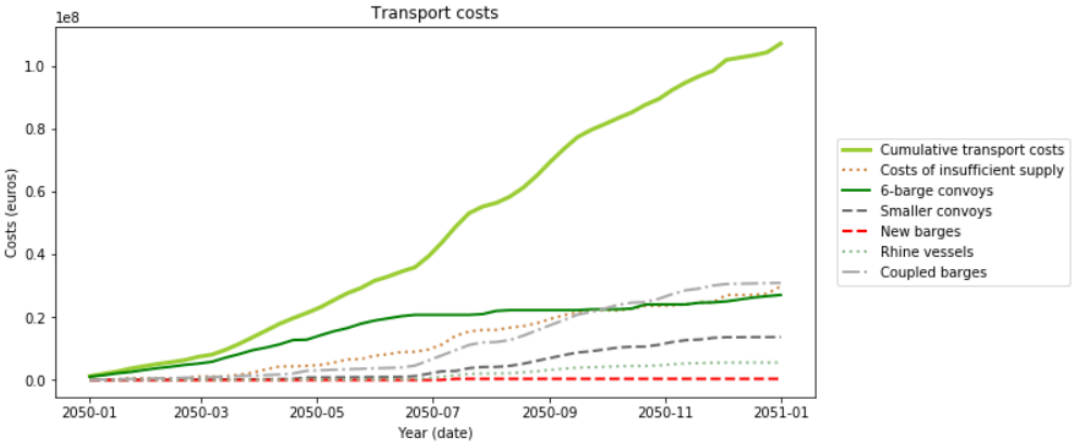

Figure F.8: Cumulative costs in RUST-scenario with smaller barges

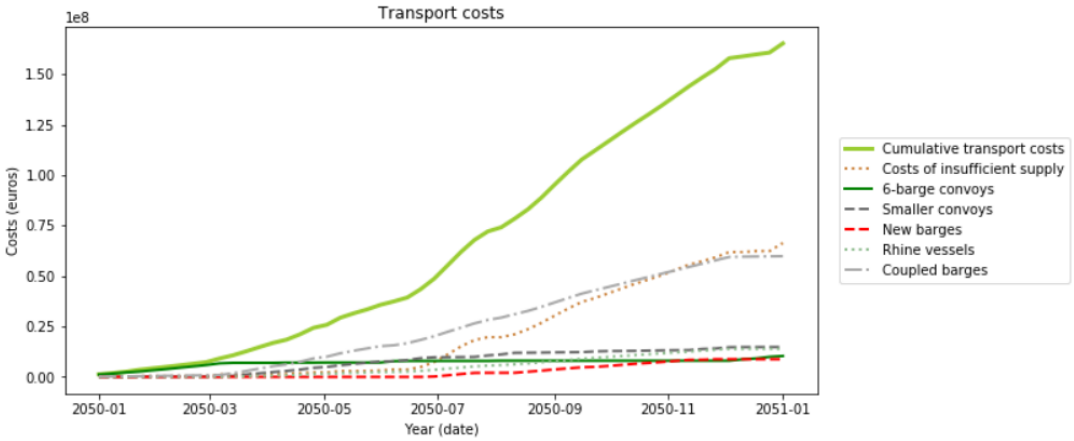

Figure F.9: Cumulative costs in STOOM-scenario with smaller barges

F.2. Results river training

The ideal number of river training works is checked for the infrastructural measure in the range from 1 to 5. A river training work is considered to hold for a stretch of 1 km. Per measure, the water depth is increased with 0.25 m. The results for each number of river training works for both the RUST- and the STOOM-scenario are shown below.

	Unit	Value RUST	Value STOOM
Number of trips			
Nr. of trips	[trips]	5,098	6,587
Nr. of trips June - November	[trips]	3,756	3,983
Nr. of trips January - May and December	[trips]	1,342	2,604
Trips 6-barge push convoys	[trips]	930	445
Trips smaller convoys	[trips]	909	842
Trips Rhine vessels	[trips]	1,363	2,253
Trips coupled barges	[trips]	1,896	3,047
Transported weight			
Transported weight	[tons]	24,090,446	20,120,957
Transport June - November	[tons]	11,757,779	7,459,297
Transport January - May and December	[tons]	12,332,667	12,661,660
Transport 6-barge push convoys	[tons]	12,329,045	6,361,945
Transport smaller convoys	[tons]	4,156,372	3,675,727
Transport Rhine vessels	[tons]	1,926,929	2,452,582
Transport coupled barges	[tons]	5,678,100	7,630,704
Transport costs			
Total costs	[€]	110,849,511	187,693,464
Costs June - November	[€]	73,788,998	145,386,225
Costs January - May and December	[€]	37,060,513	42,307,240
Costs of insufficient supply	[€]	31,213,229	89,050,687
Costs 6-barge push convoys	[€]	23,762,397	9,332,711
Costs smaller convoys	[€]	16,124,272	14,814,216
Costs Rhine vessels	[€]	6,453,646	14,457,692
Costs coupled barges	[€]	33,563,703	60,656,840

Table F.4: Output values with 1 measures infrastructural measure

	Unit	Value RUST	Value STOOM
Number of trips			
Nr. of trips	[trips]	4,720	6,556
Nr. of trips June - November	[trips]	3,464	4,008
Nr. of trips January - May and December	[trips]	1,256	2,548
Trips 6-barge push convoys	[trips]	1,021	475
Trips smaller convoys	[trips]	809	865
Trips Rhine vessels	[trips]	1,198	2,221
Trips coupled barges	[trips]	1,692	2,995
Transported weight			
Transported weight	[tons]	23,934,702	20,587,916
Transport June - November	[tons]	11,662,424	7,777,369
Transport January - May and December	[tons]	12,272,278	12,810,546
Transport 6-barge push convoys	[tons]	13,434,401	6,740,722
Transport smaller convoys	[tons]	3,708,535	3,785,380
Transport Rhine vessels	[tons]	1,702,824	2,458,952
Transport coupled barges	[tons]	5,088,942	7,602,863
Transport costs			
Total costs	[€]	106,540,026	180,573,303
Costs June - November	[€]	71,564,436	141,241,085
Costs January - May and December	[€]	34,975,590	39,332,218
Costs of insufficient supply	[€]	29,970,912	82,794,526
Costs 6-barge push convoys	[€]	28,373,627	9,877,748
Costs smaller convoys	[€]	13,856,970	14,991,224
Costs Rhine vessels	[€]	5,822,878	14,046,052
Costs coupled barges	[€]	28,616,545	59,355,182

Table F.5: Output values with 2 measures infrastructural measure

	Unit	Value RUST	Value STOOM
Number of trips			
Nr. of trips	[trips]	4,601	6,441
Nr. of trips June - November	[trips]	3,376	4,006
Nr. of trips January - May and December	[trips]	1,225	2,435
Trips 6-barge push convoys	[trips]	1,055	505
Trips smaller convoys	[trips]	782	864
Trips Rhine vessels	[trips]	1,140	2,161
Trips coupled barges	[trips]	1,624	2,911
Transported weight			
Transported weight	[tons]	24,014,913	20,699,493
Transport June - November	[tons]	11,686,920	7,978,222
Transport January - May and December	[tons]	12,327,993	12,721,271
Transport 6-barge push convoys	[tons]	13,864,793	7,081,998
Transport smaller convoys	[tons]	3,602,709	3,765,808
Transport Rhine vessels	[tons]	1,630,425	2,419,454
Transport coupled barges	[tons]	4,916,986	7,432,233
Transport costs			
Total costs	[€]	105,345,267	176,636,679
Costs June - November	[€]	69,900,316	138,275,136
Costs January - May and December	[€]	35,444,951	38,361,543
Costs of insufficient supply	[€]	30,089,187	80,233,737
Costs 6-barge push convoys	[€]	28,312,829	10,554,964
Costs smaller convoys	[€]	13,544,402	15,069,689
Costs Rhine vessels	[€]	5,434,649	13,555,743
Costs coupled barges	[€]	28,139,519	57,484,307

Table F.6: Output values with 3 measures infrastructural measure

	Unit	Value RUST	Value STOOM
Number of trips			
Nr. of trips	[trips]	4,120	6,089
Nr. of trips June - November	[trips]	2,903	4,115
Nr. of trips January - May and December	[trips]	1,217	1,974
Trips 6-barge push convoys	[trips]	1,220	675
Trips smaller convoys	[trips]	632	907
Trips Rhine vessels	[trips]	868	1,878
Trips coupled barges	[trips]	1,400	2,629
Transported weight			
Transported weight	[tons]	24,402,904	21,747,081
Transport June - November	[tons]	11,824,638	8,970,155
Transport January - May and December	[tons]	12,578,266	12,776,926
Transport 6-barge push convoys	[tons]	15,887,567	9,009,757
Transport smaller convoys	[tons]	2,933,869	3,829,105
Transport Rhine vessels	[tons]	1,566,649	2,676,559
Transport coupled barges	[tons]	4,014,819	6,231,660
Transport costs			
Total costs	[€]	100,940,314	163,789,092
Costs June - November	[€]	65,686,060	125,998,928
Costs January - May and December	[€]	35,254,254	37,790,165
Costs of insufficient supply	[€]	27,280,161	67,773,119
Costs 6-barge push convoys	[€]	35,460,791	16,557,380
Costs smaller convoys	[€]	10,629,564	16,691,707
Costs Rhine vessels	[€]	3,953,310	12,157,798
Costs coupled barges	[€]	24,103,065	51,052,426

Table F.7: Output values with 4 measures infrastructural measure

	Unit	Value RUST	Value STOOM
Number of trips			
Nr. of trips	[trips]	4,207	6,120
Nr. of trips June - November	[trips]	3,073	4,068
Nr. of trips January - May and December	[trips]	1,134	2,052
Trips 6-barge push convoys	[trips]	1,161	622
Trips smaller convoys	[trips]	689	876
Trips Rhine vessels	[trips]	966	1,963
Trips coupled barges	[trips]	1,391	2,659
Transported weight			
Transported weight	[tons]	23,990,756	21,210,197
Transport June - November	[tons]	11,754,100	8,631,355
Transport January - May and December	[tons]	12,236,656	12,578,842
Transport 6-barge push convoys	[tons]	15,148,249	8,395,272
Transport smaller convoys	[tons]	3,190,126	3,753,441
Transport Rhine vessels	[tons]	1,391,788	2,220,596
Transport coupled barges	[tons]	4,260,594	6,840,888
Transport costs			
Total costs	[€]	101,912,706	165,845,635
Costs June - November	[€]	67,030,224	129,425,574
Costs January - May and December	[€]	34,882,482	36,420,060
Costs of insufficient supply	[€]	29,515,246	73,089,408
Costs 6-barge push convoys	[€]	32,287,915	13,219,958
Costs smaller convoys	[€]	11,640,105	15,911,926
Costs Rhine vessels	[€]	4,613,656	12,706,367
Costs coupled barges	[€]	24,027,447	51,322,589

Table F.8: Output values with 5 measures infrastructural measure

The data from these tables is used to compute the relative measure effectiveness and cost-benefit ratio for each number of infrastructural measures in order to determine the optimal number of measures. The results are given in Figures F.10a, F.10b, F.10c, F.10d, F.10e and F.10f. The ideal number of measures provides the highest measure effectiveness, i.e. highest growth of transported cargo, and has the lowest cost-benefit ratio, i.e. the implementation costs are less than the benefit in costs. Four river training works in the RUST-scenario show the smallest reductions of transported cargo, apart from applying one single measure. One single measure, however, gives a negative value for the cost-benefit ratio (here denoted by 0). This signals that a negative damage, i.e. higher costs after implementation of the adaptation measure, is expected. One single measure is therefore no longer an option. Applying four river training works then clearly is the best option of the RUST-scenario. When comparing this value to the STOOM-scenario, four measures are seen to have a high measure effectiveness and a low cost-benefit ratio. From both considered climate scenarios, it can thus be concluded that applying four river training works is the optimal number of infrastructural measures.

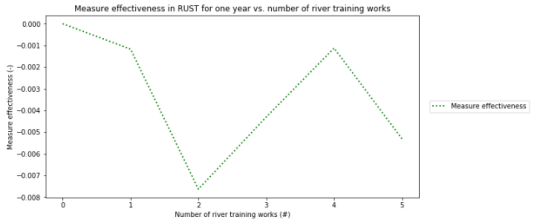

(a) Infrastructural measure effectiveness in RUST-scenario for one year

(b) Infrastructural measure effectiveness in STOOM-scenario for one year

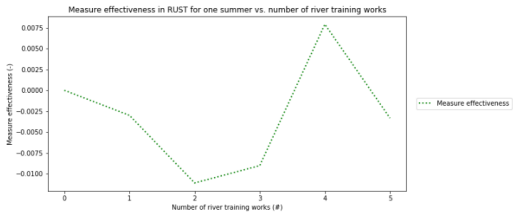

(c) Infrastructural measure effectiveness in RUST-scenario for one summer

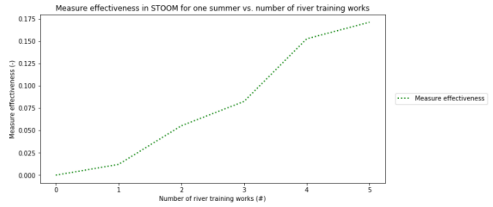

(d) Infrastructural measure effectiveness in STOOM-scenario for one summer

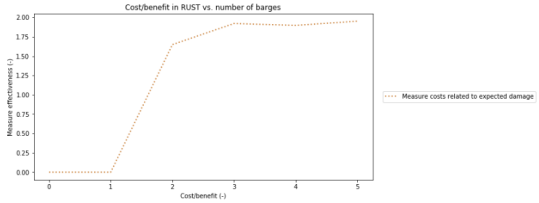

(e) Cost-benefit ratio in RUST-scenario for one year

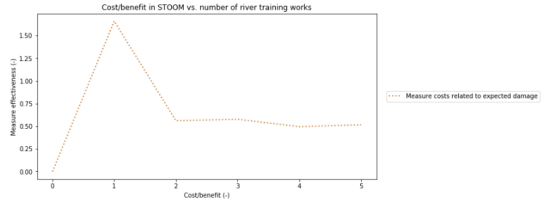

(f) Cost-benefit ratio in STOOM-scenario for one year

Figure F.10: Selection of optimal number of river training works

The results of the simulation after adding these infrastructural measures are shown below for both climate scenarios.

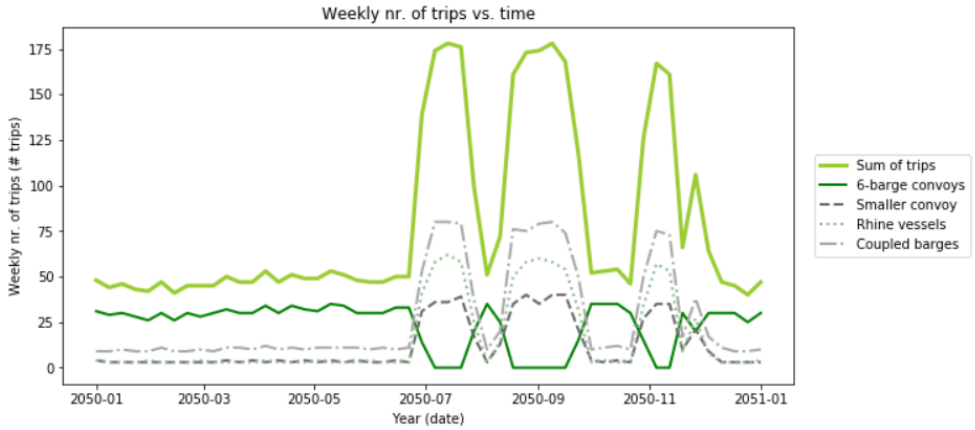

Figure F.11: Number of trips in RUST-scenario with river training works

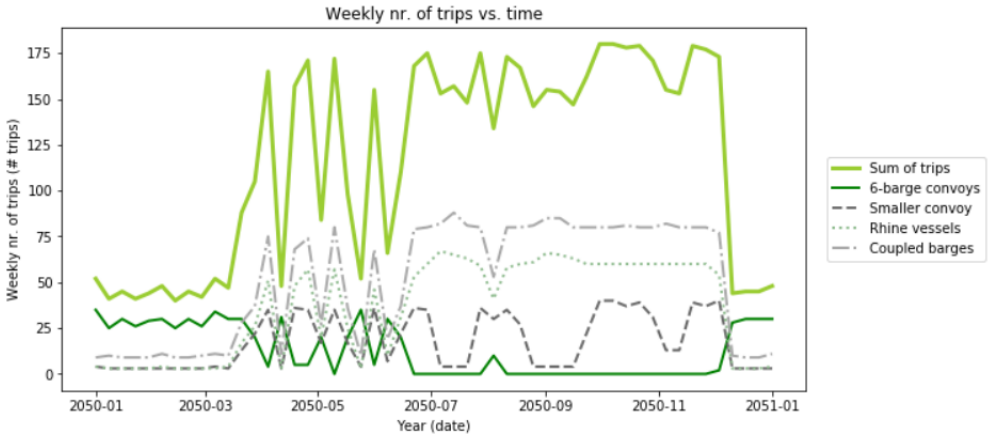

Figure F.12: Number of trips in STOOM-scenario with river training works

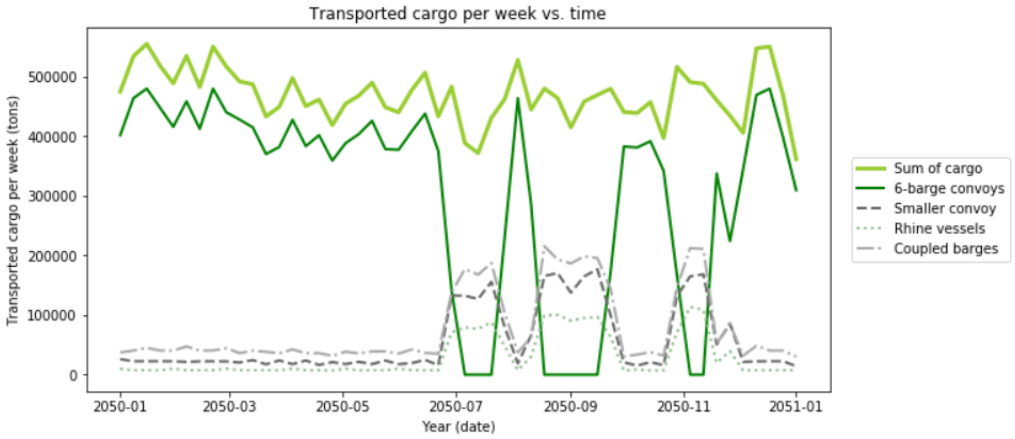

Figure F.13: Transported cargo in RUST-scenario with river training works

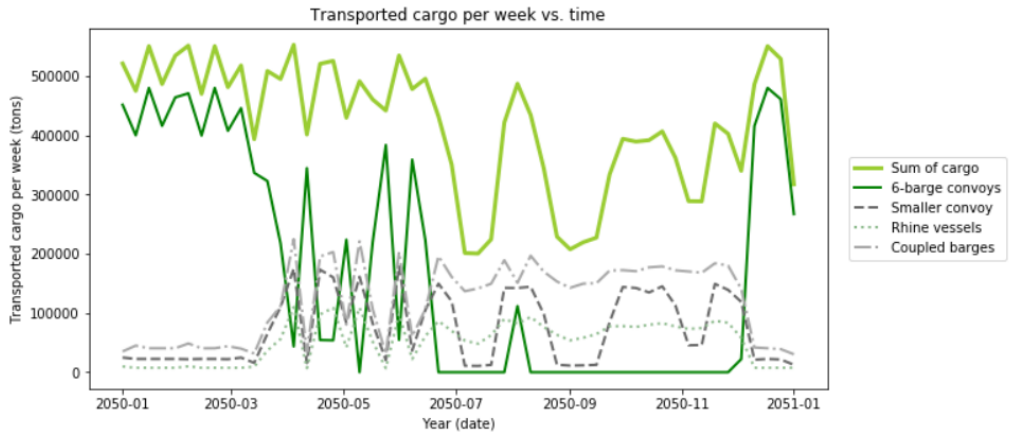

Figure F.14: Transported cargo in STOOM-scenario with river training works

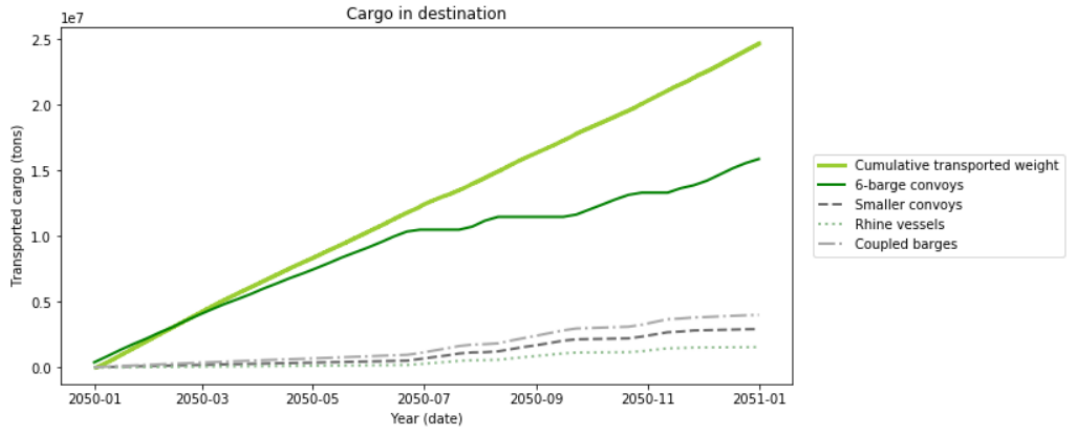

Figure F.15: Cumulative cargo in RUST-scenario with river training works

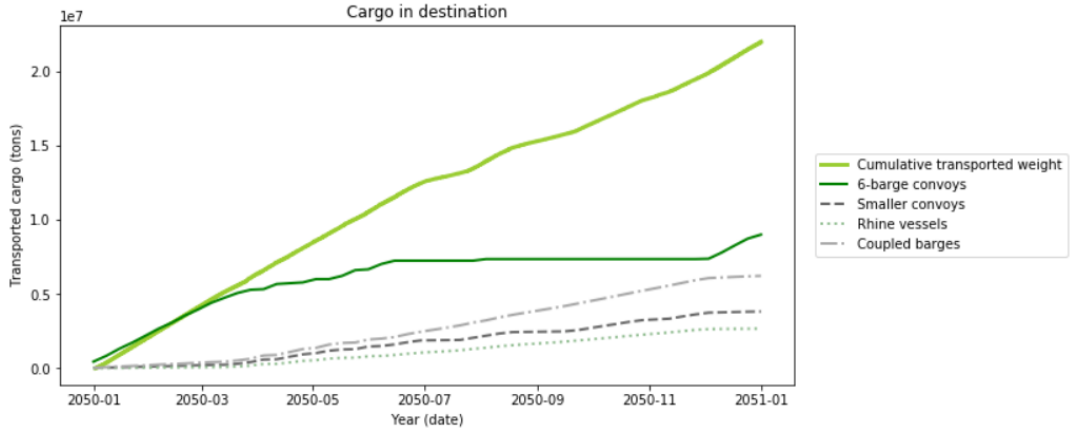

Figure F.16: Cumulative cargo in STOOM-scenario with river training works

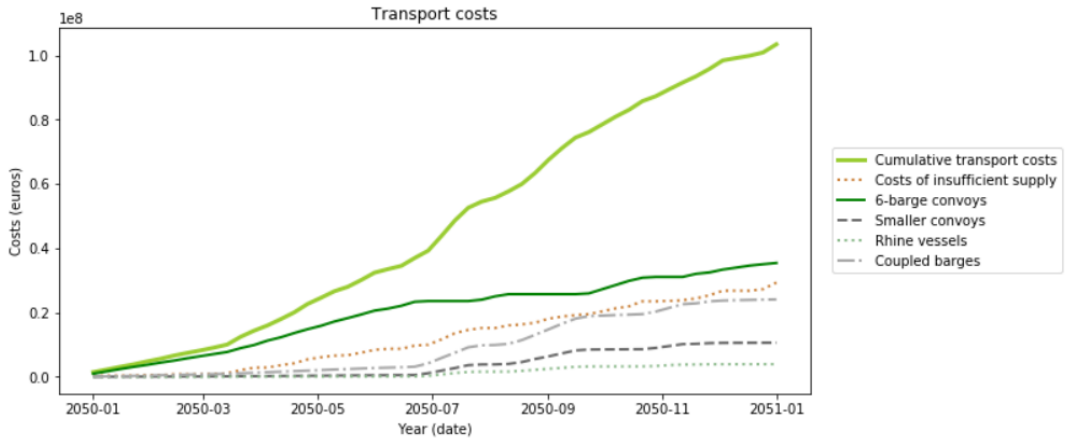

Figure F.17: Cumulative costs in RUST-scenario with river training works

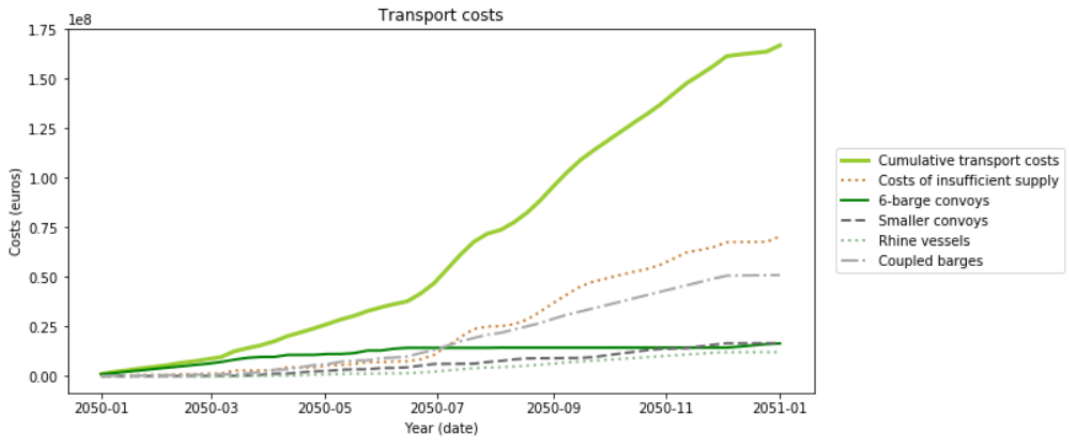

Figure F.18: Cumulative costs in STOOM-scenario with river training works

G

Stockpile calculation

G.1. Calculation iron ore stockpile

The total stockpile volume required for the iron ore is given by the following equation:

$$Volume\ stockpile = \frac{Optimal\ storage\ iron\ ore - Present\ stockpile}{Dumping\ weight\ iron\ ore}$$

The volume of the iron ore stockpile is given by:
Sides:

$$V_{sides} = (a - 2 * c) * 0.5 * c * Height * 2$$

$$c = \frac{Height}{\tan(Dumpingangle)}$$

where:

a	[m]	Length of stockpile
c	[m]	Width of one side; c = d
Dumping angle	[°]	Dumping angle of iron ore
Height	[m]	Height of iron ore stockpile

Body:

$$V_{body} = (a - 2 * c) * (b - 2 * c) * Height$$

where:

a	[m]	Length of stockpile
b	[m]	Width of stockpile
Height	[m]	Height of iron ore stockpile

Heads:

$$V_{heads} = (b - 2 * c) * 0.5 * d * Height * 2$$

$$d = \frac{Height}{\tan(Dumping\ angle)}$$

where:

b	[m]	Width of stockpile
d	[m]	Width of one side; d = c
Dumping angle	[°]	Dumping angle of iron ore
Height	[m]	Height of iron ore stockpile

The total volume is then given by:

$$V_{total} = (V_{sides} + V_{body} + V_{heads}) * n$$
$$V_{total} = 240,766 * n$$

By using the dumping weight, the optimal storage in tons can be translated to required volume of the stockpile. This can then be compared with the equation of the total volume to find the number of rows. From this it follows that the required number of rows of the iron ore stockpile for the RUST-scenario is equal to 1.85, i.e. 2. For the STOOM-scenario, the stockpile of iron ore requires 6.00, i.e. 6 rows.

G.2. Calculation coal stockpile

The calculation of the required storage area for coal follows the same method. The method only requires different input. The simplified total volume of coal is given by:

$$V_{total} = (V_{sides} + V_{body} + V_{heads}) * n$$
$$V_{total} = 565,326 * n$$

By using the dumping weight, the optimal storage in tons can be translated to required volume of the stockpile. This can then be compared with the equation of the total volume to find the number of rows. From this it follows that the required number of rows of the coal stockpile for the RUST-scenario is equal to 0.79, i.e. 1. For the STOOM-scenario, the stockpile of coal requires 2.56, i.e. 3 rows.

When schematized in a rectangular-shaped stockpile, an estimation can be done for the total required storage area. These schematizations can be seen in Figures G.1a and G.1b. The required storage area for both scenarios is given in Table G.1.

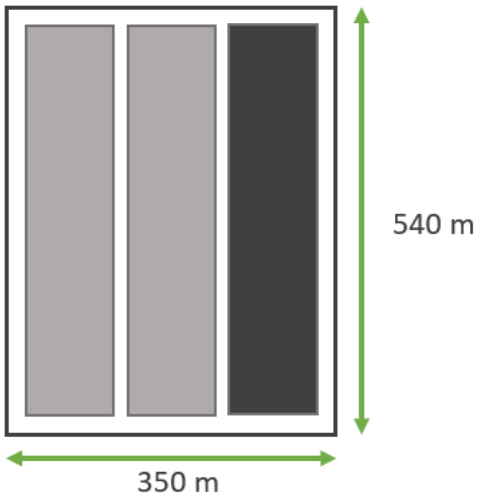

(a) Schematized storage area for the RUST-scenario

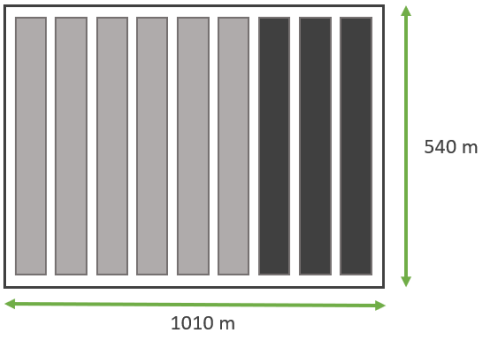

(b) Schematized storage area for the STOOM-scenario

Figure G.1: Schematized lay-outs for the required storage area in the RUST- and STOOM-scenario. The grey stripes depict the rows of iron ore, the black stripes depict the rows of coal

	Unit	Value
Storage area RUST	[m^2]	189,000
Storage area STOOM	[m^2]	545,400

Table G.1: Summary of the required storage area for the RUST- and STOOM-scenario

H

Code archive

The IWT performance model has been developed with the Open Complex Logistics Simulation (OpenCLSim) package. The package is available on the digital academic repository Zenodo. A link to this package can be found in Figure H.1. OpenCLSim is a tool for rule driven scheduling of cyclic activities for in-depth comparison of alternative operating strategies.

The IWT performance model is able to assess the impact of low water depths on the network performance of IWT systems, by evaluating key performance indicators as the transported cargo and the transport costs. A link to the repository in which the IWT performance model has been carefully built up can be found in Figure H.3. The considered base scenario that was used in the application of chapter 5 can be found in Figure H.3. This base scenario was then adjusted in order to evaluate the effectiveness of several adaptation measures. The links to these adjusted simulations are given in Figures H.4, H.5 and H.6.

Figure H.1: Link to OpenCLSim package on the Zenodo repository

Figure H.2: Link to the Network Capacity Analysis repository on the TU Delft Github

Figure H.3: Link to the simulation of the base scenario

Figure H.4: Link to the simulation of the equipment measure

Figure H.5: Link to the simulation of the infrastructural measure

Figure H.6: Link to the simulation of the stockpile measure